

TA7
.C6
CER 93-94-1
copy 2

LABORATORY NOTES ON STRATIFICATION OF SANDS

by

Pierre Y. Julien

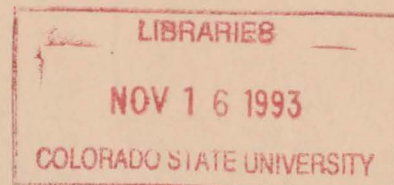
and

Yasser Raslan

Report CER 93-94-PYJ-YR-1

Engineering Research Center
Colorado State University
Fort Collins, CO 80523
USA

November, 1993



LABORATORY NOTES ON STRATIFICATION OF SANDS

by

Pierre Y. Julien

and

Yasser Raslan

Report CER 93-94-PYJ-YR-1

**Engineering Research Center
Colorado State University
Fort Collins, CO 80523
USA**

November, 1993



U18401 0685446

TA-
7
CG
CER 93-94-1
ESBL

TABLE OF CONTENTS

1.	INTRODUCTION	1
2.	EXPERIMENTS ON SEGREGATION AND LAMINATION	3
2.1	Introduction	3
2.2	Segregation Experiments	5
2.2.1	Sediment mixture	5
2.2.2	Experimental setup and procedures	5
2.3	Lamination Experiments	13
2.3.1	Experimental set up	13
2.3.2	Settling in air at horizontal position	15
2.3.3	Lamination and Segregation in air	15
2.3.4	Lamination in fresh water	19
2.3.5	Lamination in salt water	19
2.3.6	Lamination in vacuum	19
3.	EXPERIMENTS ON STRATIFICATION	26
3.1	Introduction	26
3.2	Large Laboratory Flume	26
3.3	Flume operation and Procedures	29
3.4.1	Horizontal slope run (run 1)	31
3.4.2	Positive slope run (run 2)	38
3.4.3	Negative slope run (run 3)	46
3.5	Compilation of Results	54
3.6	Stratified Delta	66
4.	CONCLUSIONS	72
4.1	Particle Segregation	72
4.2	Lamination in Air	72
4.3	Lamination in Fresh Water and Salt Water	73
4.4	Lamination in Vacuum	73
4.5	Stratification in a Large Laboratory Flume	73
5.	REFERENCES	76

LIST OF FIGURES

Figure 1.	Sieve analysis for the white sand	6
Figure 2.	Sieve analysis for the black sand	7
Figure 3.	Sieve analysis for the sand mixture	8
Figure 4.	The plexiglas plate	10
Figure 5.	U-shaped settling tube	13
Figure 6.	Vacuum settling tube	14
Figure 7.	Sketch of the 4 ft-wide flume	27
Figure 8.	Experimental flowchart	32
Figure 9.	The deposition of step 1-U1	34
Figure 10.	The deposition of step 1-U2	35
Figure 11.	The deposition of step 1-U3	36
Figure 12.	The deposition of step 1-U4	37
Figure 13.	The deposition of step 2-U2	40
Figure 14.	The deposition of step 2-U3	41
Figure 15.	The deposition of step 2-D1	42
Figure 16.	The deposition of step 2-D2	44
Figure 17.	The deposition of step 2-D3	45
Figure 18.	The deposition of step 3-U1	47
Figure 19.	The deposition of step 3-U2	48
Figure 20.	The deposition of step 3-U3	50
Figure 21.	The deposition of step 3-U4	51
Figure 22.	The deposition of step 3-D1	52
Figure 23.	The deposition of step 3-D2	53
Figure 24.	The deposition of step 3-D3	55

LIST OF TABLES

Table 1.	Characteristics of sands	8
Table 2.	Pump characteristics	28
Table 3.	Summary of runs	31
Table 4.	Summary results for run 1	38
Table 6.	Summary results for run 3	56
Table 7.	Data summary for all runs	57

LIST OF PICTURES

Picture 1.	Example of kinetic energy of rolling particles	4
Picture 2.	Coarse sand, fine sand, and sand mixture	9
Picture 3.	Top view of particle segregation	11
Picture 4.	Bottom view of particle segregation	12
Picture 5.	Laminae formation in air	16
Picture 6.	Lamination in air	16
Picture 7.	Thick laminae formation in air	17
Picture 8.	Thick lamination in air	17
Picture 9.	Lamination and segregation in air - lower side	18
Picture 10.	Lamination and segregation in air - upper side	18
Picture 11.	Lamination in fresh water	20
Picture 12.	Lamination in salt water - 35 mg/ℓ NaCl concentration	20
Picture 13.	Lamination in salt water - 350 mg/ℓ NaCl concentration	21
Picture 14.	Vacuum pressure gage	23
Picture 15.	Particle segregation near the angle of repose	23
Picture 16.	Lamination in vacuum at -560 mm of Hg	24
Picture 17.	Vacuum settling at -560 mm of Hg - clear lamination	25
Picture 18.	The 4 ft-wide flume	30
Picture 19.	Details of the downstream end of the flume	30
Picture 20.	Longitudinal view of step 1-U1	34
Picture 21.	Longitudinal view of step 1-U2	35
Picture 22.	Longitudinal view of step 1-U3	36
Picture 23.	Longitudinal view of step 1-U4	37
Picture 24.	Longitudinal view of step 2-U2	40
Picture 25.	Longitudinal view of step 2-U3	41
Picture 26.	Longitudinal view of step 2-D1	42
Picture 27.	Longitudinal view of step 2-D2	44
Picture 28.	Longitudinal view of step 2-D3	45
Picture 29.	Longitudinal view of step 3-U1	47
Picture 30.	Longitudinal view of step 3-U2	48
Picture 31.	Longitudinal view of step 3-U3	50
Picture 32.	Longitudinal view of step 3-U4	51
Picture 33.	Longitudinal view of step 3-D1	52
Picture 34.	Longitudinal view of step 3-D2	53
Picture 35.	Longitudinal view of step 3-D3	55
Picture 36a.	Time sequence of ripple formation	58
Picture 36b.	Time sequence of ripple formation	58
Picture 36c.	Time sequence of ripple formation	59
Picture 36d.	Time sequence of ripple formation	59
Picture 36e.	Time sequence of ripple formation	60
Picture 37a.	Examples of climbing ripples	61
Picture 37b.	Examples of climbing ripples	61
Picture 37c.	Examples of climbing ripples	62
Picture 38.	Topset and foreset slopes of a dune in formation	63

Picture 39.	Upstream degradation of stratified deposits during dune formation	63
Picture 40.	Example of combined aggradation and degradation during dune formation . . .	64
Picture 41.	Combined aggradation and degradation during dune formation	64
Picture 42.	Typical stratified deposit of a long dune	65
Picture 43.	Typical delta in formation	66
Picture 44.	Coarse particles rolling on top of fine particles on topset slope	67
Picture 45.	Stratified deposit in formation	67
Picture 46a.	Typical dried delta	69
Picture 46b.	Typical dried delta, enlarged view	69
Picture 47.	Top view of a dry delta	70
Picture 48.	Side view of a dry delta	70
Picture 49.	Cross-section of a dry delta	71
Picture 50.	Enlarged cross-section of a dry delta	71

LIST OF SYMBOLS

d_s	Diameter of particle
d_{10}	Particle size of which 10% of mixture is finer
d_{25}	Particle size of which 25% of mixture is finer
d_{50}	Particle size of which 50% of mixture is finer
d_{75}	Particle size of which 75% of mixture is finer
d_{90}	Particle size of which 90% of mixture is finer
f	Darcy-Weisbach friction factor
Fr	Froude number
h	Average flow depth
Q	Flow discharge
S_f	Friction slope
U_*	Shear velocity
V_m	Mean velocity
τ_o	Bed shear stress

ACKNOWLEDGEMENTS

Our deepest appreciation goes to M. Guy Berthault for his financial support and great enthusiasm during the review of the experimental results. This program of study has been completed with the thoughtful and dedicated laboratory assistance of Dr. S. Abt, Mr. J. Davis, S. Hogan, J. Burgi and J. Wargadalam. We are grateful to Mrs. Jenifer Davis for upgrading the manuscript and M. Ellis for the specialized photographic services.

1. INTRODUCTION

This experimental study stems from several years of research on stratification at the Hydraulics Laboratory of the Colorado State University Engineering Research Center. Several experimental series have been carried out by Julien and Chen (1989a, 1989b) and Julien and Lan (1989, 1990a). The last experimental report entitled "Laboratory experiments on lamination, stratification and desiccation" by Julien and Lan (1990b) summarizes the laboratory measurements on lamination and stratification of over 12 sand mixtures of particles of different size, density and shape. The conditions under which segregation of sand mixtures occurs were delineated, stratification experiments on at least two sand mixtures provided conclusive evidence that the segregation mechanism causes definite stratification patterns in steady non-uniform flows under a continuous supply of sediment particles. Desiccation experiments with natural sands of Bijou Creek showed definite layering and preferential fracturations of dried sediment deposits. The results of these experiments in a small recirculating flume (15 cm wide, 15 cm deep and 240 cm long) will be published in the Bulletin de la Société Géologique de France in November 1993 (Julien et al. 1993).

The interest in pursuing additional experiments on the topic arises from numerous discussions entertained after the presentation at the 3rd Congrès Français de Sédimentologie in Brest by Berthault et al. (1991). It became apparent that additional laboratory experiments in a large flume with sediment deposits up to 20 cm would enable the simulation of gradual changes in water elevation on sediment deposits. An experimental program simulating cycles of gradual increase and decrease in water depth with time was designed for three bed slope conditions (positive, horizontal and adverse).

Additional considerations were given to the problem of lamination. Since several scientists consider that lamination results from the effects of turbulence on graded sediment mixtures, it has been convened to test whether lamination is possible under vacuum conditions.

This report presents detailed information on the laboratory conditions under which the experiments were carried out. The first part of this report pertains to the experiments on lamination, while the second part outlines the experimental results on stratification in the wide-rectangular recirculating flume.

A video-tape of selected laboratory results entitled "Fundamental Experiments on Stratification" has been prepared as a dynamic documentary supplement to the photographs presented herein.

2. EXPERIMENTS ON SEGREGATION AND LAMINATION

2.1 Introduction

The reader is referred to Julien and Lan (1990) for a detailed literature review on lamination. Recent hypotheses include: 1) Bridge and Best (1988) "it appears that laminae can be formed by both the migration of low-relief bedwaves and the turbulent bursting process"; 2) Paola, Wiele and Reinhart (1989) "Extremely low amplitude bedforms...Initial deposition from small scale turbulent fluctuations in shear stress followed by sieving out mechanism resulting in a smooth surface process termed glazing"; and 3) Julien and Lan (1990) "the lamination process involves the motion of a layer of heterogeneous sediments. Through lateral movement, the finer particles fall within the interstices of the rolling coarser particles. The coarse particles then roll on top of the fines and microscale separation of the particles is then obtained." Lamination therefore seems limited to three processes: bedforms, turbulence and/or segregation.

Besides the thorough investigation of Julien and Lan (1990), the results of complementary experiments are presented herein to examine whether bedforms and turbulence play a significant role. The segregation experiment from earlier studies have been repeated to show the same particle segregation characteristics of heterogeneous sand mixtures under lateral motion. The analysis first focused on seeking a physical explanation of the segregation mechanism.

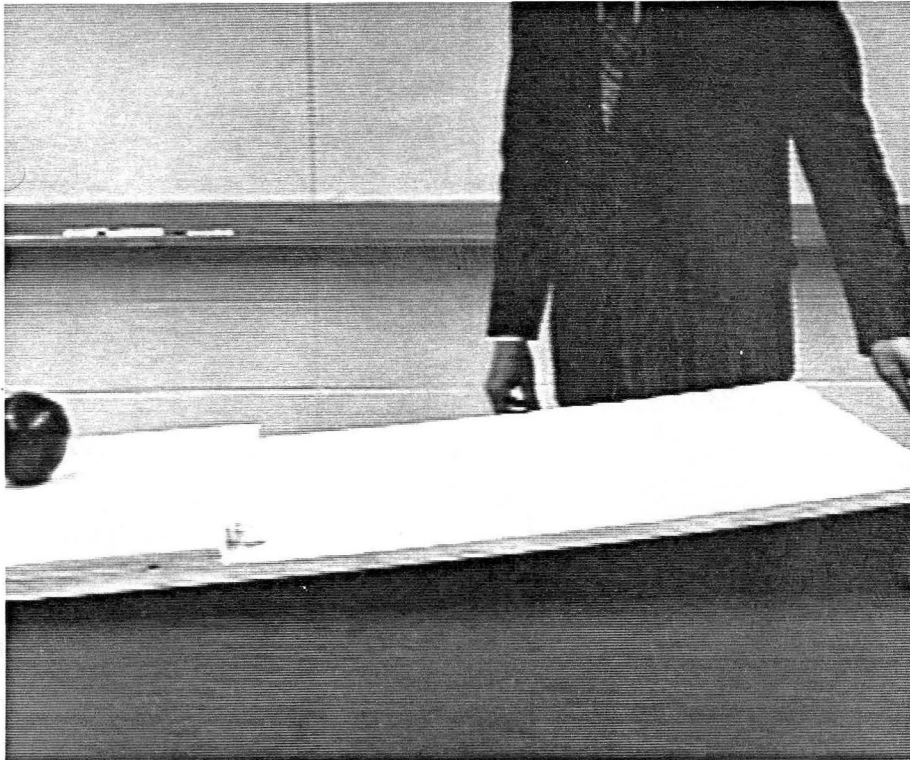
The physical process of segregation can be explained with reference to the kinetic energy of rolling particles on a plane surface. When a sphere of radius r and mass m rolls on a horizontal surface at an angular velocity w and translation velocity V , the moment of inertia of the solid sphere is $I = \frac{2}{5} m r^2$ and the kinetic energy E of the falling sphere is given by

$$E = \frac{1}{2}mV^2 + \frac{1}{2}I\omega^2 \quad (1)$$

for these conditions $V=r\omega$, on obtains

$$E = \frac{7}{10}m\omega^2r^2 = \frac{7}{10}mV^2 \quad (2)$$

This indicates that the kinetic energy of a rolling sphere increases with mass m and the square of the velocity V . At a given rolling velocity, the kinetic energy increases directly with the particle mass, thus for solid particles of constant mass density, coarse particles have a higher kinetic energy than fine particles. This explains the greater mobility of coarse particles in heterogeneous mixtures. Picture 1) illustrates this phenomenon, in front of surface irregularities, the coarse particle in black keeps rolling while the small particle in white stops in front of the obstacle.



Picture 1. Example of kinetic energy of rolling particles

2.2 Segregation Experiments

2.2.1 Sediment mixture

Two types of sands were mixed to obtain a single sediment mixture for the experiments. The first type is coded as ERC#6 which is a white fine sand with median diameter $d_{50}=0.2$ mm. The visual observations indicated that ERC#6 is rounded in shape. Settling in the air showed that the angle of repose for the ERC#6 is 35.5° . Figure 1 shows the grain size distribution of this sand.

The second type is a black coarse sand coded as B2040 with median grain diameter $d_{50}=0.6$ mm. The visual observations of this sand indicated that this sand has an angular shape. Settling in air showed that the angle of repose is equal to 39.5° . Figure 2 shows the grain size distribution for the B2040. Table 1 outlines the characteristics of the fine sand ERC#6 and the coarse sand B2040 including d_{10} , d_{25} , d_{50} , d_{75} , d_{90} .

For the whole set of experiments, a mixture of fine and coarse sand was prepared and well mixed with a proportion of 50/50 by volume. By using two different colors, shapes and densities, it was possible to observe particle movement and the formation and characteristics of laminated and stratified sand deposits. Figure 3 shows the grain size distribution of the mixture and Picture 2) shows ERC#6, B2040 and the sand mixture.

2.2.2 Experimental setup and procedures

The equipment used for this segregation experiment was a simple plexiglass plate. The transparent plate as shown in Figure 4 measures 30 cm length, 25 cm width and 1 cm deep so that the sand mixture can move freely onto this plate.

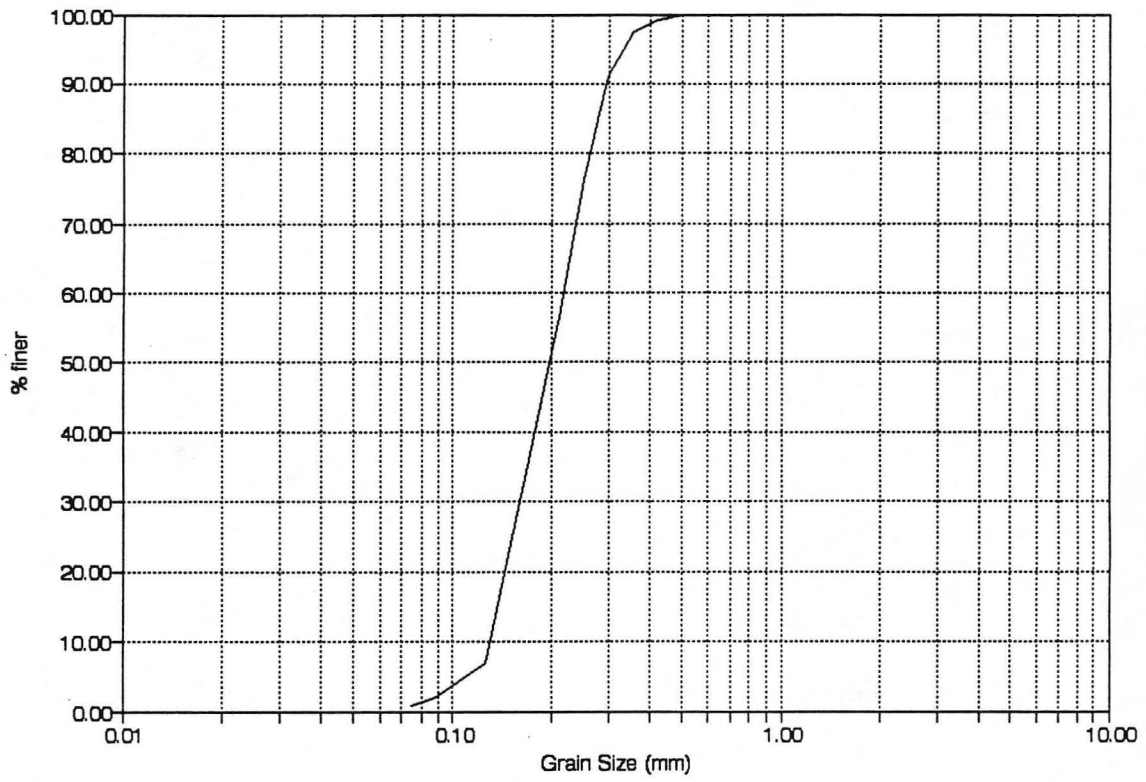


Figure 1. Sieve analysis for the white sand

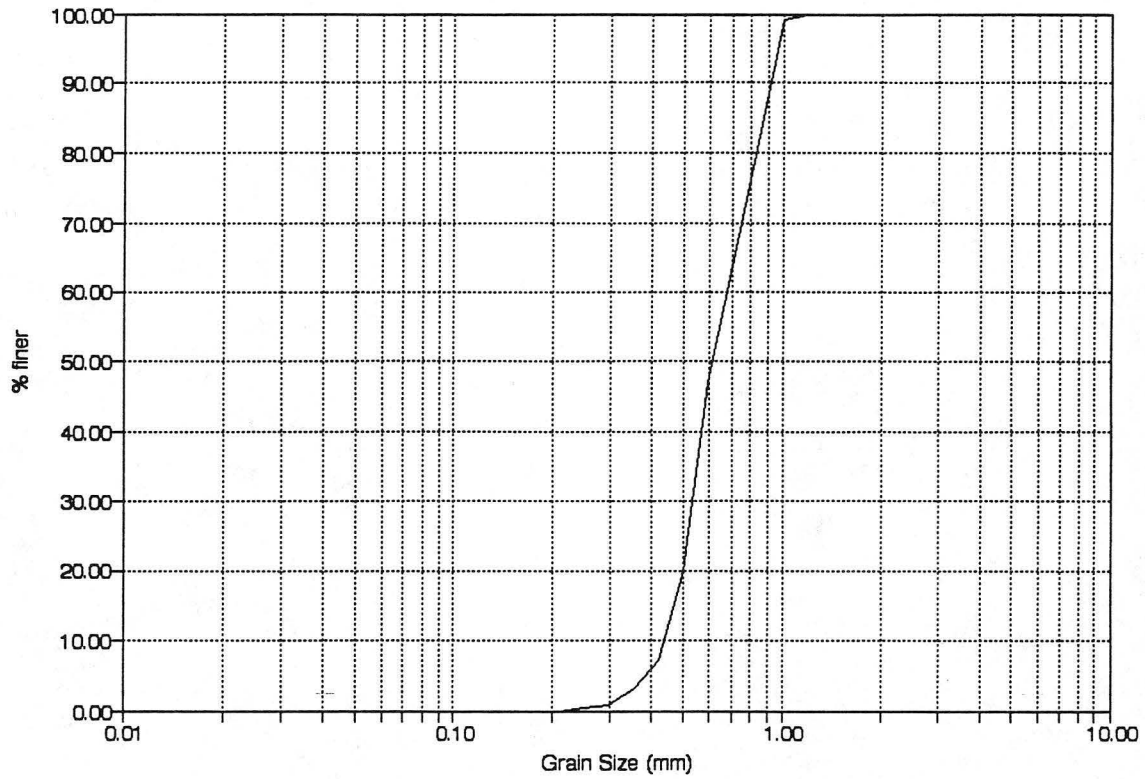


Figure 2. Sieve analysis for the black sand

Table 1. Characteristics of sands

Sand	Color	Density	Angle of repose in air	Angularity	D ₁₀ mm	D ₂₅ mm	D ₅₀ mm	D ₇₅ mm	D ₉₀ mm
B2040	Black	2.7	39.5°	Angular	0.45	0.52	0.6	0.8	0.9
ERC#6	White	2.5	35.5°	Rounded	0.15	0.16	0.2	0.25	0.29

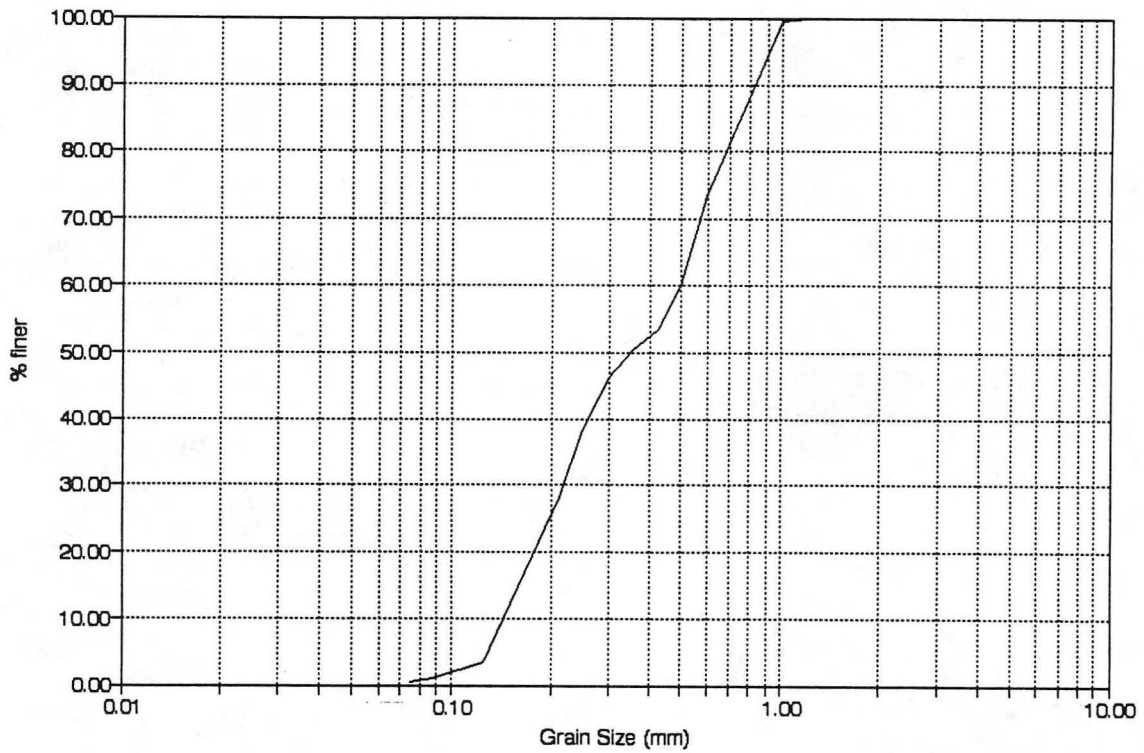
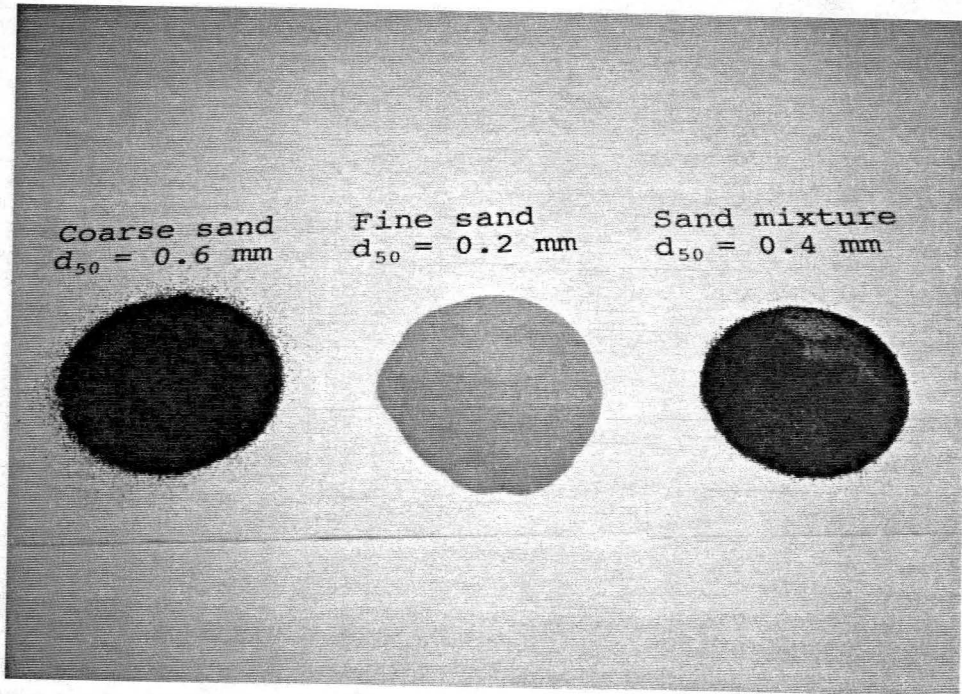
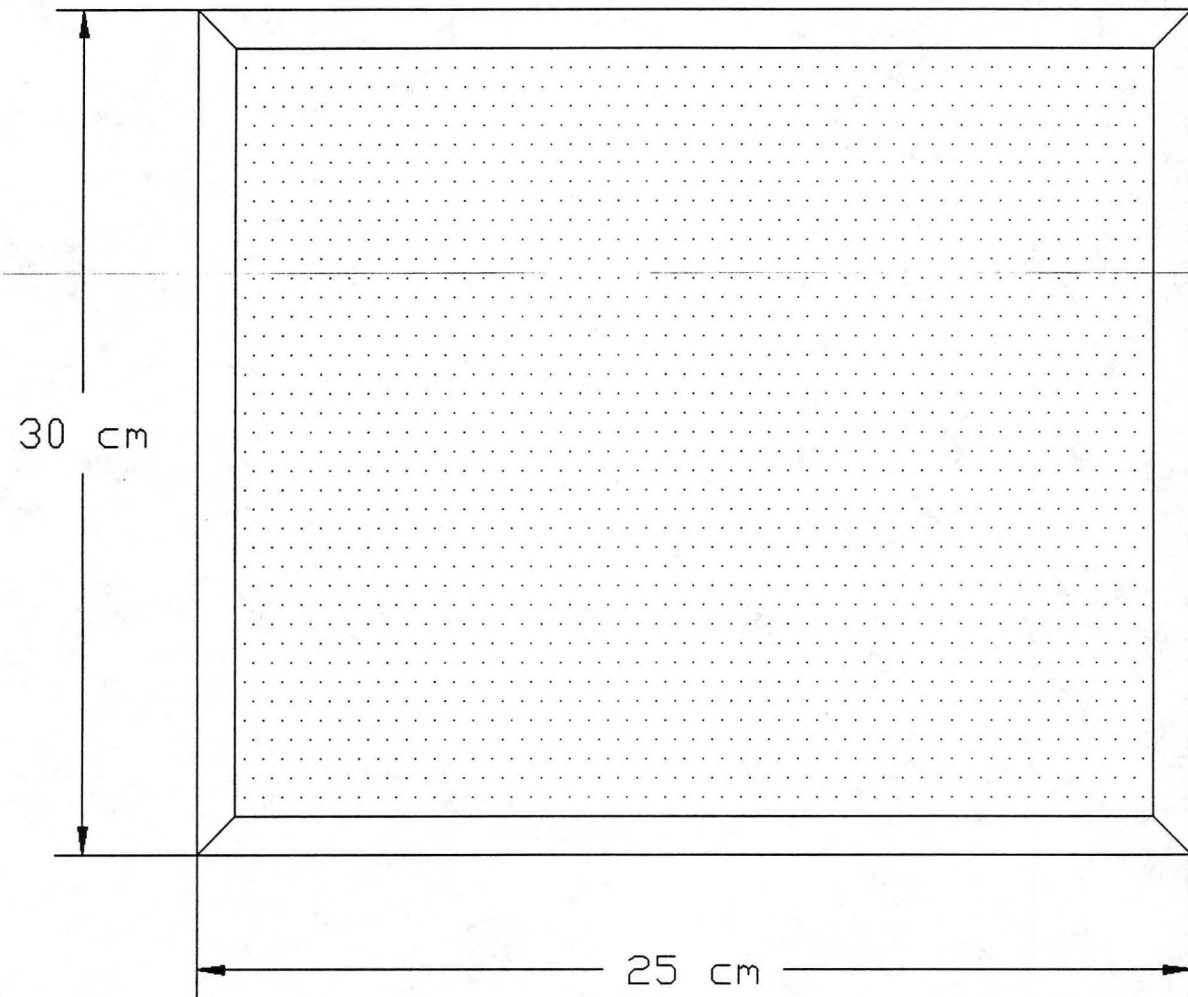


Figure 3. Sieve analysis for the sand mixture



Picture 2. Coarse sand, fine sand, and sand mixture



The plexiglas plate
Figure (4)

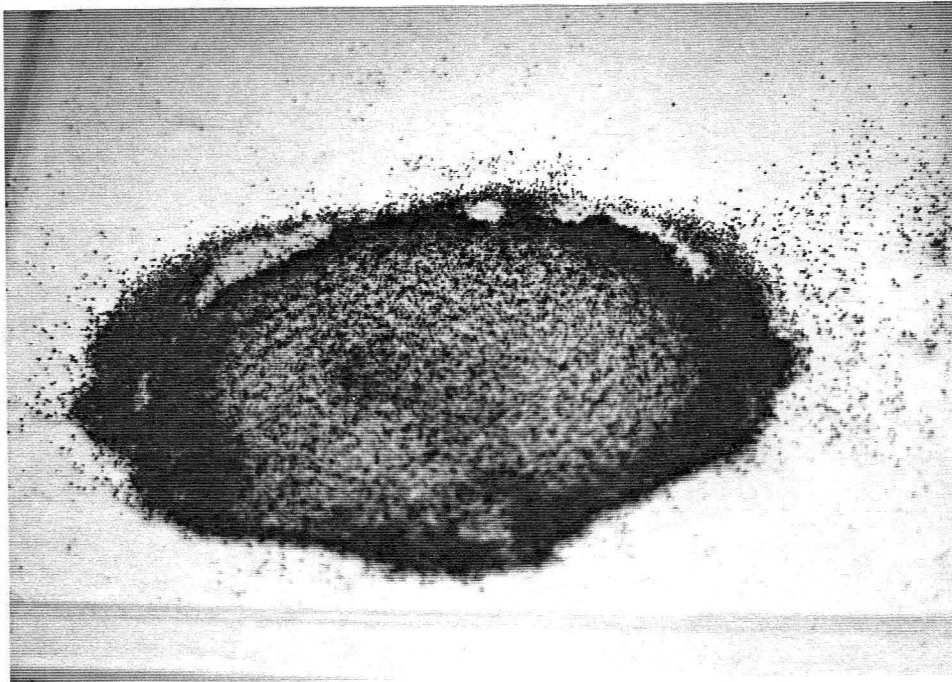
Figure 4. The plexiglas plate

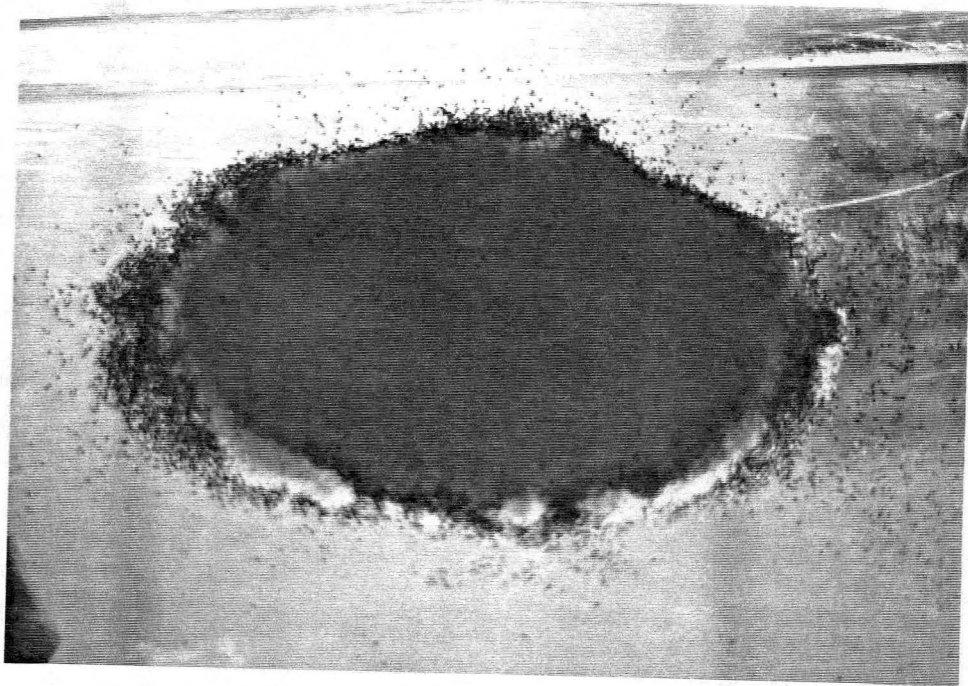
The mixture previously prepared from the black coarse sand and the white fine sand was used in this experiment. About 250 cm^3 volume of this sand mixture is poured onto the plexiglass plate. The plate is set in a horizontal position on a table. The plexiglass plate was then gently shaken laterally on the table. A layer of coarse sand particles appears on top of fine white particles within a few seconds.

2.2.3 Results

As the result of lateral motion, it was possible to observe a layer of black coarse particles on top. By looking underneath, through the plexiglass, a white layer of fine sand could be seen clearly. Through lateral motion of the plexiglas plate on a horizontal plane, segregation of coarse and fine particles occurs and the coarse particles roll on top of fine particles. Picture 3 shows the top of the plate where black particles cover the surface. Picture 4 shows the bottom of the plate covered with white particles.

The segregation process is limited to the change in kinetic energy of coarse particles confers them an increased mobility viewed as an ability to roll on top of finer particles.





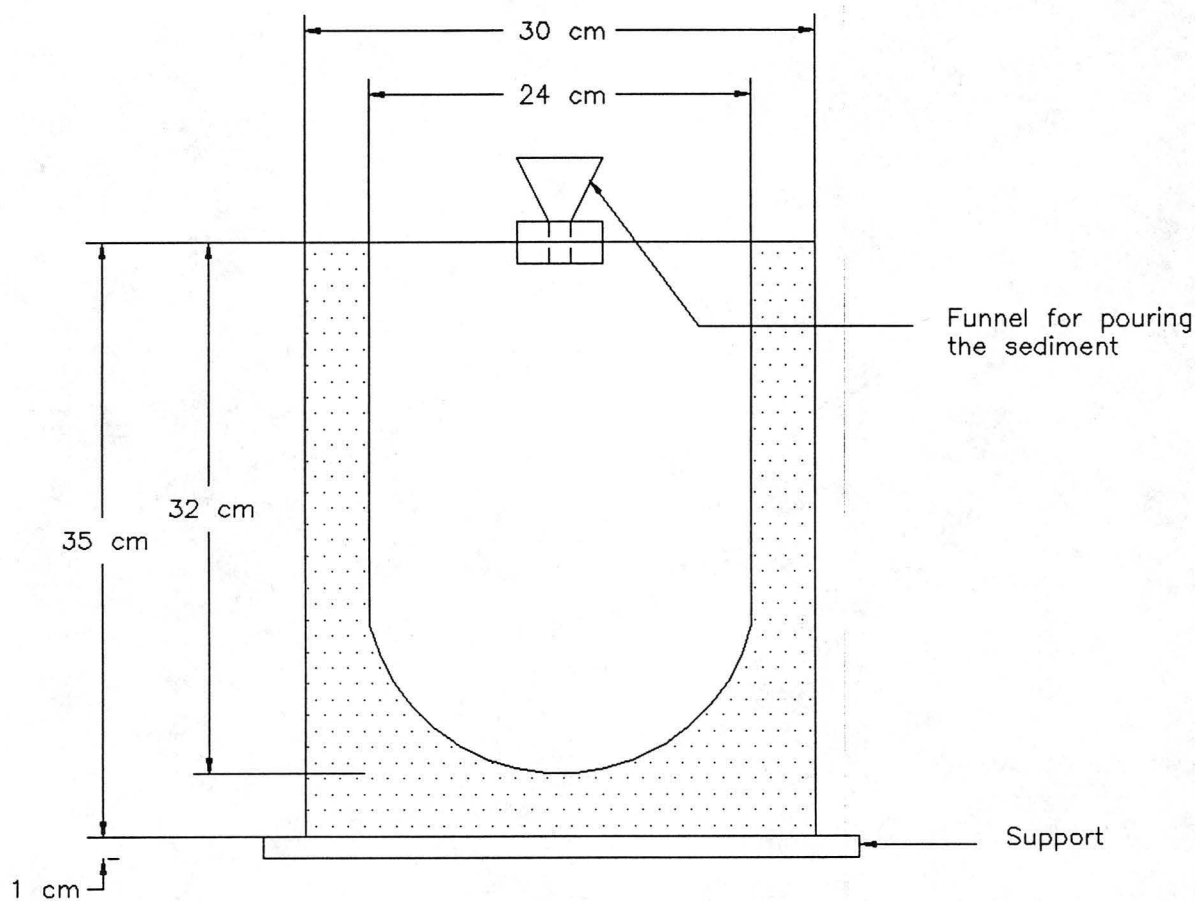
Picture 4. Bottom view of particle segregation

2.3 Lamination Experiments

2.3.1 Experimental set up

For these experiments, two special settling tubes were designed and assembled to test settling in air, fresh and salt water and in vacuum.

Figure 5 shows a graphic presentation for the first experimental set up used for testing settling in air and water. The first apparatus is a simple U-shaped plexiglass container with rectangular outside dimensions as shown on Figure 5. Inside, the container has a U shape with height equal to 32 cm and width equal to 24 cm. The inside thickness of the container is equal to 1 cm, in order to visualize the internal structure of the deposit under two-dimensional settling. A plastic funnel is held fixed on top of the container by a removable plexiglass support.



The second set apparatus has been specifically designed for testing settling in vacuum. This plexiglas vacuum settling tube is symmetric in shape about its horizontal axis as shown on Figure 6. It has a rectangular outer dimensions. Inside this container, an orifice separates two funneled chambers. The base width of the chambers is 24 cm, which gradually decreases to 0.3 cm at the orifice. The upper chamber is connected to a 1.16 hp vacuum pump.

Five settling experiments were conducted using both settling tubes and the above-mentioned sediment mixture: 1) vertical settling in air; 2) tilted settling in air; 3) settling in fresh water, 4) settling in salt water, and 5) settling in vacuum. The experimental results are documented in the subsections 2.3.2 and 2.3.6 respectively.

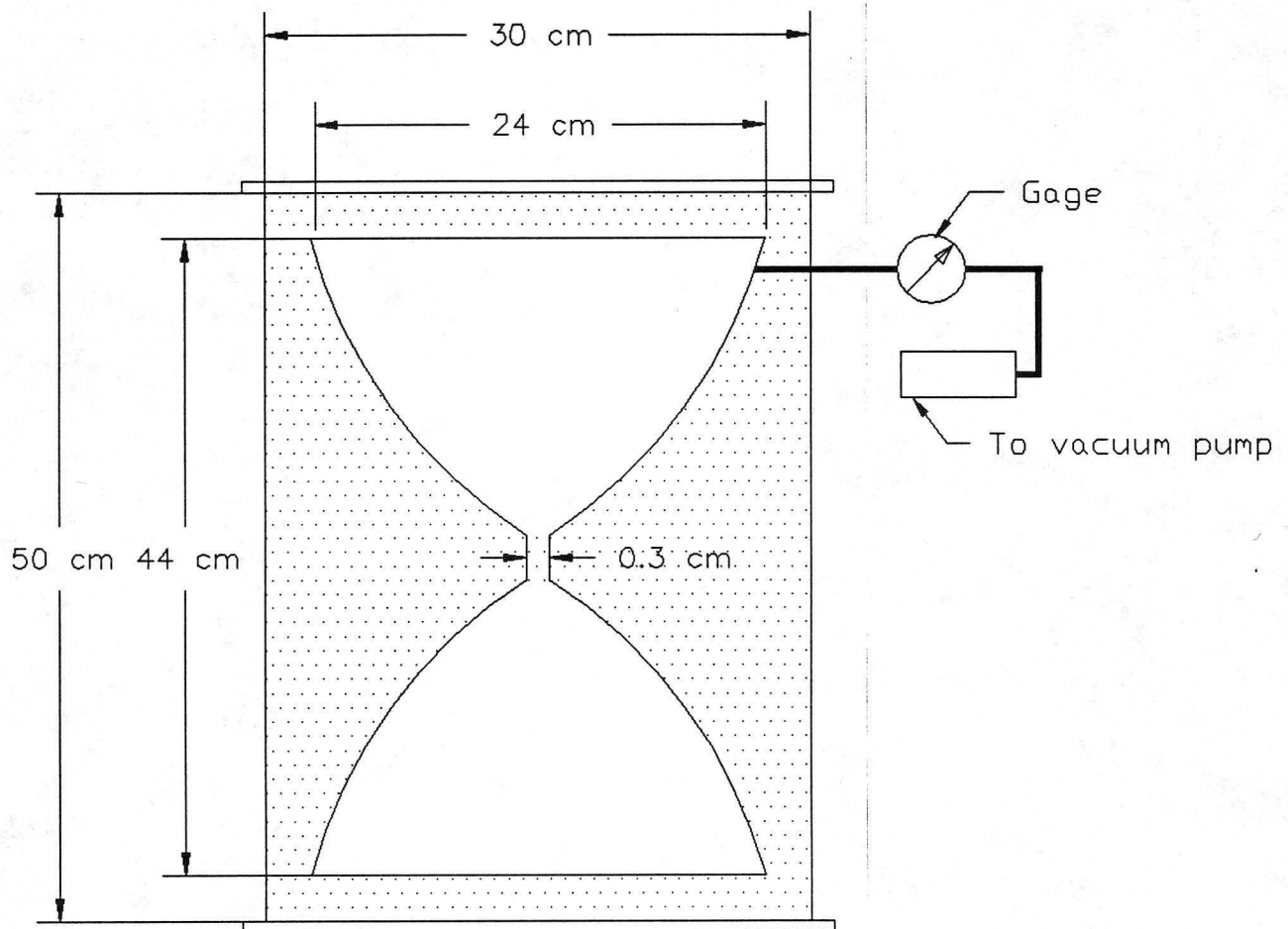


Figure 6. Vacuum settling tube

2.3.2 Settling in air at horizontal position

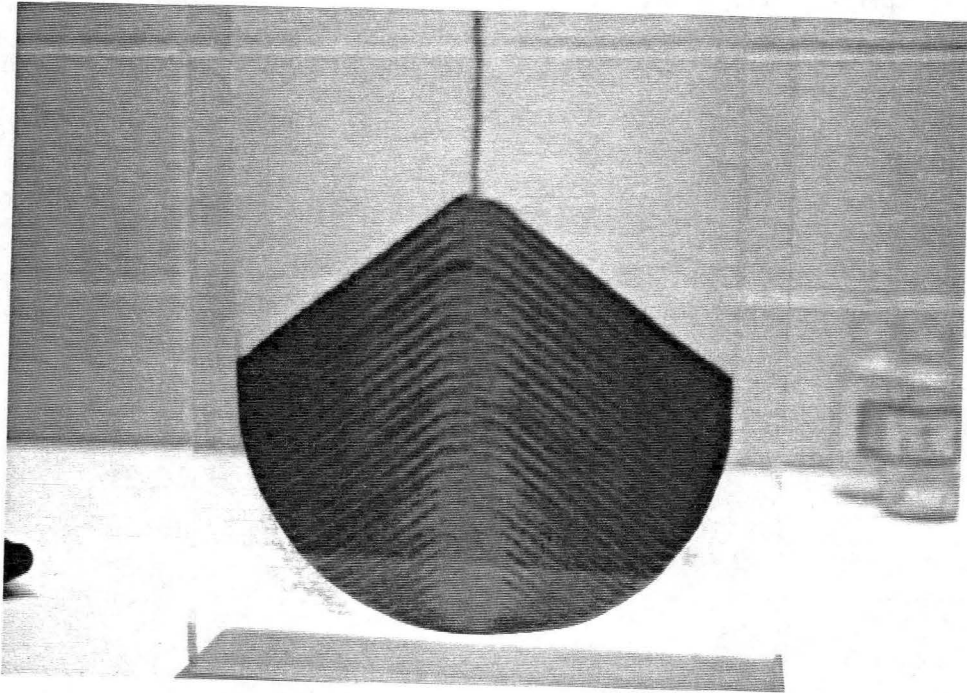
The U-tube is used for this settling experiment. The apparatus is held stationary on a horizontal plane for vertical settling inside the U-tube. The mixture is poured gently onto the funnel at a rate of $3.78 \text{ cm}^3/\text{sec}$.

While pouring the mixture, laminae formation could not clearly be seen at large falling heights because of the splash induced by impacting particles. Over time, the falling height decreases and laminae started to form as can be seen on Picture 5. Laminae could be seen clearly through the plexiglas sides of the settling tube. The laminae thickness of the black coarse sand reduces gradually toward the center of the container as shown in Picture 6. Conversely, the laminae thickness of the fine white sand gradually decreases toward the lower parts of the slide, as a result of rolling of coarse particles over fine particles. The segregation mechanism is explained in Section 2.2. The formation of thick laminae was possible from vertical settling in air as shown on Picture 7 and 8.

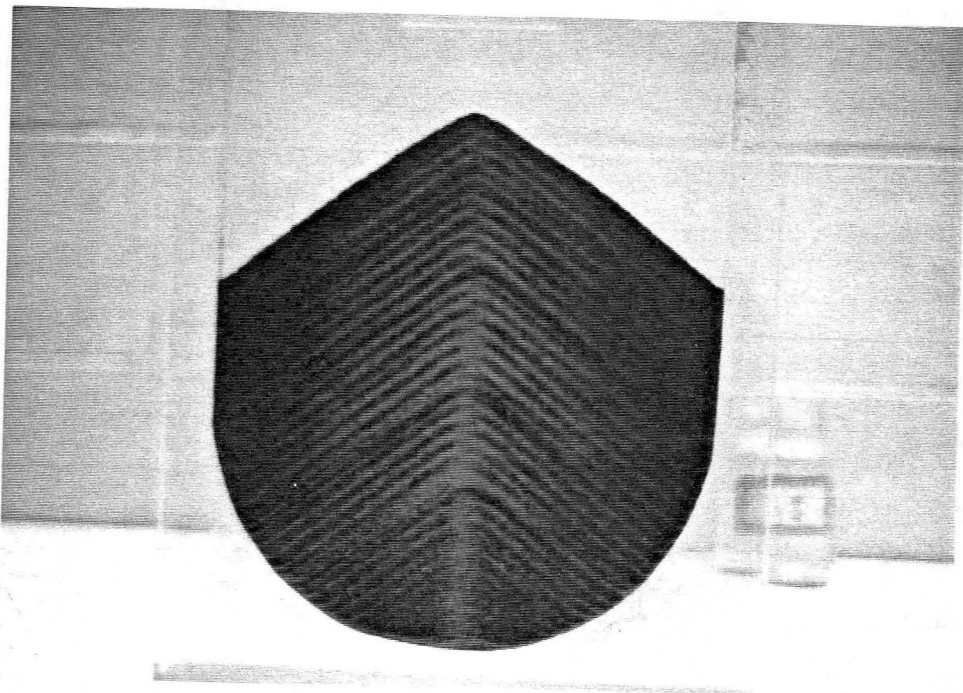
2.3.3 Lamination and Segregation in air

The previous procedures were repeated with the same U-shaped settling tube. But, instead of vertical settling, tilted settling is induced by tilting the settling tube at an inclination with the vertical approaching 30° . The mixture is poured onto the funnel at the same feeding rate of $3.78 \text{ cm}^3/\text{sec}$.

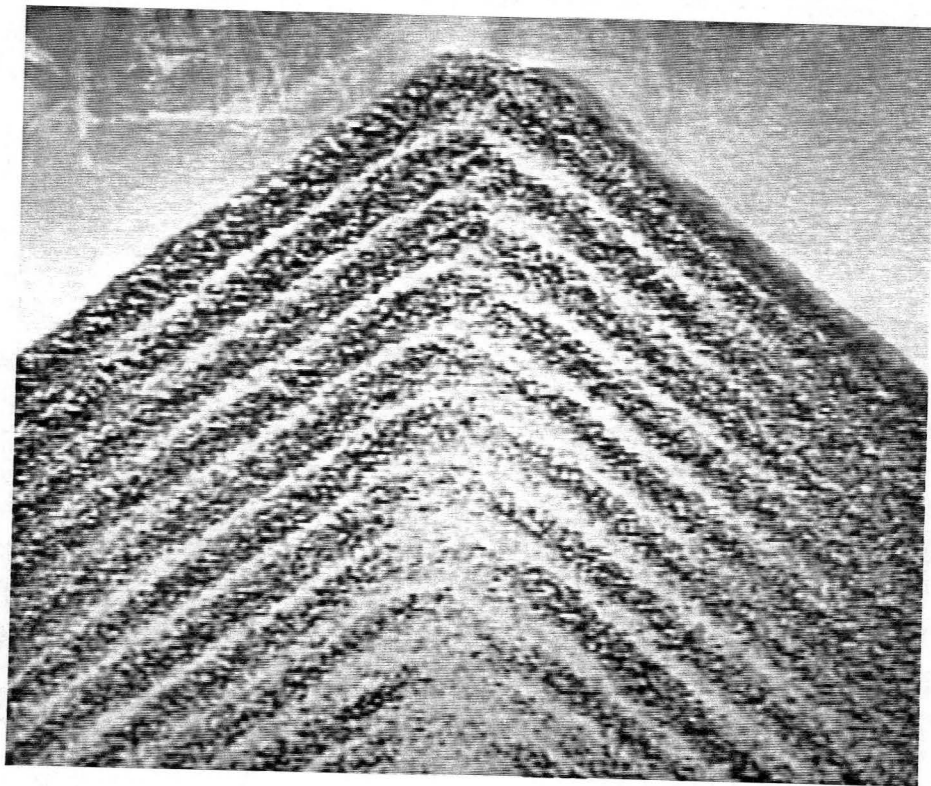
As the mixture is poured into the U-shaped settling tube, the fine white particles segregate and accumulate near the lower side wall of the settling tube while the coarse black particles move over the fine layer. At the end of the pouring process, a clear preferential accumulation of white particles can be seen on the lower side (Picture 9), while coarse black particles accumulated on the upper side as shown on Picture 10.



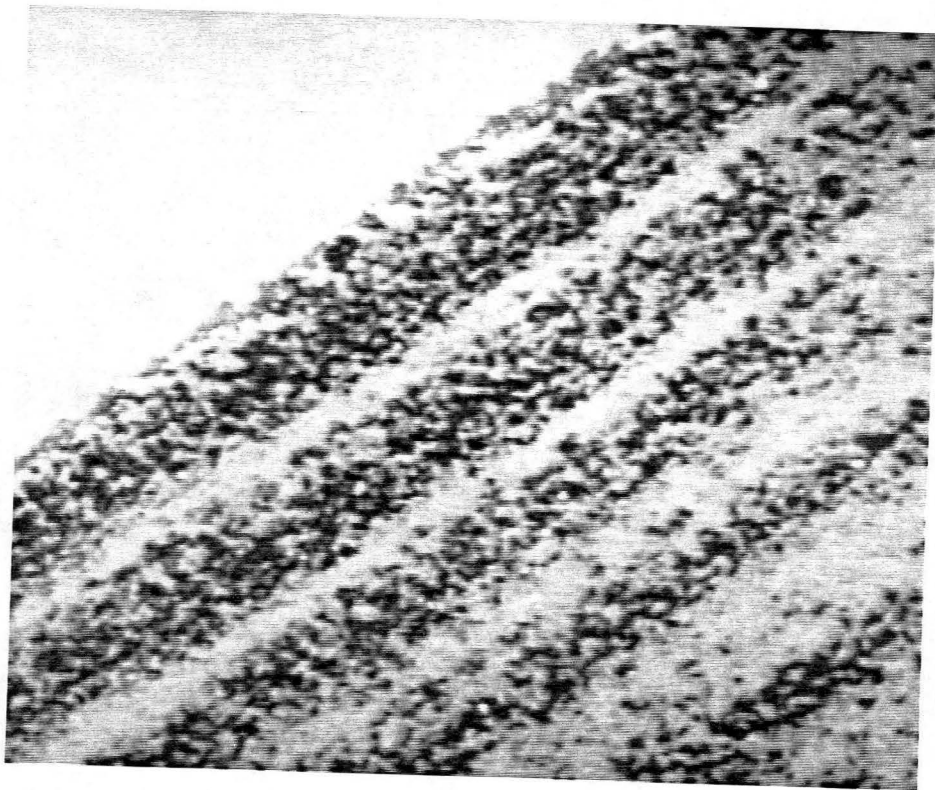
Picture 5. Laminae formation in air



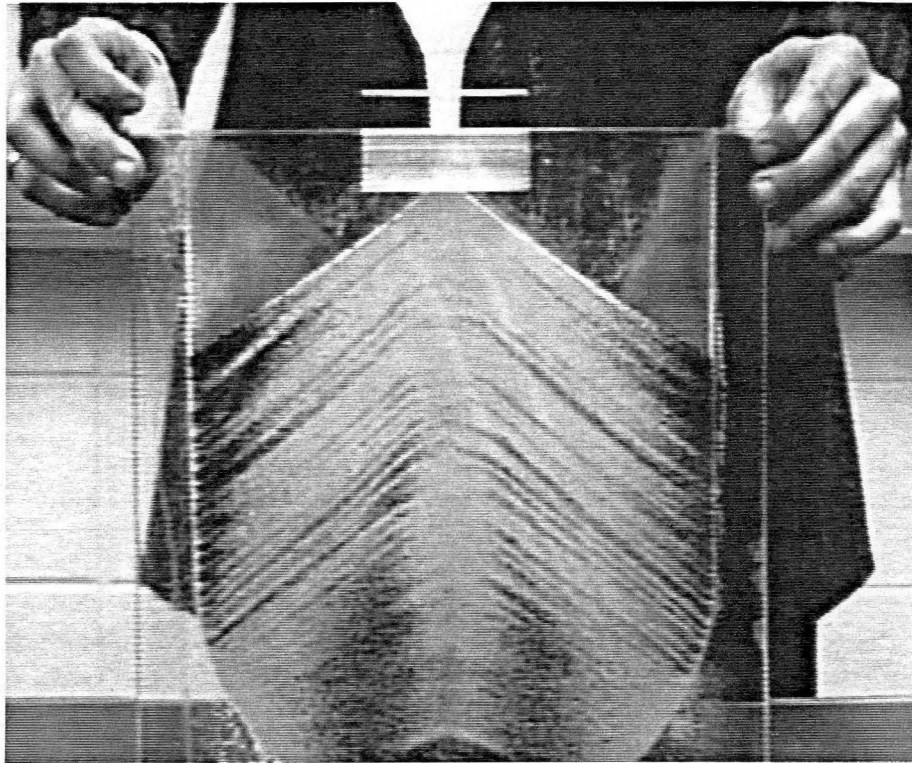
Picture 6. Lamination in air



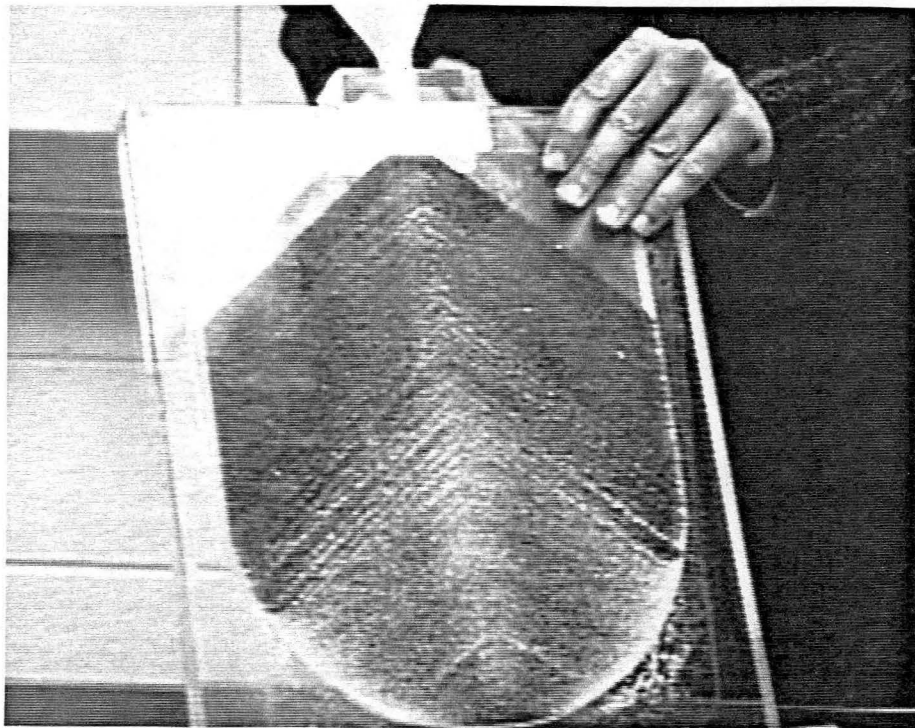
Picture 7. Thick laminae formation in air



Picture 8. Thick lamination in air



Picture 9. Lamination and segregation in air - lower side



Picture 10. Lamination and segregation in air - upper side

2.3.4 Lamination in fresh water

In this experiment, the U-shaped settling tube is used for settling in fresh water. But, in this case the container was half filled with water prior to the experiment. The sediment mixture is poured at a rate of $3.78 \text{ cm}^3/\text{s}$.

While pouring the sediment, fine sands remained in suspension in the water, thus inducing preferential settling of the fines, near the sides of the settling tube. The settling velocity and the angle of repose of the mixture are less under water than in air. But, lamination still could be observed in the U-shaped settling tube shown on Picture 11.

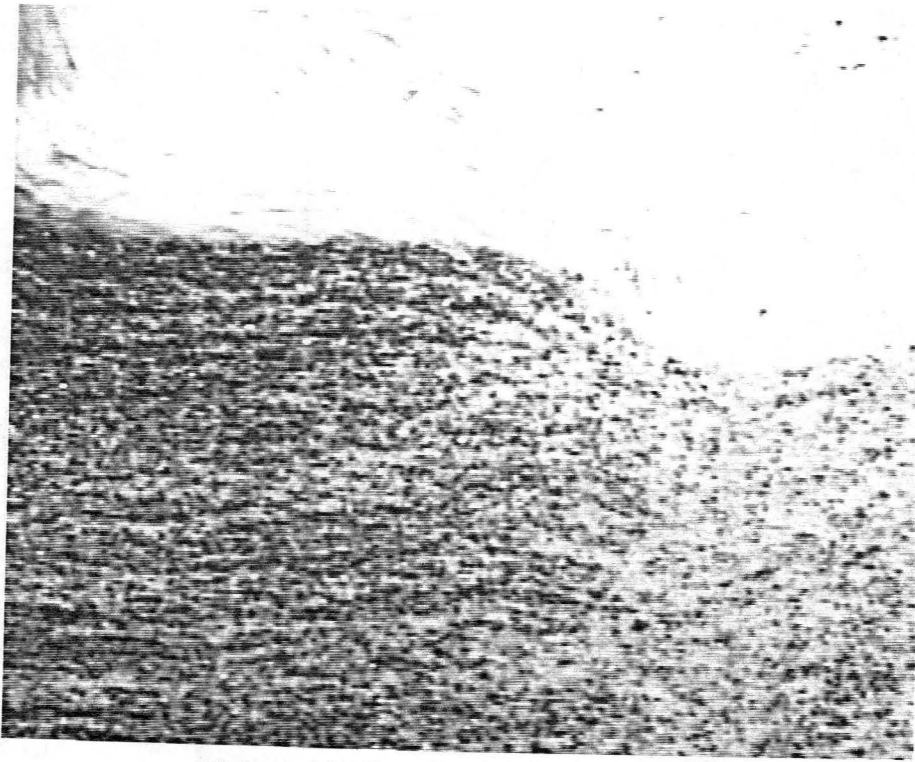
2.3.5 Lamination in salt water

The same procedures are repeated herein in the salt (NaCl) water at a concentration of 35 g/l and near salt saturation at 350 g/l.

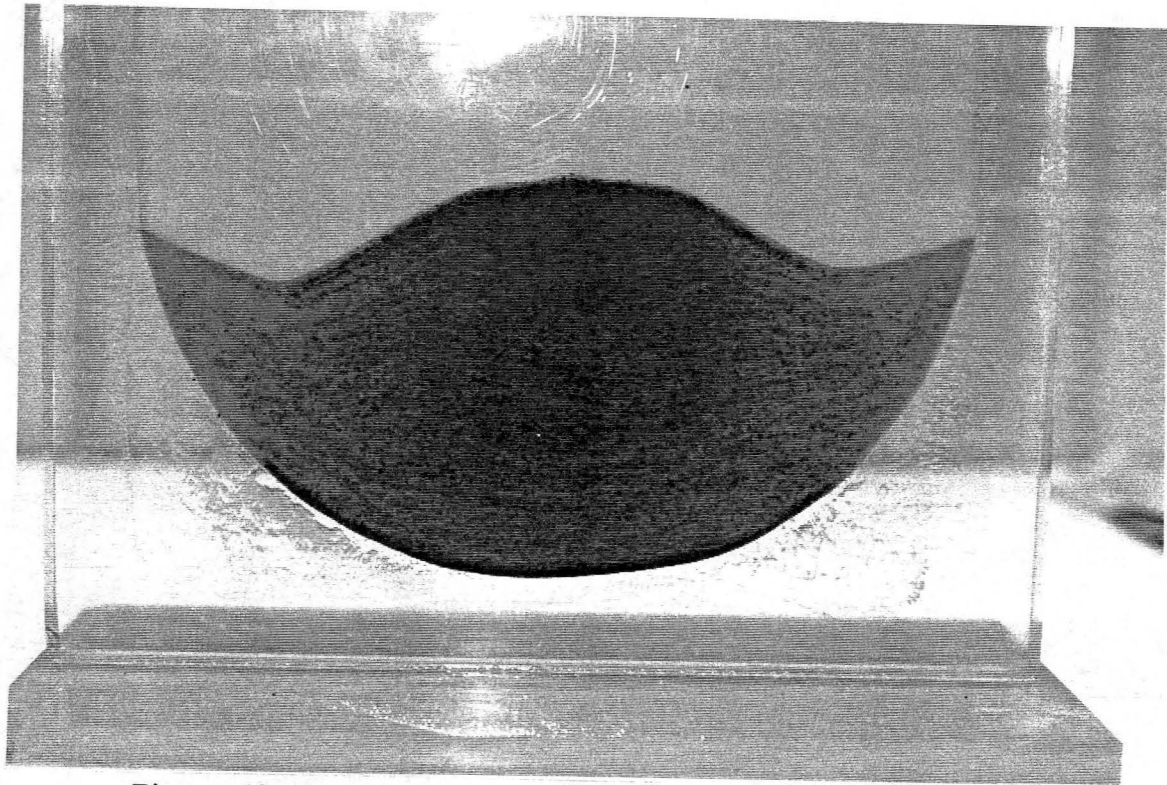
Despite changes in mass density from fresh water to salt water, no major differences in laminae formation were observed. Pictures 12 and 13 show the formation of laminae in the salt water at these two concentration.

2.3.6 Lamination in vacuum

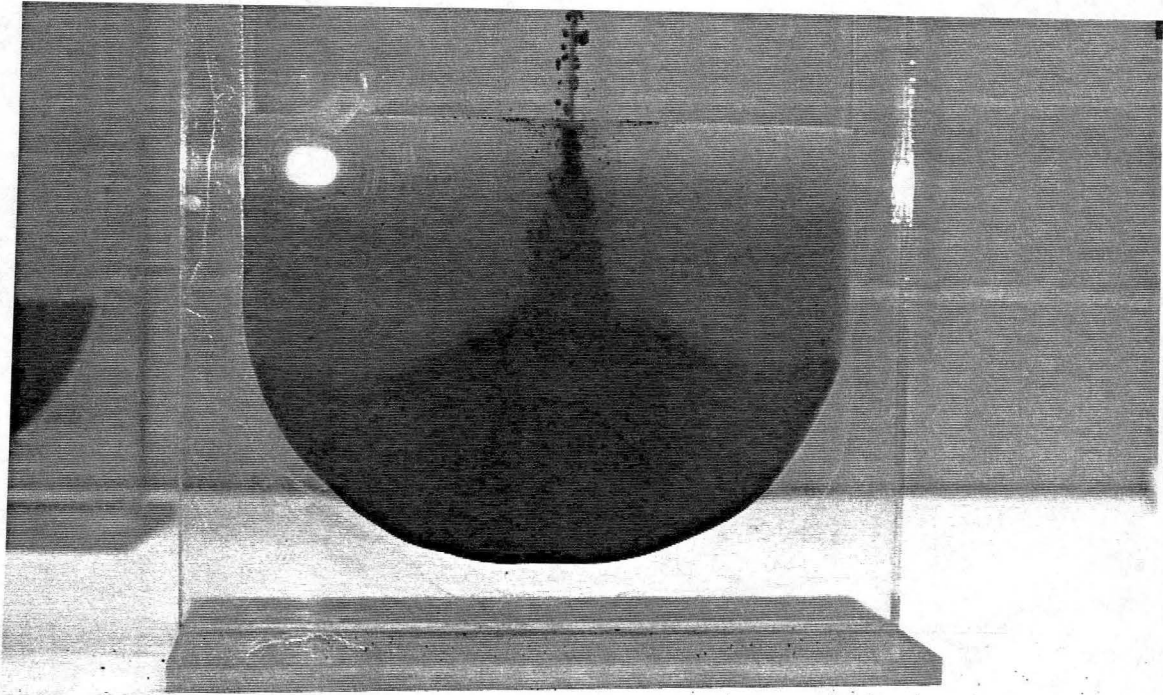
The previously mentioned vacuum settling tube was used for this experiment. The container was positioned down on a horizontal plane. The upper chamber was connected to a vacuum pump through a plastic tube, a pressure gage and a valve were mounted on the tube line. The valve was opened and the vacuum pump was actioned to pump the air outside of the vacuum settling tube. During the experiment, the pressure was maintained at -560 mm of Hg (or -22 in of Hg), which is 0.29 atmosphere. The valve was then closed and the vacuum pump was switched off, thus maintaining a constant vacuum at -560 mm of Hg within the settling tube during the experiment.



Picture 11. Lamination in fresh water



Picture 12. Lamination in salt water - 35 mg/l NaCl concentration

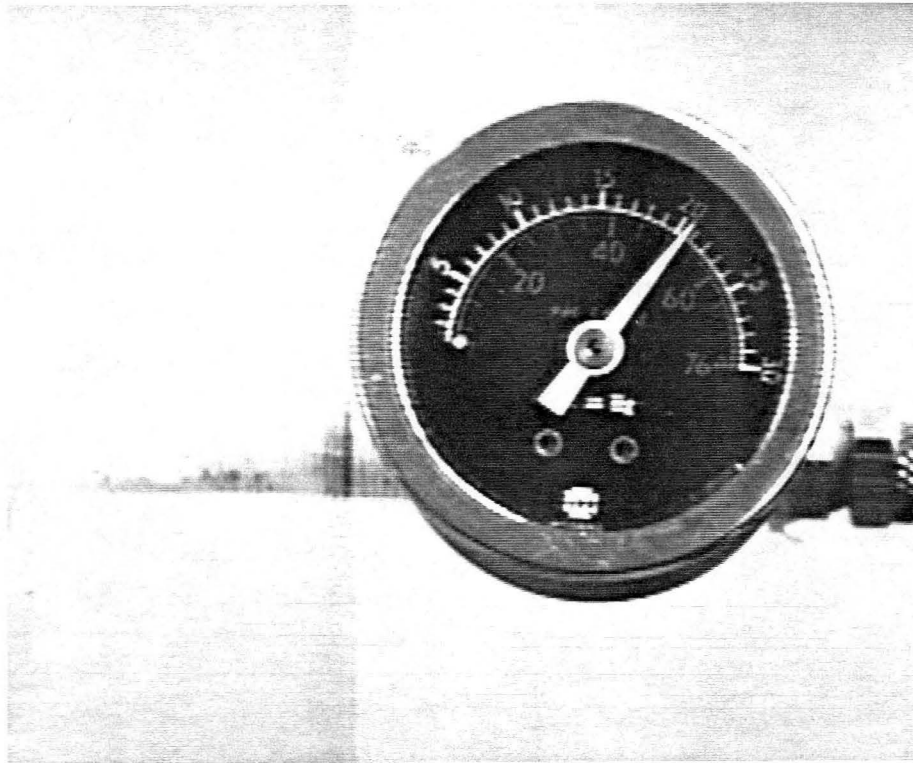


Picture 13. Lamination in salt water - 350 mg/l NaCl concentration

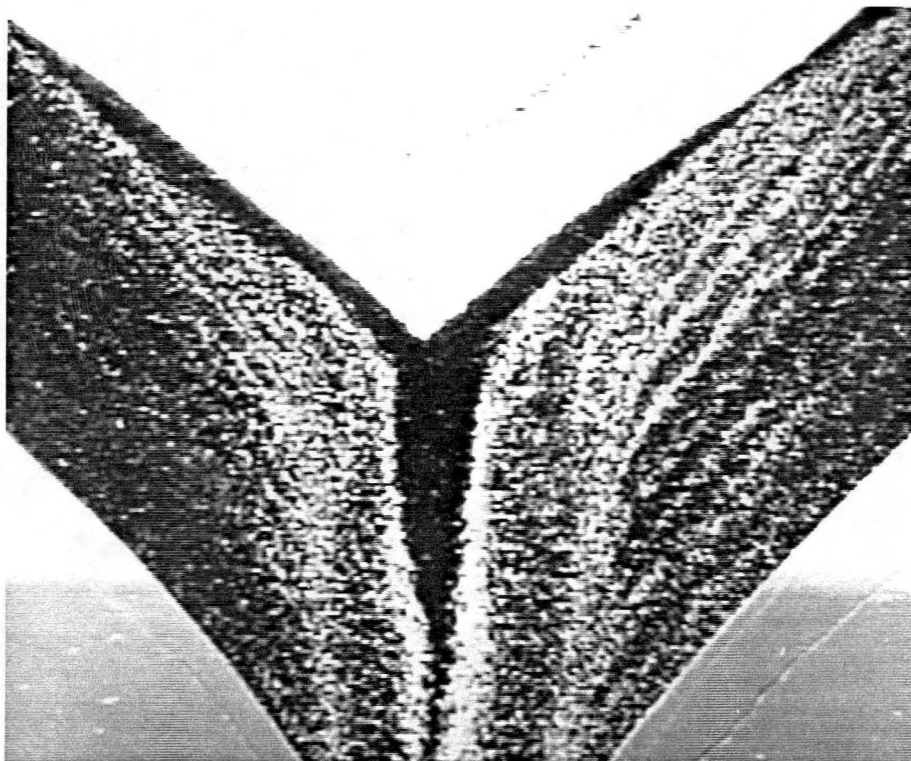
To start the experiment, the container was turned upside down, allowing the mixture to pass through the orifice and settle in the lower chamber. The feeding rate controlled by the orifice opening between the two chambers was fixed at a rate of $3.25 \text{ cm}^3/\text{sec}$. The vacuum pressure gage at the end of the experiment shown on Picture 14 shows that the pressure remained close to -560 mm of Hg during the experiment.

The first interesting feature is the observation of the segregation process in the upper chamber at the angle of repose of the sediment mixture, as shown on Picture 15. This demonstrates that the particle segregation process can take place not only on horizontal surfaces, but on surface angles up to the angle of repose (exceeding 35° with the horizontal).

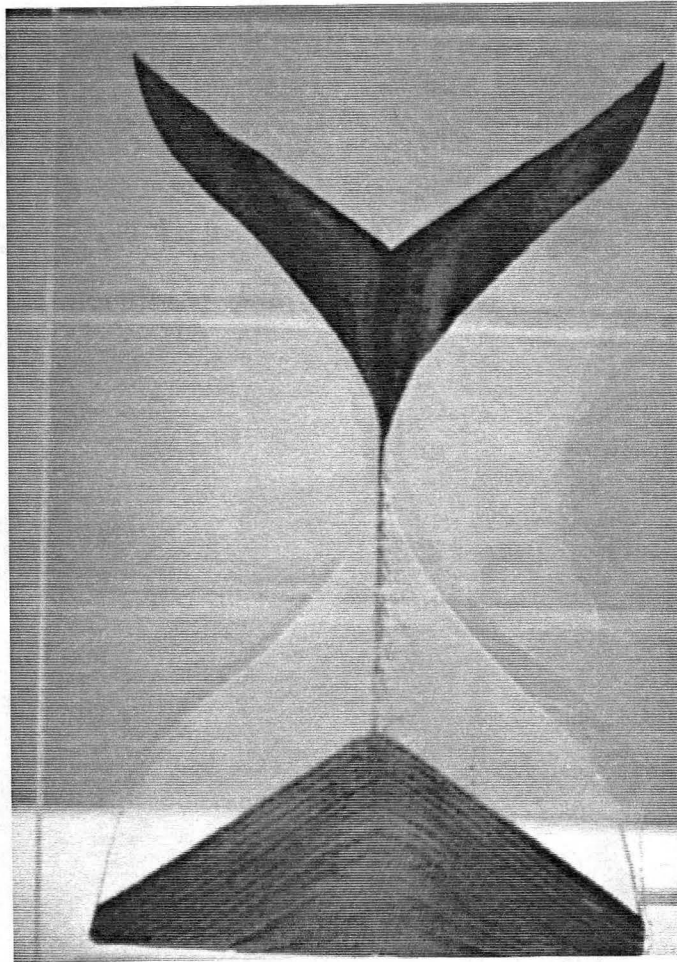
After settling, clear laminae formed under vacuum, as in the air. Pictures 16 and 17 show the laminae formation during the experiment at a vacuum pressure of -560 mm of Hg. This experiment demonstrates that lamination is possible without turbulence. The role played by the periodic cycles of turbulence including bursts and sweeps must therefore be discarded.



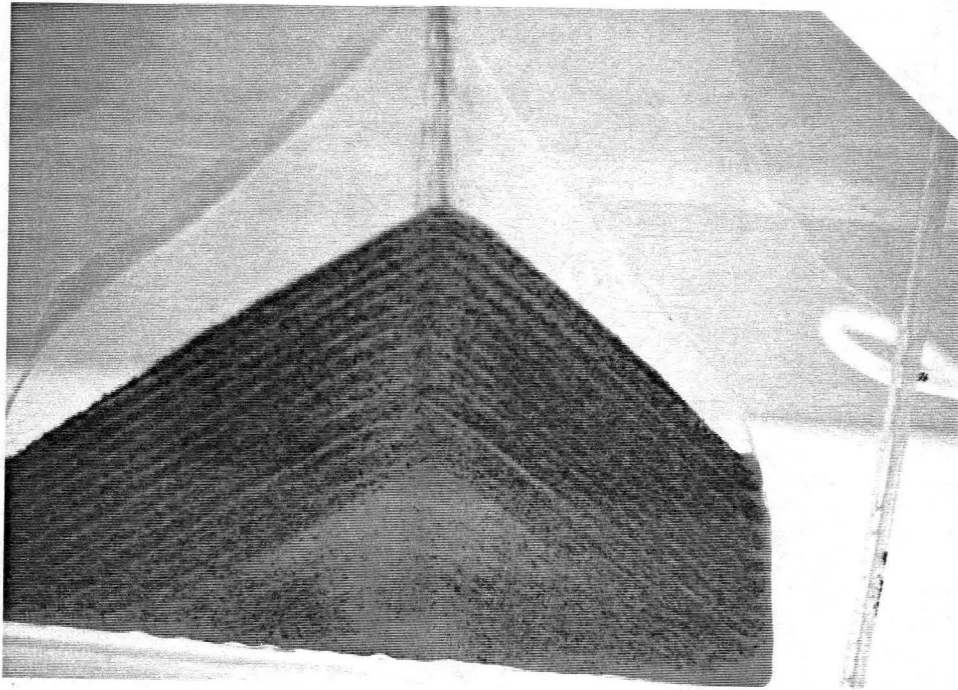
Picture 14. Vacuum pressure gage



Picture 15. Particle segregation near the angle of repose



Picture 16. Lamination in vacuum at -560 mm of Hg



Picture 17. Vacuum settling at -560 mm of Hg - clear lamination

3. EXPERIMENTS ON STRATIFICATION

3.1 Introduction

Large scale stratification experiments were conducted to examine the effect of changing flow depth, while keeping constant discharge and a continuous sediment supply, on the stratification structure of sands.

3.2 Large Laboratory Flume

The experimental work was carried out in a tilting recirculating laboratory flume at the Engineering Research Center of Colorado State University. The flume sketched on Figure 7 can recirculate both water and sediment. The flume is 1.2 m wide, 18 m long and 0.6 m deep. The downstream end of the flume wall is transparent with plexiglas on both sides. The transparent portion of the flume covers 7.2 m with has six windows, each measuring 1.2 m long. In the center of each window, a transparent staff gage is glued to the flume sidewalls for measuring the flow depth and the accumulated sediment depth.

The flume is provided with Pitot tube which is assembled with a point gage on a rolling carriage freely moving on top of the entire flume-length. The Pitot tube is used for measuring the flow velocity at different depths. The Pitot tube is connected to manometers, through which the velocity head could be measured. Then, the velocity in m/s could be calculated by:

$$V = \sqrt{2gh}$$

where, h is the velocity head in m, and g is the gravitational acceleration.

The flume is provided with multi-manometer system through which the water surface slope can be checked and the flow depth measurement as well.

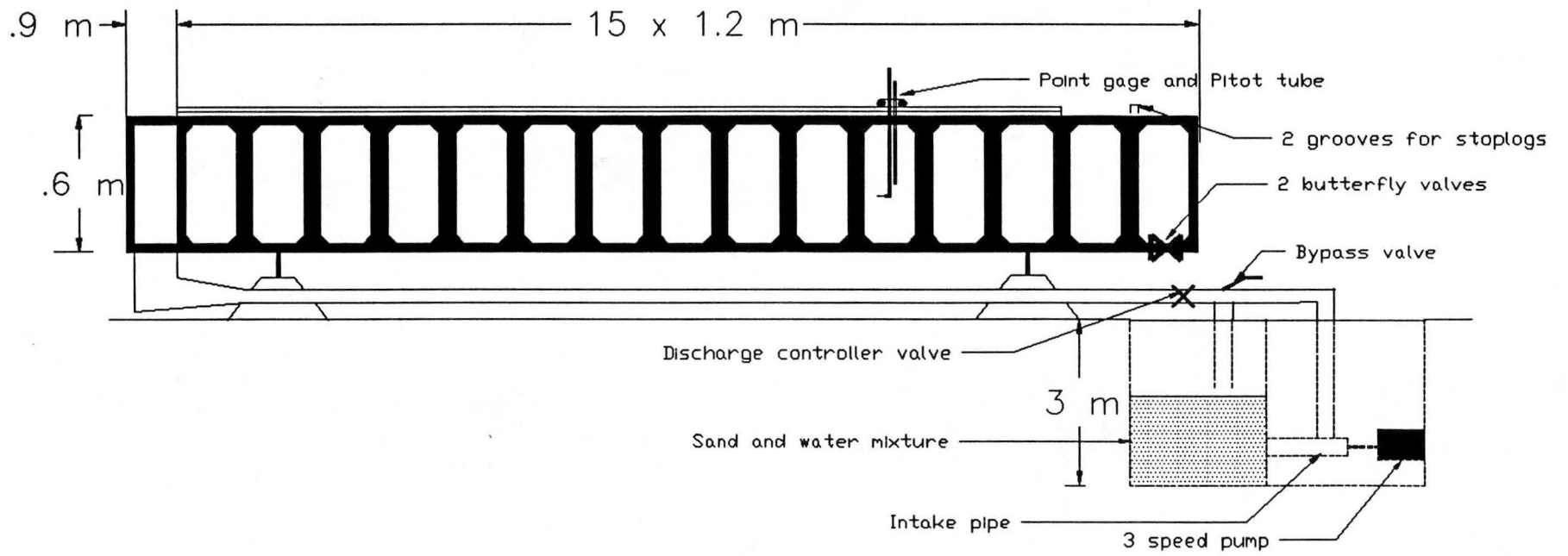


Figure 7. Sketch of the 4 ft-wide flume

Flow discharge could be measured through a Venturi meter. The head difference could be read from the Venturi meter; then, by using calibration chart, the head difference could be transferred into discharge. Unfortunately, clogging of the Venturi meter tubes with fine sand occasionally gave inaccurate discharge measurements. The discharge was also measured using the broad crested weir method at the downstream end of the flume. The discharge measurements were then checked by the mean velocity measurement from the Pitot tube.

A 50 hp pump recirculates the water-sediment mixture. This pump can handle different discharges at different rotational speeds. Table 2 below shows the pump operation power at different speeds:

Table 2. Pump characteristics

Horse Power	r.p.m.	Amps
10	440	31.5
18	586	36.5
40	881	54.6

The flume slope which can be adjusted electrically, has a range of -0.2% to 2.0%. At the far downstream end of the flume, two butterfly valves were fixed on the flume floor, controlled the flume outlet flow. The valves could be adjusted manually to accommodate different flow depths inside the flume.

Near the downstream end of the flume, 2 grooves on the side wall of the flume were used to insert tailgates in order to adjust the flow condition inside the flume. Each tailgate is 3 cm high. The return water falls into a large mixing chamber where the sediment mixture is kept under a high

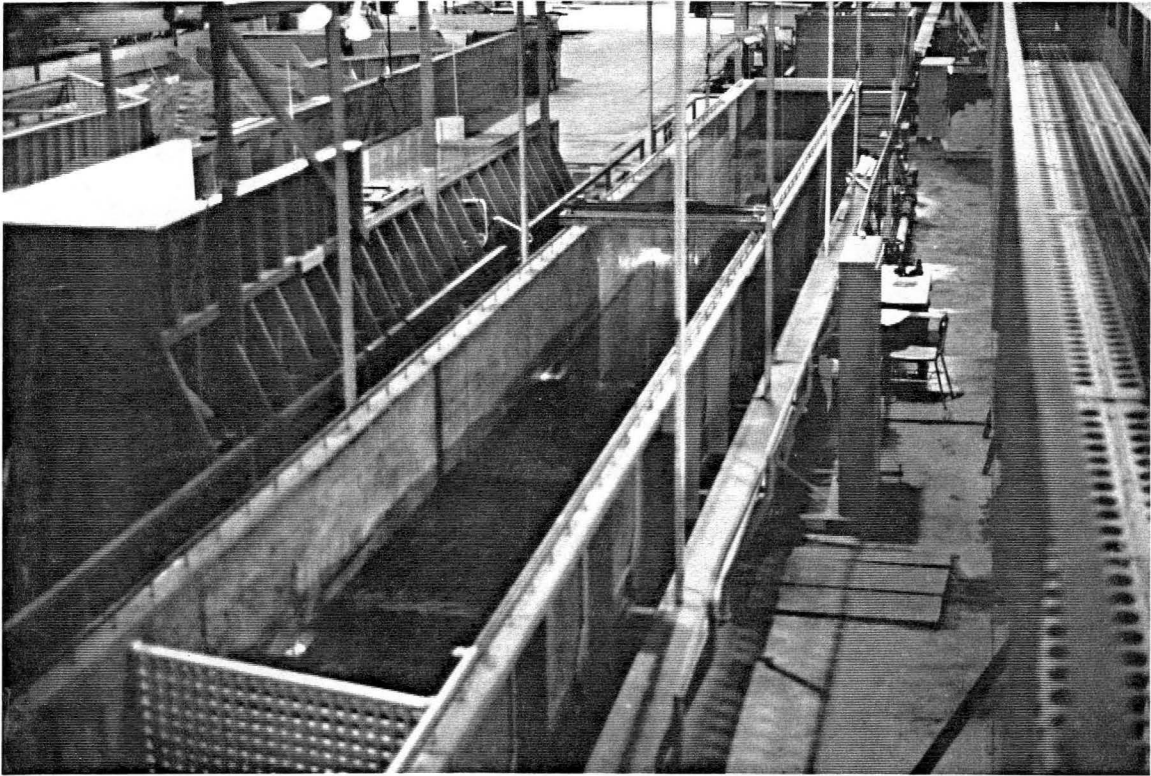
level of turbulence near the pump intake. This set up ensures adequate mixing of the sediment and a continuous supply of sand throughout the entire experiment.

3.3 Flume operation and Procedures

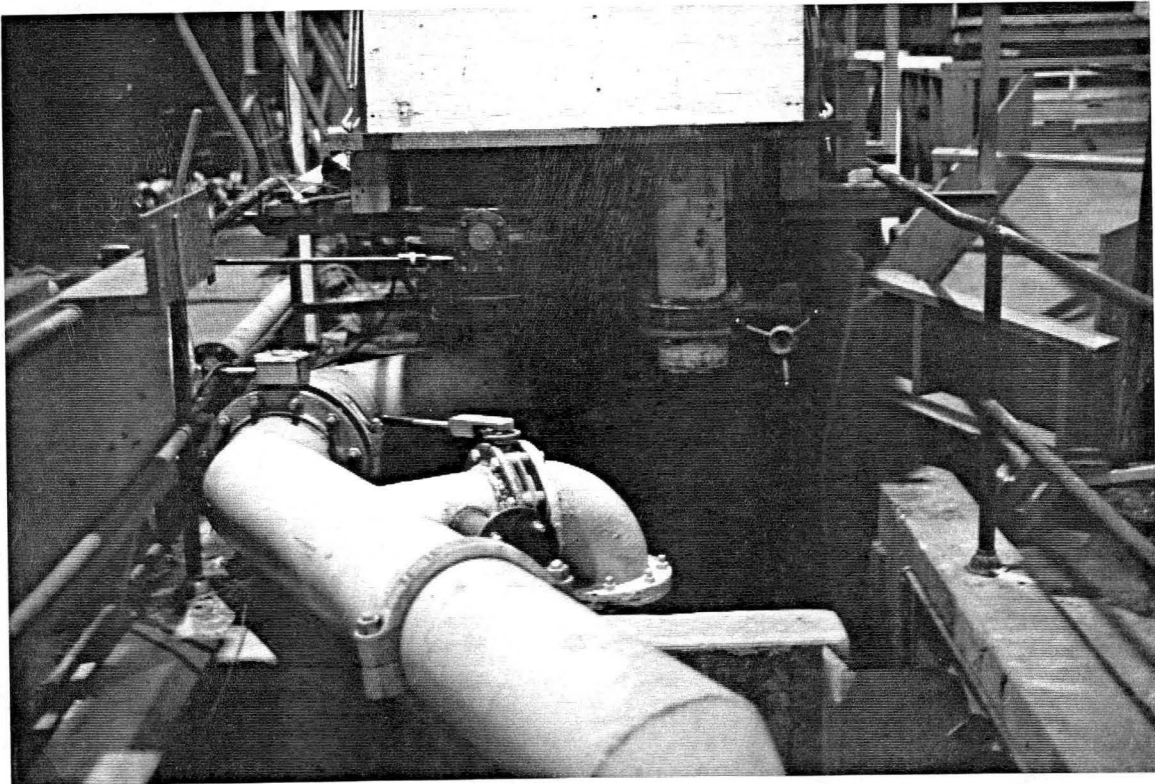
Prior to the experiment, a large volume (about 2.8 m³) of the sediment mixture ERC#6 and B2040 was supplied in the mixing chamber. Clear water was supplied to the mixing chamber from the city facilities.

As the pump is turned on, the by-pass is slightly open to allow a substantial return of water to the mixing chamber to induce turbulent mixing of the sediment. The water and sediment mixture are pumped into the main pipeline underneath the flume to the upstream end of the flume. The high velocities in the pipeline sustains adequate mixing of the sediment. Flow straighteners and wooden wave suppressors are fixed to the upstream end of the flume to reduce the turbulence level and provide uniform upstream flow conditions. The pump speed could be adjusted, typically the medium and high speeds provided the best mixing and overall flow conditions. The discharge could be adjusted through a pipeline valve. The flow depth in the flume was adjusted through the 2 butterfly valves and/or the stop logs. Also the flume slope could be adjusted electrically.

In this experimental program, 3 main sets of runs were performed for: 1) horizontal slope; 2) positive slope; and 3) negative slope. Every set of run is divided into steps either steps U where the stage is going up or steps D where the stage is going down. All runs were performed on a unique sand mixture of fine and coarse sands. Table 3 summarizes the condition under which every set is performed. Notationwise, Step 1-U4 decides the fourth observation with horizontal slope while the water level was rising.



Picture 18. The 4 ft-wide flume



Picture 19. Details of the downstream end of the flume

Table 3. Summary of runs

Run number	Step	Slope	Stage
1	1-U	Horizontal	Up
	1-D	Horizontal	Down
2	2-U	Mild	Up
	2-D	Mild	Down
3	3-U	Adverse	Up
	3-D	Adverse	Down

3.4 Experimental Results

This section presents the results of the experimental work and the calculated parameters. Pictures presenting the runs are also shown in this section. Figure 8 presents a flow chart summarizing the different steps. The following sub-sections summarize the observations;

3.4.1 Horizontal slope run (run 1)

- (1) Objectives of this run: Examining stratification under different flow depths.
- (2) Experimental conditions and data summary:
 - Horizontal flume, $S_f=0$.
 - Sand mixture of $d_{50}=0.4$ mm.
 - Six tail gates (each is 3 cm height)

The following is a summary of the steps:

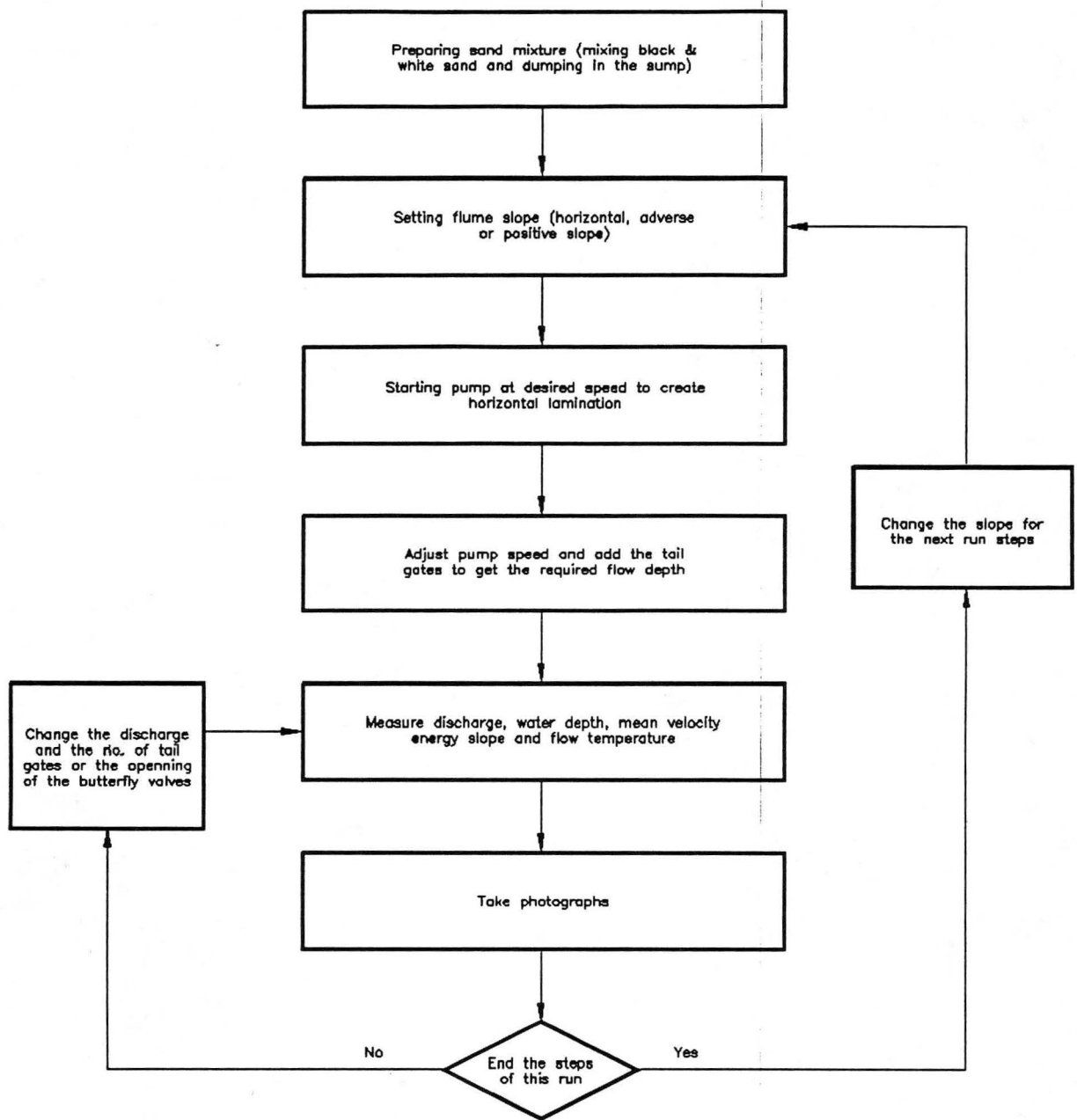


Figure 8. Experimental flowchart

Step 1-U1

This step performed under constant discharge of $0.125 \text{ m}^3/\text{sec}$. Smooth water surface profile and plane bed were observed as shown on Picture 20. The slope of the topset of the delta formation was 1.25%. The bottomset slope of the delta was measured as 0.625%. Figure 9 shows the bed structure at mid point in the flume.

Step 1-U2

Constant discharge $0.125 \text{ m}^3/\text{sec}$. The flow level is increased by closing the butterfly valves. White ripples were observed near the downstream end of the flume. Figure 10 shows that the top layer of the laminae was degraded and the delta was formed on top. Picture 21 shows a longitudinal profile of the flume during this run.

Step 1-U3

The discharge was held constant at $0.125 \text{ m}^3/\text{sec}$. Flow depth is increased by controlling the butterfly valves. Ripples were observed with length equal to 3 cm and height equal to 0.6 cm as shown in Picture 22. Figure 11 shows the sedimentary structure of the bed at mid point. From Figures 9 and 10, it can be seen that ripples replaced the deltaic formation of the previous step as the flow depth was increased.

Step 1-U4

The discharge was $0.125 \text{ m}^3/\text{sec}$. Flow depth was slightly increased by closing the butterfly valves. As the flow depth was increased downstream, ripples of small magnitude started to form as shown on Picture 23 and Figure 12. This implies that a delta essentially replaced the ripples of the previous step.

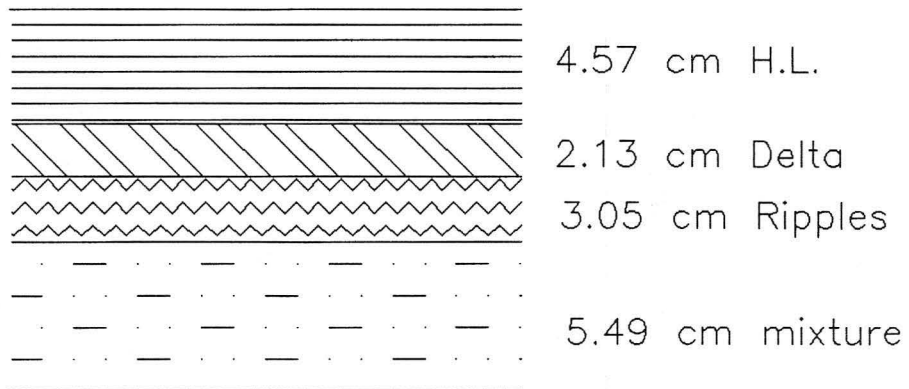
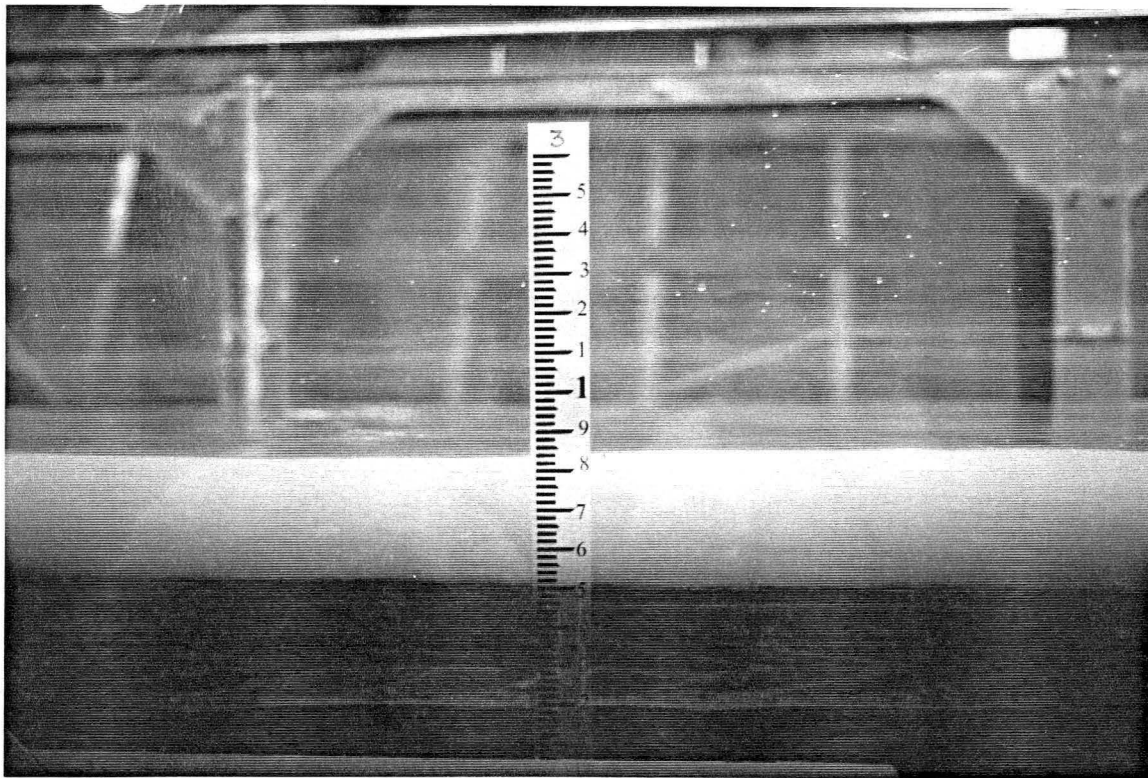


Figure 9. The deposition of step 1-U1



Picture 20. Longitudinal view of step 1-U1

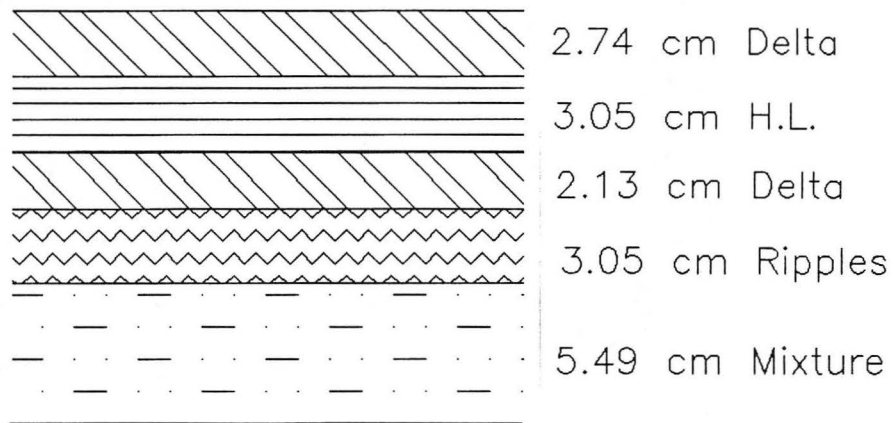
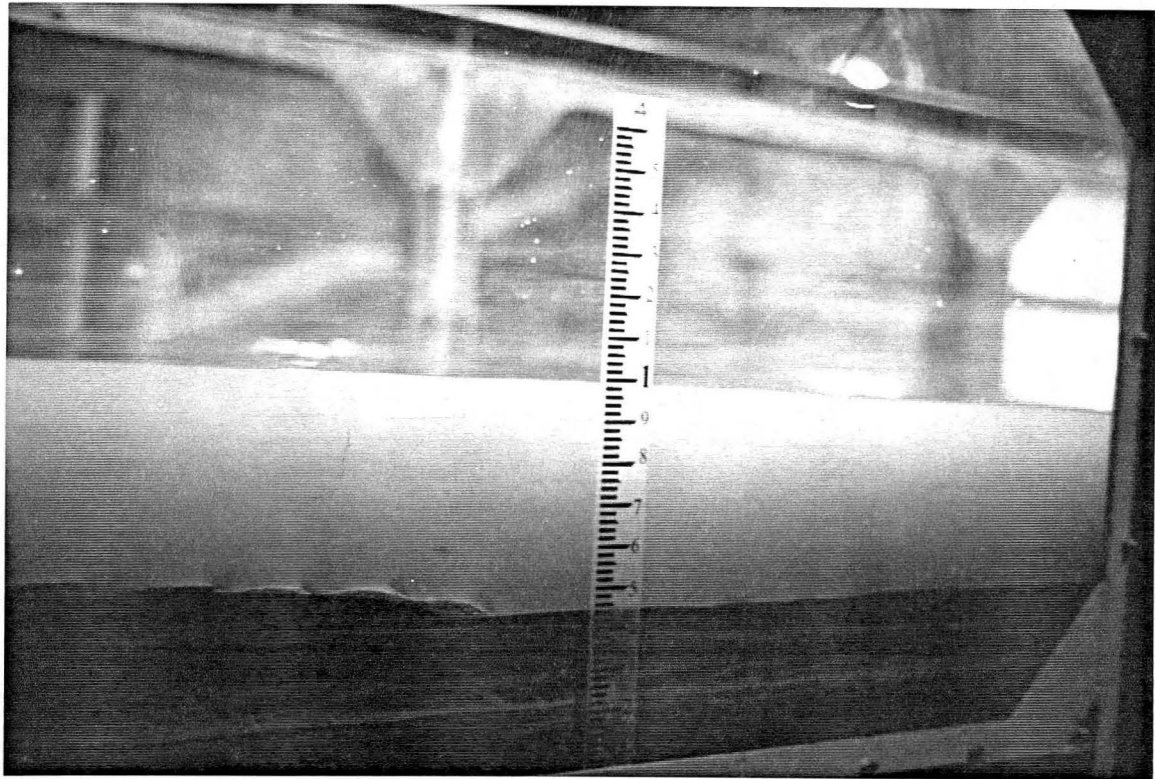


Figure 10. The deposition of step 1-U2



Picture 21. Longitudinal view of step 1-U2

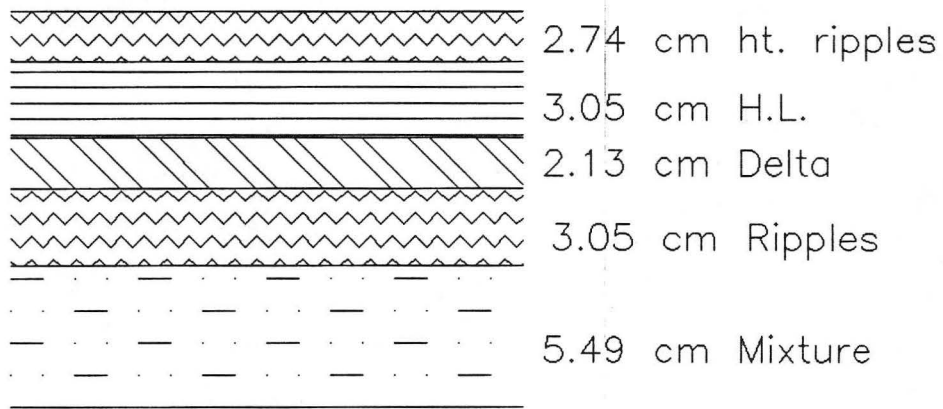
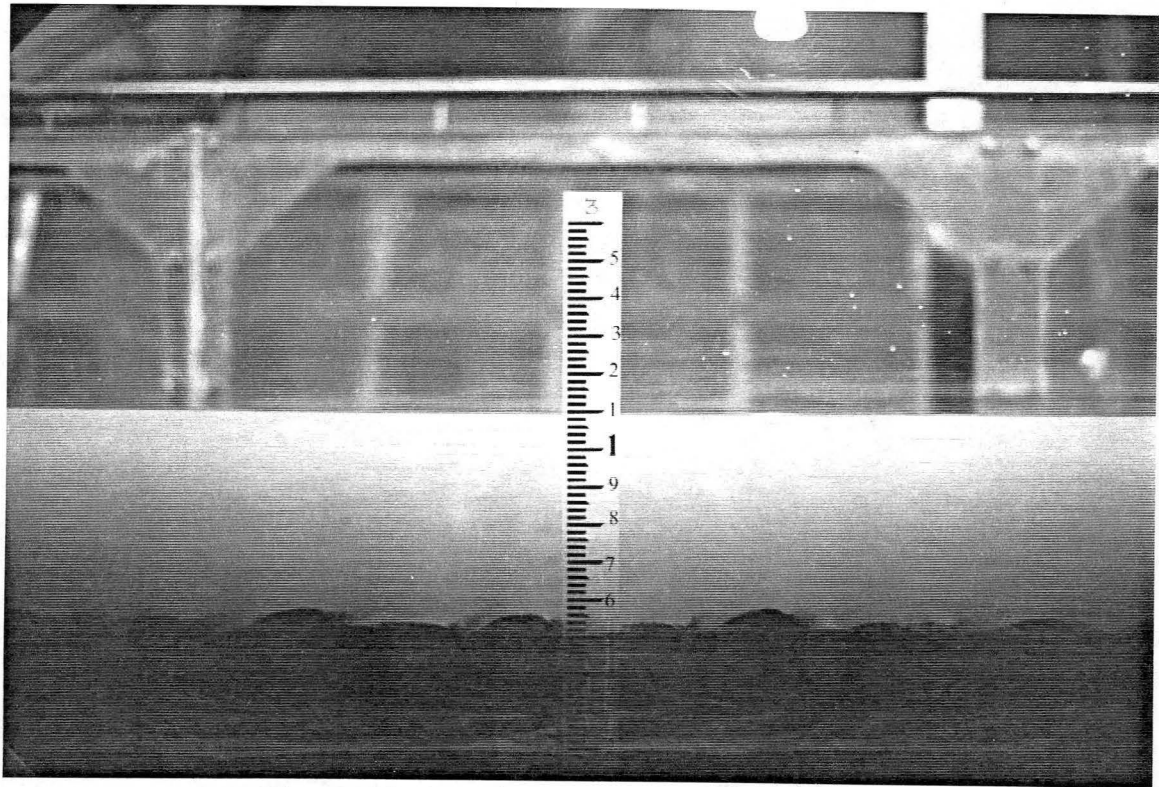


Figure 11. The deposition of step 1-U3



Picture 22. Longitudinal view of step 1-U3

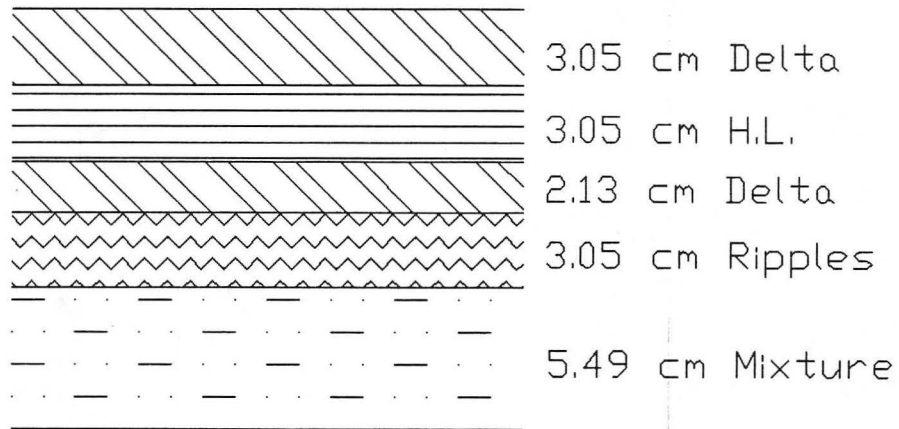
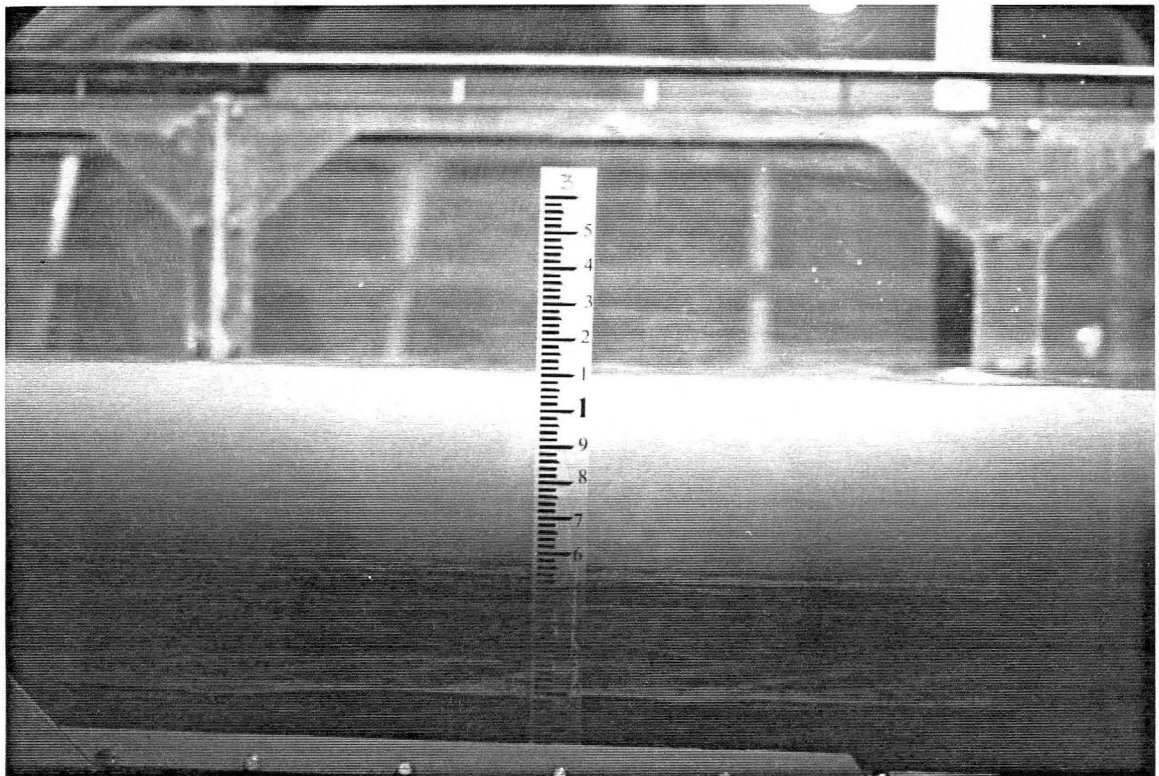


Figure 12. The deposition of step 1-U4



Picture 23. Longitudinal view of step 1-U4

Step 1-B

As the tailwater depth decreased at a constant discharge, scour was initiated at the downstream end of the flume and a nick point propagated upstream. The flow became locally supercritical and the degradational features of the bed were of little interest as the bed rapidly scoured over time. Table 4 summarizes the steps of run 1.

Table 4. Summary results for run 1

Step	Gate	Q m ³ /s	h cm	V _m cm/s	S _f	Shear N/m ²	Fr	U* m/s	f	bedforms
1-U1	6	0.125	10.31	101.03	0.00558	4.81	1	0.0694	0.038	plane bed
1-U2	6	0.125	13.77	75.65	0.00507	5.56	0.65	0.0746	0.078	ripples
1-U3	6	0.125	17.12	60.85	0.00449	5.86	0.47	0.0766	0.127	ripples
1-U4	6	0.125	18.54	56.18	.00439	6.09	0.42	0.0781	0.155	small ripples
1-B	3	0.125	--	--	--	--	--	--	--	scour

3.4.2 Positive slope run (run 2)

1- Objective of this run:

Examine the bed deposit slope under a positive flume floor slope. Examine the sand stratification at different flow depths, under a continuous supply of the heterogeneous sand mixture.

2- Experimental conditions and data summary:

- Constant discharge at Q=0.125 m³/s.
- Positive flume slope (+0.5%).
- Sand mixture of d₅₀ =0.4 mm.
- Number of tailgates ranged from 2 to 6.

Step 2-U1

The discharge for this run was constant at $0.125 \text{ m}^3/\text{s}$. Two tailgates were inserted at the downstream end of the flume. The bed surface as characterized by plane bed with parallel lamination. Pictures were not available for this step.

Step 2-U2

The number of tailgates was increased to 4 and the discharge was held constant at $0.125 \text{ m}^3/\text{s}$. As a result, water surface level increased, and induced the formation of white ripples, primarily at the downstream end of the flume. Figure 13 shows the bed structure observed during this run. Picture 24 shows a double delta formed on top of the ripple structure.

Step 2-U3

The flume was operated under the same constant discharge at $0.125 \text{ m}^3/\text{s}$. The number of tail gates was increased to 6 and the flow depth increased accordingly. Picture 25 does not reflect the measurements taken earlier. Figure 14 shows that white ripples formed on top of the delta from Step 2-U2.

Step 2-D1

The number of tailgates was reduced to 4, while the discharge was kept constant at $0.125 \text{ m}^3/\text{s}$. As a result, flow level is decreased. Plane bed was observed along with a smooth water surface profile. The slope of the topset of the delta was measured as 0.125% and the bottomset was measured 1.25%. Figure 15 shows the bed structure and Picture 26 shows the longitudinal section of the flume.

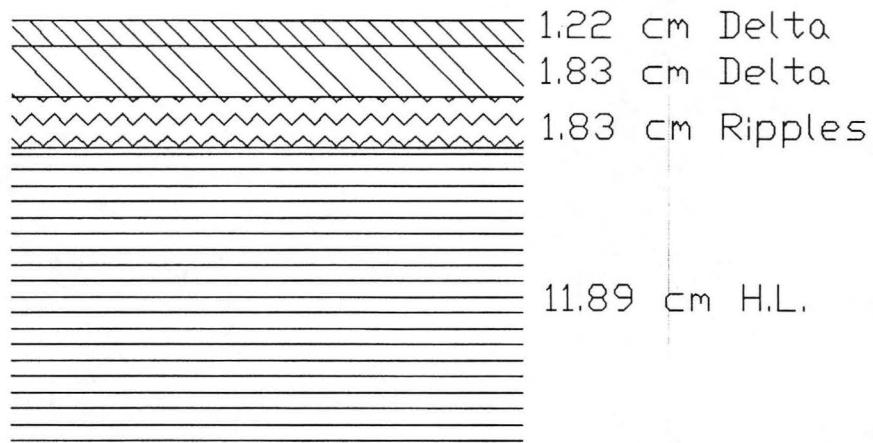
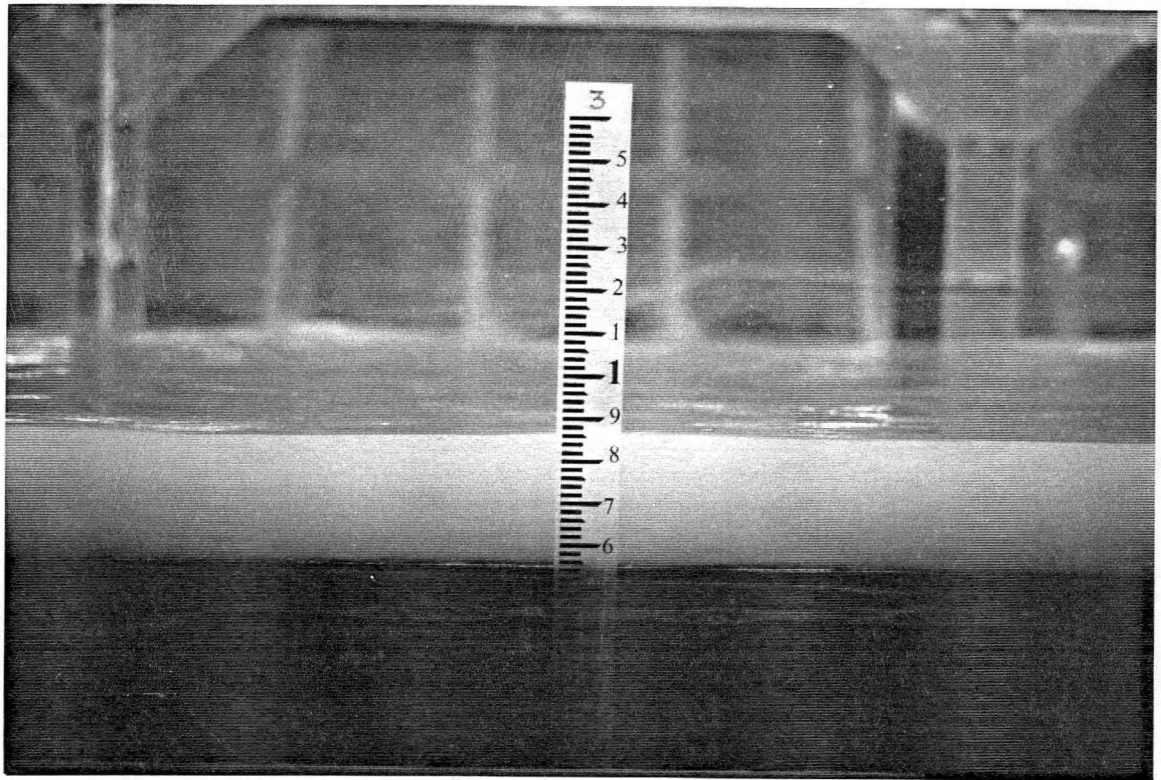


Figure 13. The deposition of step 2-U2



Picture 24. Longitudinal view of step 2-U2

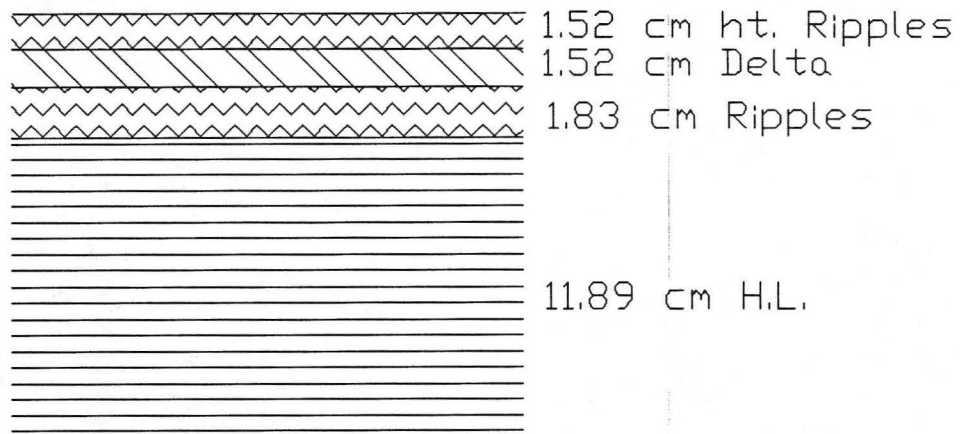
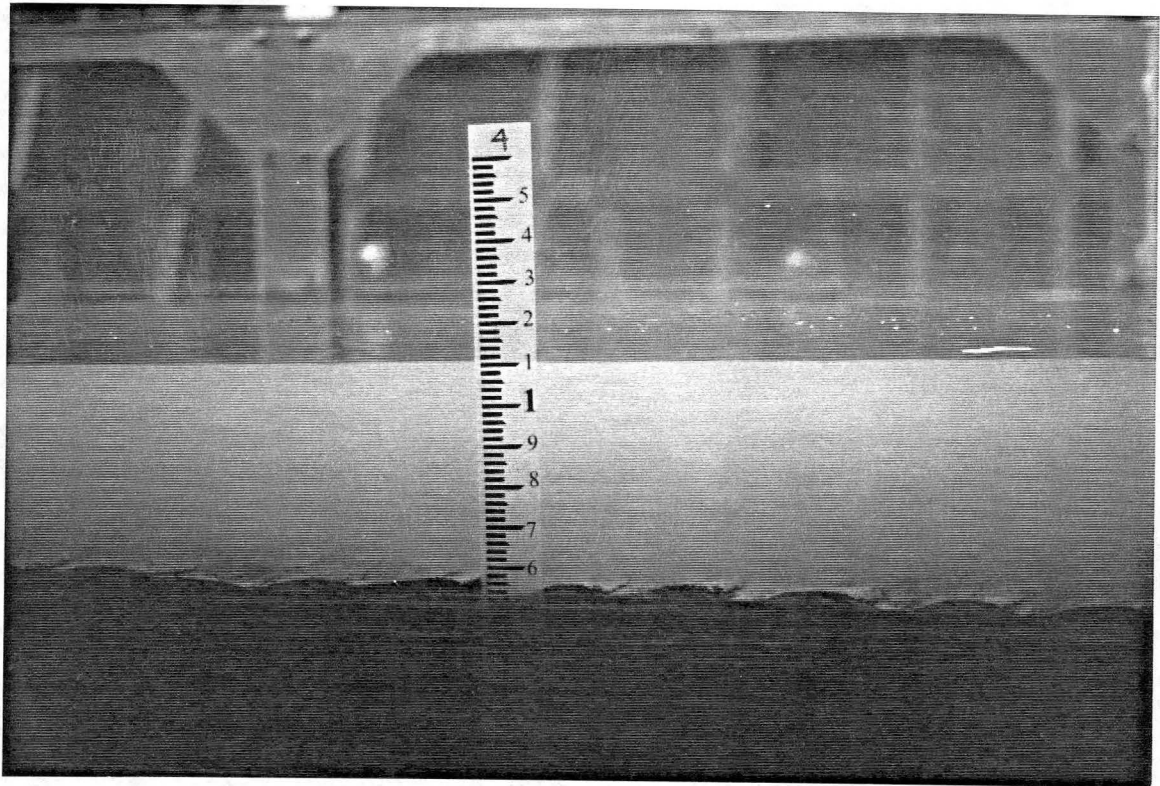


Figure 14. The deposition of step 2-U3



Picture 25. Longitudinal view of step 2-U3

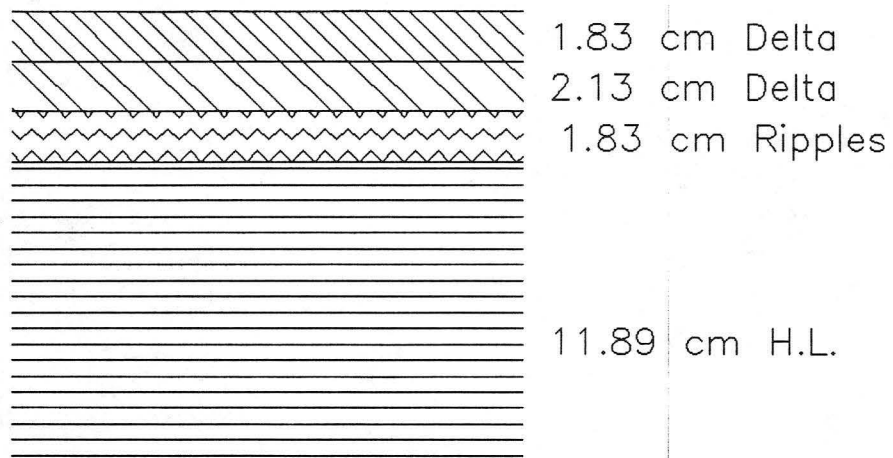
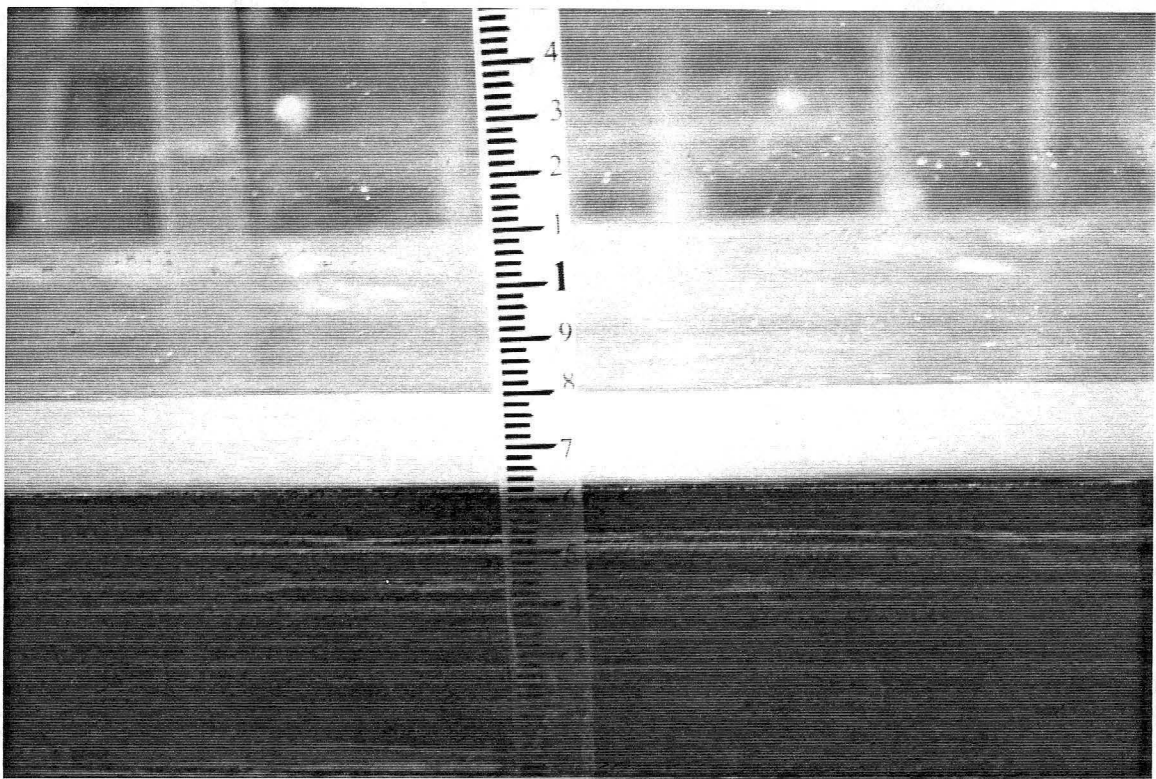


Figure 15. The deposition of step 2-D1



Picture 26. Longitudinal view of step 2-D1

Step 2-D2

This step is performed after decreasing the discharge to a steady discharge of 0.04 m³/s and only 2 tailgates. The top layer is characterized by the progression of a thick delta over the previously formed ripples as shown in Figure 16. The topset slope of the delta was -0.5%, the bottomset slope was measured at 2.17%. Picture 27 shows a longitudinal section through the flume.

Step 2-D3

The same hydraulic conditions were continued as the previous step. A slight increase in the flow depth took place due to the aggradation of the bed. The delta formed in this step is thicker than the one in the previous step as shown in Figure 17. Picture 28 shows longitudinal section on the flume during this step. Table 5 summarizes all the result from run 2.

Table 5. Summary results for run 2

Step	Gate	Q m ³ /s	h cm	V _m cm/s	S _f	Shear N/m ²	Fr	U _* m/s	f	Bedform
2-U1	2	0.125	8.53	122.12	0.01897	13.88	1.33	0.1179	0.075	plane bed
2-U2	4	0.125	13.56	76.82	0.003735	4.05	0.67	0.0636	0.055	ripples delta
2-U3	6	0.125	18.9	55.11	---	---	0.4	---	---	ripples
2-D1	4	0.125	7.37	141.34	0.00264	1.7	1.66	0.0412	0.007	plane bed
2-D2	2	0.04	6.6	50.50	0.00763	4.44	0.63	0.067	0.139	delta
2-D3	2	0.04	7.11	46.88	0.01211	7.54	0.56	0.087	0.275	delta

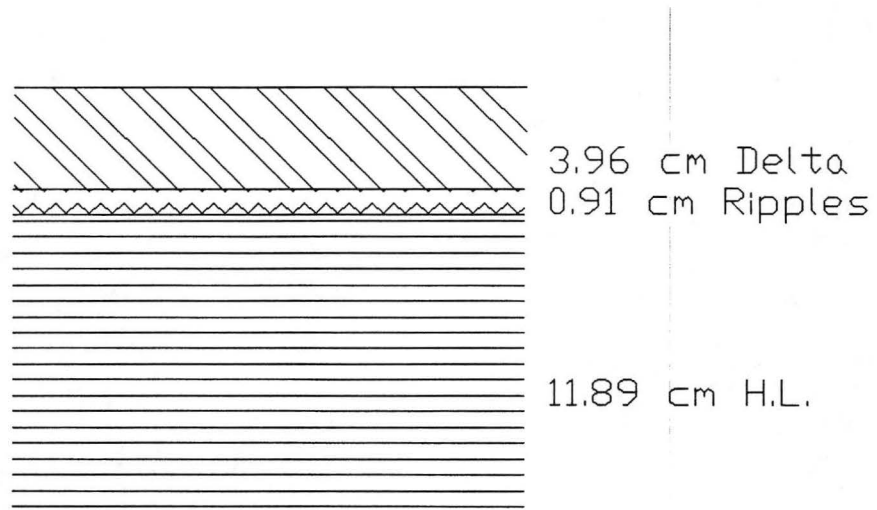
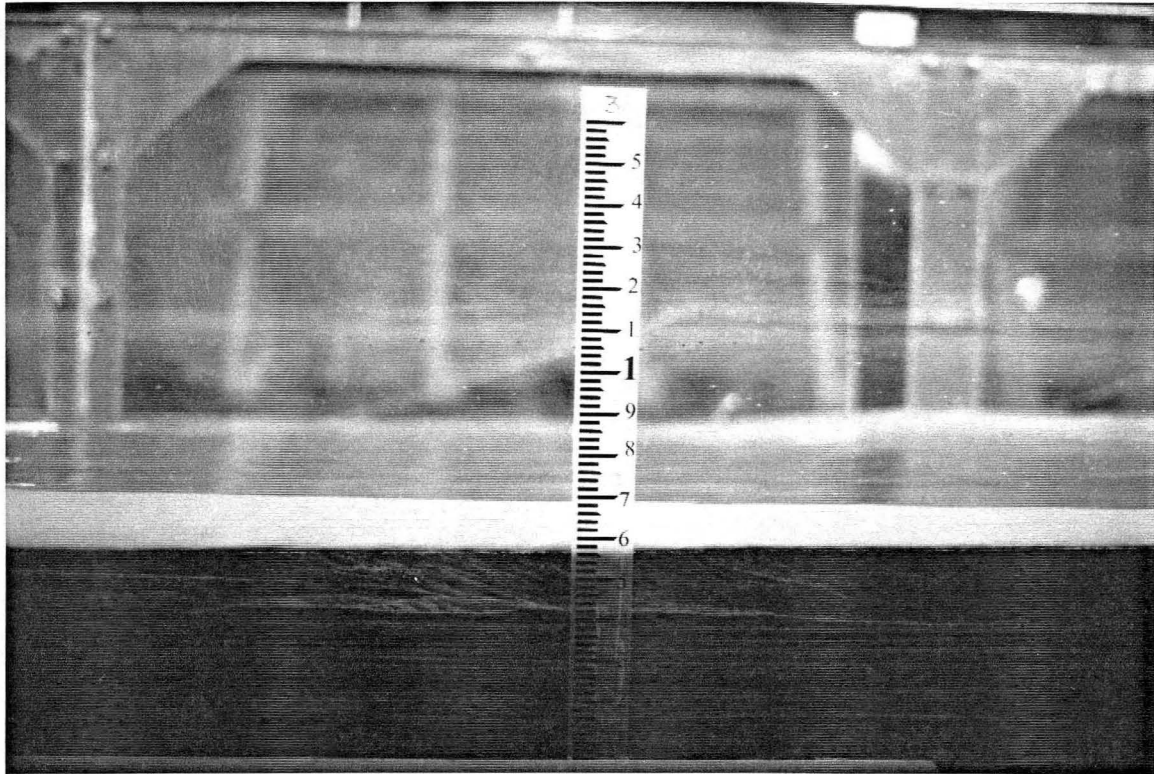


Figure 16. The deposition of step 2-D2



Picture 27. Longitudinal view of step 2-D2

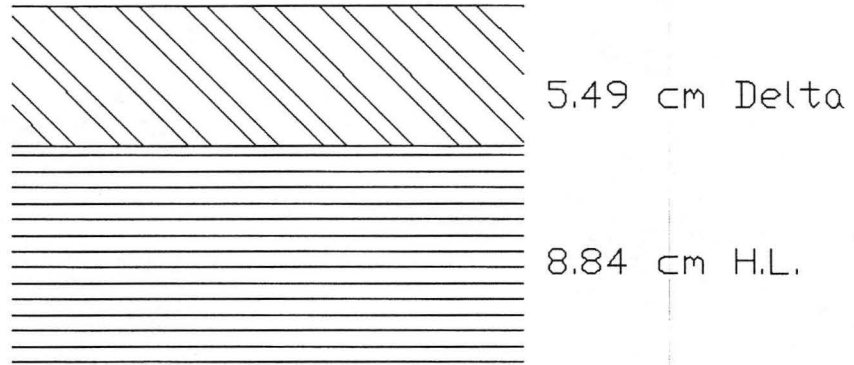
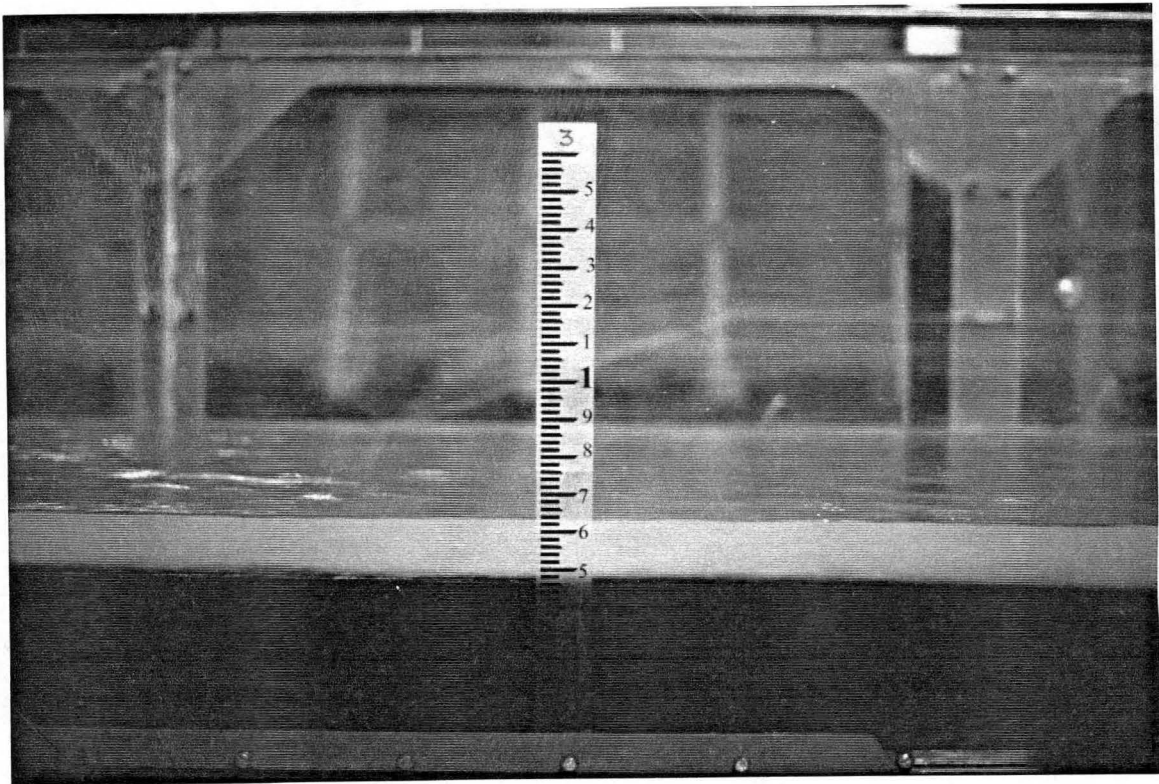


Figure 17. The deposition of step 2-D3



Picture 28. Longitudinal view of step 2-D3

3.4.3 Negative slope run (run 3)

1. Objectives of these runs:

Examining the influence of adverse slope of the flume floor on the stratification of sands.

The effect of the stage on the delta formation.

2. Experimental conditions and data summary:

- Adverse flume slope (-0.2%).
- Sand mixture of $d_{50}=0.4$ mm.
- No. of tail gates used are 2, 3 and 5 tail gates.

Step 3-U1

The discharge used for this step was $0.04 \text{ m}^3/\text{sec}$. A smooth water surface profile was observed during the run. Plane bed was originally formed, then ripples started to propagate in the downstream direction. The delta topset slope was measured 0.63%. The slope of the bottomset was measured 0.675%. The delta thickness was measured 4.57 cm as shown in Figure 18. Picture 29 shows the initial plane bed.

Step 3-U2

Flow depth was increased by adding two more tail gates and increasing the discharge to $0.125 \text{ m}^3/\text{sec}$. This run represents a nonequilibrium situation. The water surface profile was rough and the whole bed was covered by ripples as shown in Picture 30. Figure 19 shows the change in the top layer due to the ripple formation.

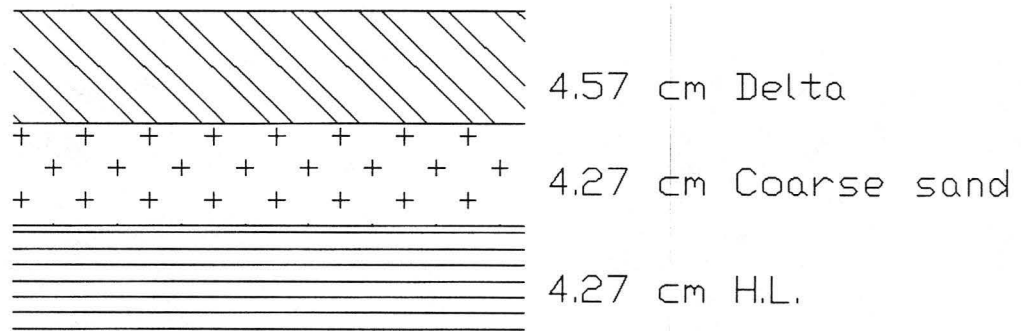
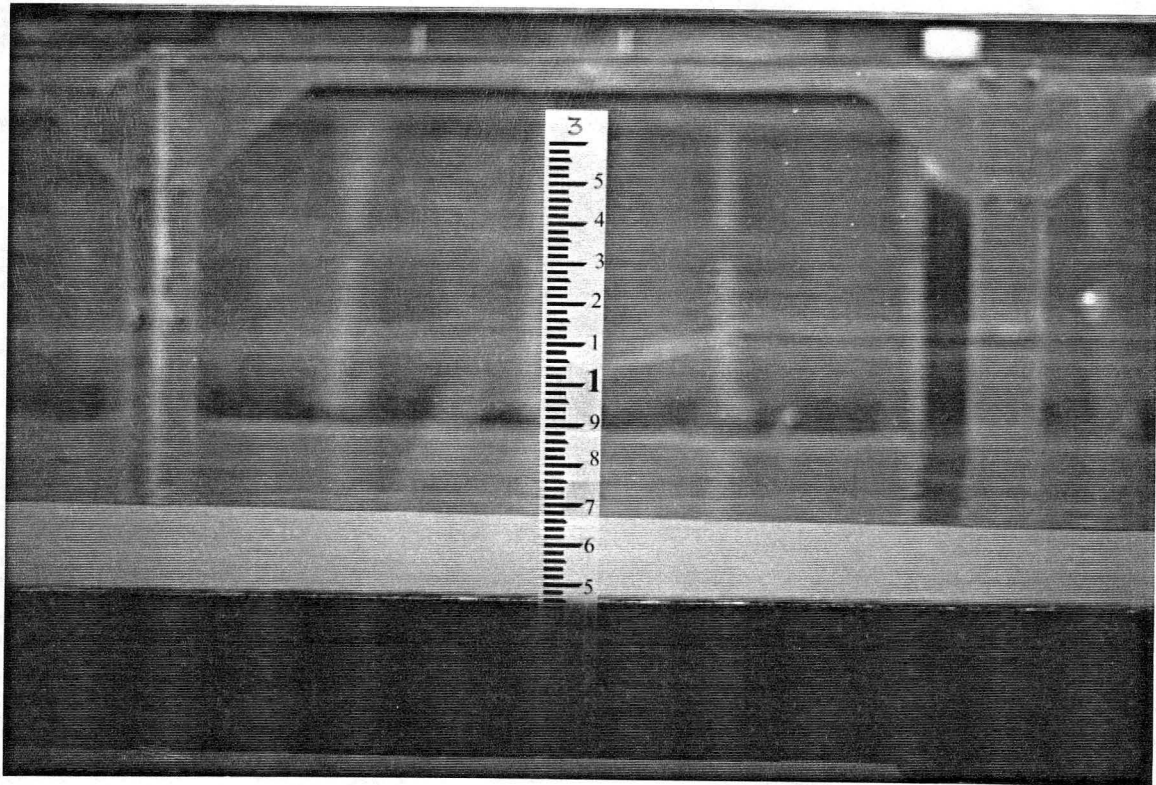


Figure 18. The deposition of step 3-U1



Picture 29. Longitudinal view of step 3-U1

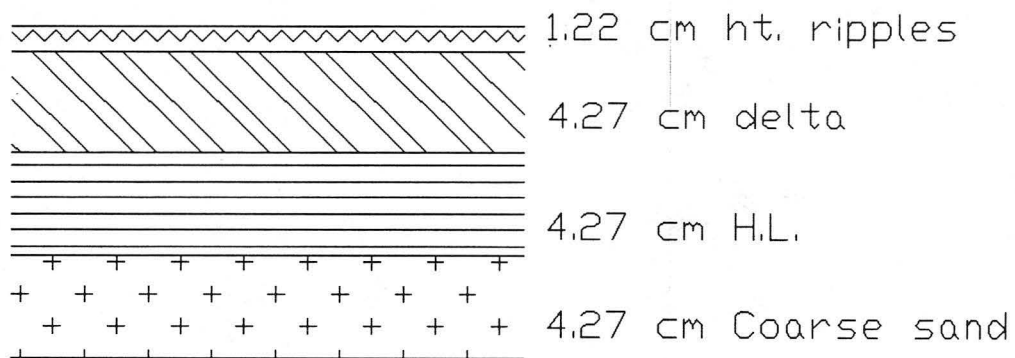
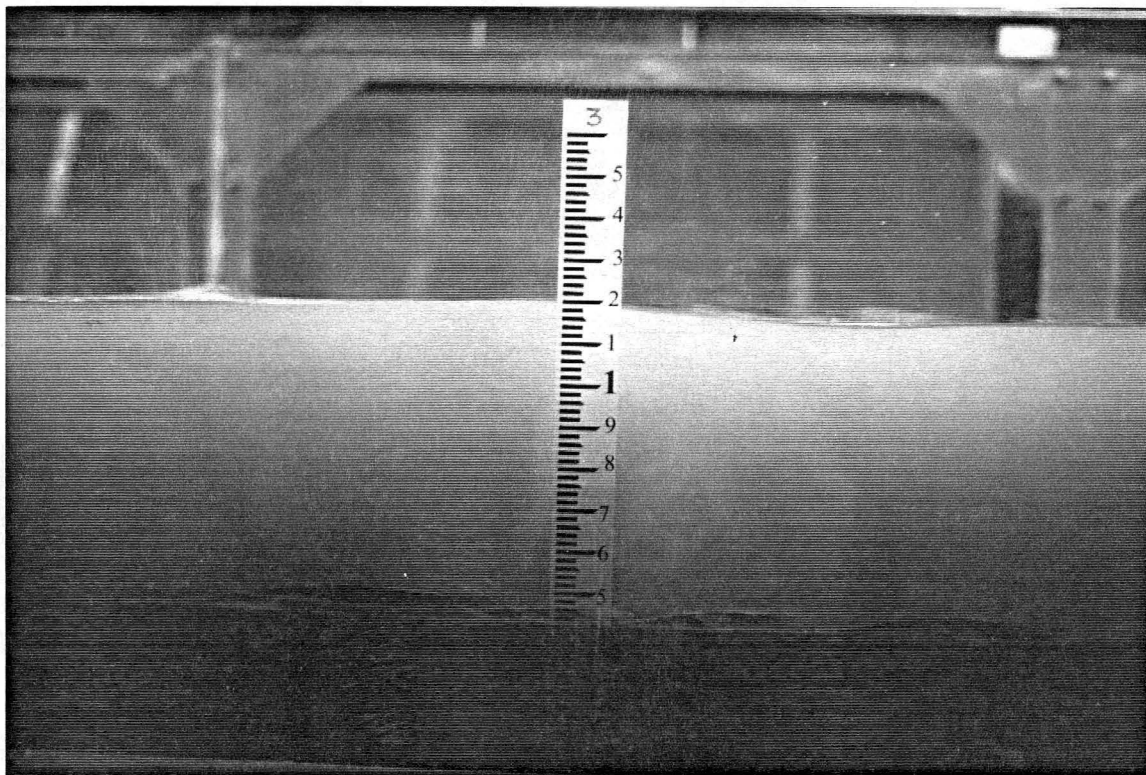


Figure 19. The deposition of step 3-U2



Picture 30. Longitudinal view of step 3-U2

Step 3-U3

This run was performed under the same hydraulic conditions as the previous one. More time was allowed for this measurements. As shown in Picture 31, the bed profile is characterized by a delta similar to long dunes. The sedimentary structure as shown in Figure 20 represents a section through one of the dunes.

Step 3-U4

The hydraulic conditions stayed the same as the previous one except for the tailgates which were increased to 5 tail gates. The measurements were taken 25 minutes after the previous one, so, it represents near equilibrium conditions. Dunes were observed during this run as shown in Picture 32. The dunes were averaged 240 cm length and 7 cm height. The sedimentary structure is shown in Figure 21 through one of the dunes.

Step 3-D1

The discharge for this run was decreased to $0.04 \text{ m}^3/\text{sec}$ and the number of tail gates were reduced to 3 tail gates. Flow depth was reduced, as a result, the bed was degraded and tended to form dunes as shown in Picture 33. By examining the sedimentary structure of the previous step and this step, it can be concluded that degradation process were resulted as shown in Figure 22.

Step 3-D2

The hydraulic conditions remained the same as the previous run. Measurements were taken 10 minutes after the measurements of the previous run. Flow depth was increased and the dunes started to grow in height and become more stable as shown in Picture 34. They were measured 120 cm length and 9.5 cm height. Figure 23 shows the sedimentary structure of the bed.

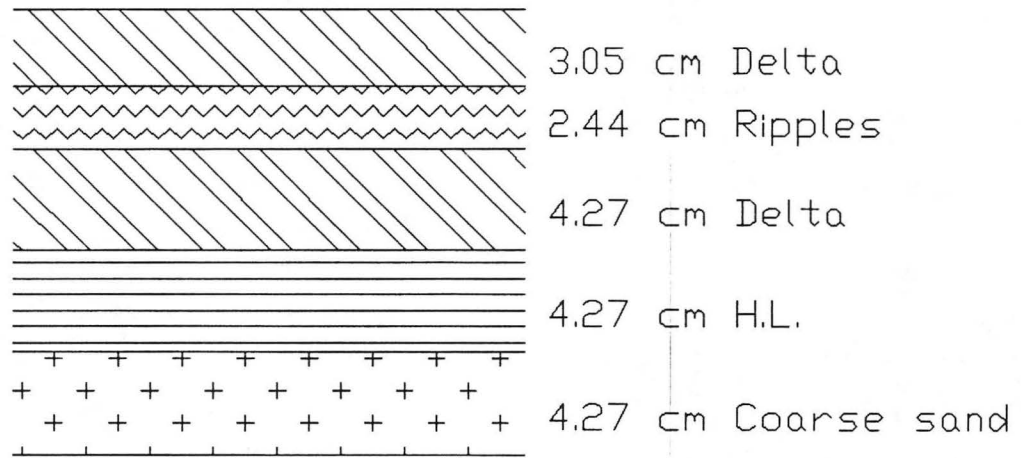
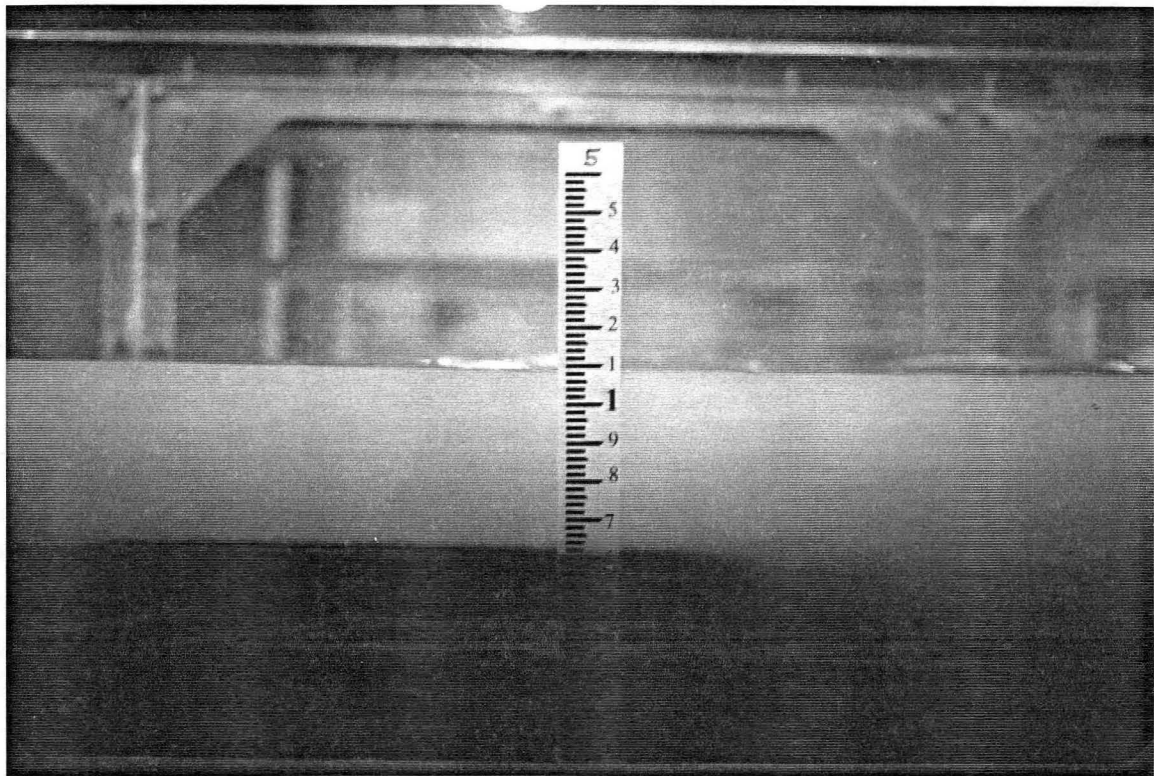


Figure 20. The deposition of step 3-U3



Picture 31. Longitudinal view of step 3-U3

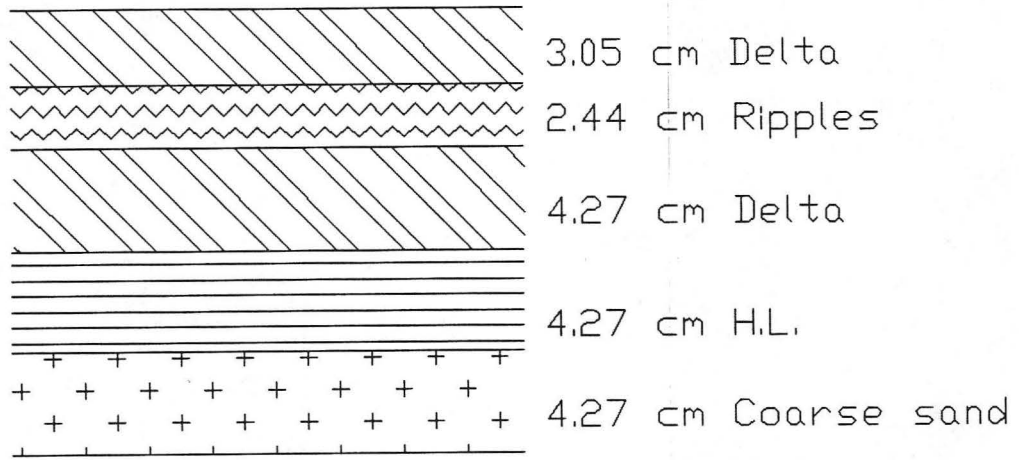
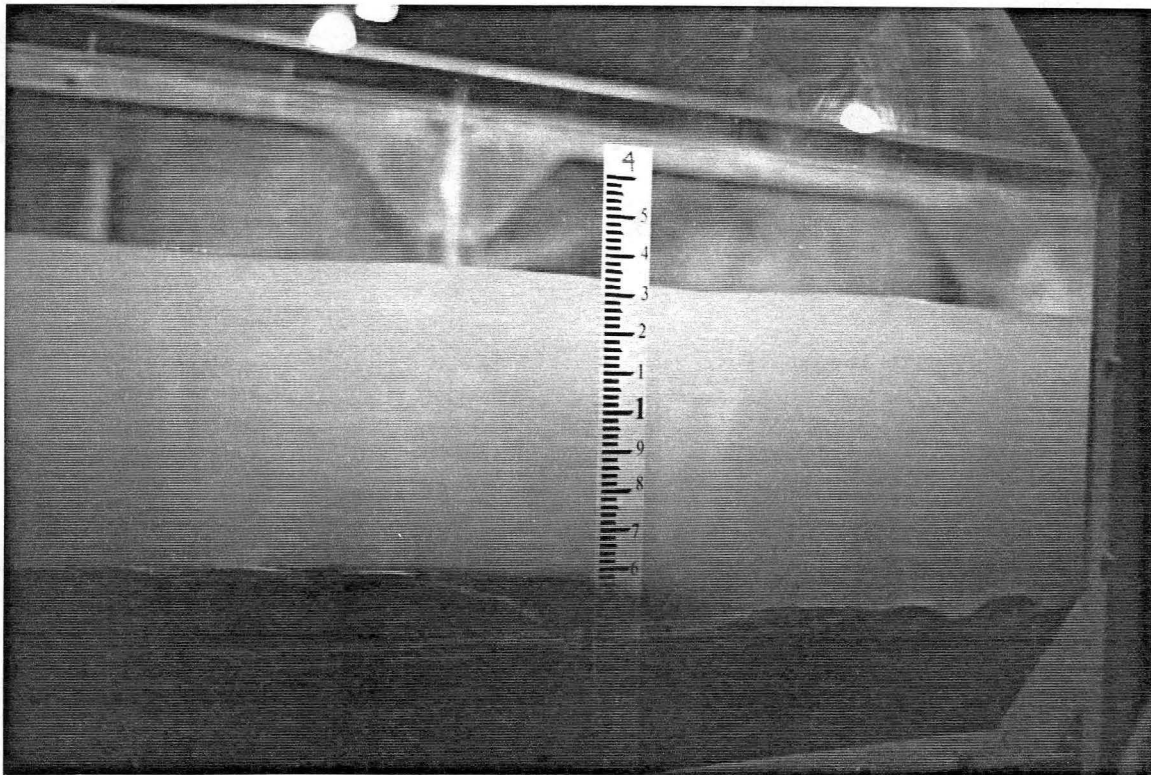


Figure 21. The deposition of step 3-U4



Picture 32. Longitudinal view of step 3-U4

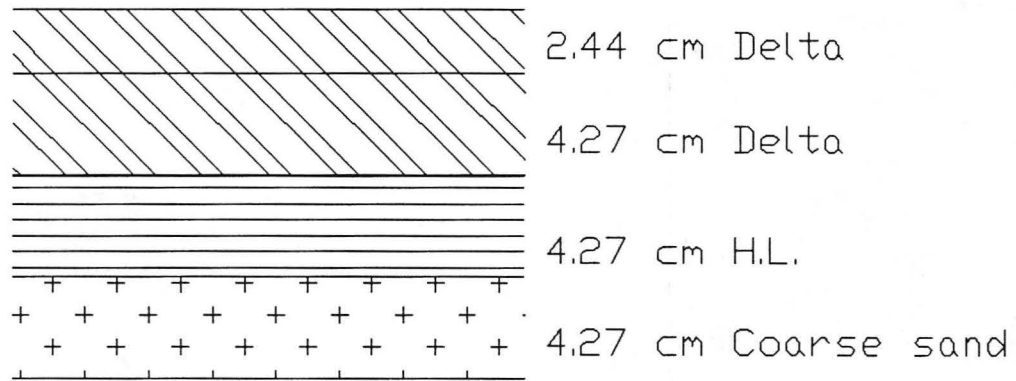
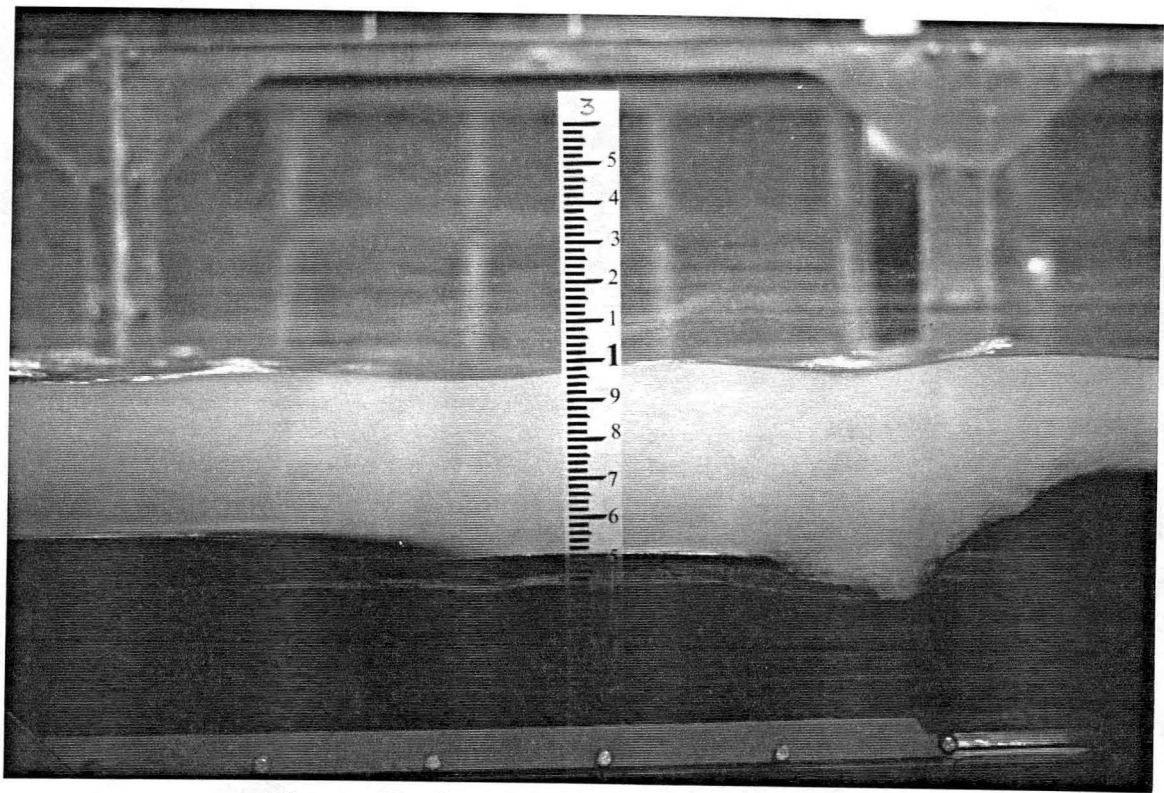


Figure 22. The deposition of step 3-D1



Picture 33. Longitudinal view of step 3-D1

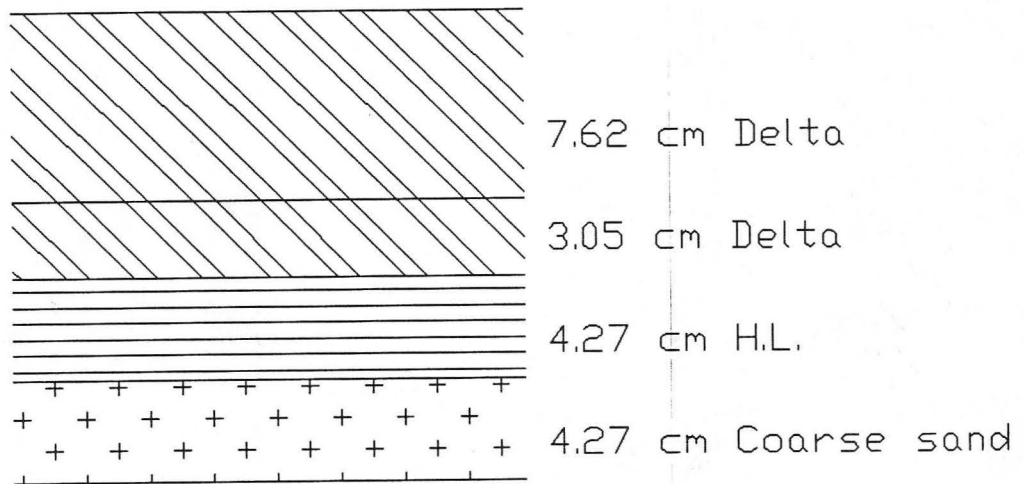
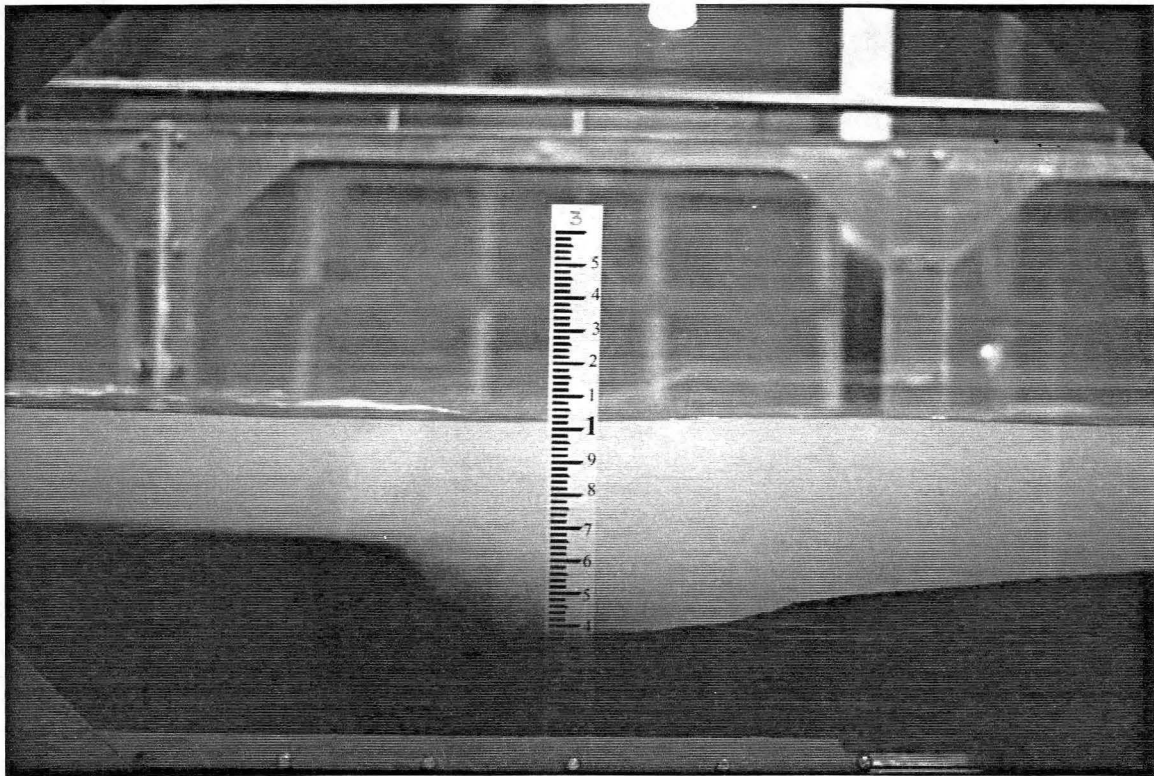


Figure 23. The deposition of step 3-D2



Picture 34. Longitudinal view of step 3-D2

Step 3-D3

The hydraulic conditions did not change from the previous run. Measurements were taken 20 minutes after the previous run. Picture 35 shows fully developed dunes under stable conditions. Figure 24 shows the sedimentary structure of the bed. Table 6 summarizes all the results from run 3.

3.5 Compilation of Results

Table 7 compiles the results for all stratification runs. The analysis of data includes the calculation of the different hydraulic parameter such as discharge Q , flow depth h , mean velocity V_m , friction stopple S_f , Froude number Fr , hydraulic radius R , shear stress, stress velocity U_* , and the Darcy-Weisbach friction factor f .

The formation of ripples was often initiated on a plane bed of fine white particles. Over time, the content of coarse black particles increased leading to the formation of relatively coarse ripples as shown on the sequence of Pictures 36a to 36e. Over time ripple configurations in the aggradation plane evolved into climbing ripples shown on Pictures 37a to 37c.

Pictures 38 and 39 show the foreset slope of a dune in formation. Features similar to deltaic formation are recognized. The upstream end of dunes in formation are characterized by scour of multiple layers in the bed. Combinations of these features are shown on Pictures 40 and 41. Long dunes often have stratified deposits as shown on Picture 42.

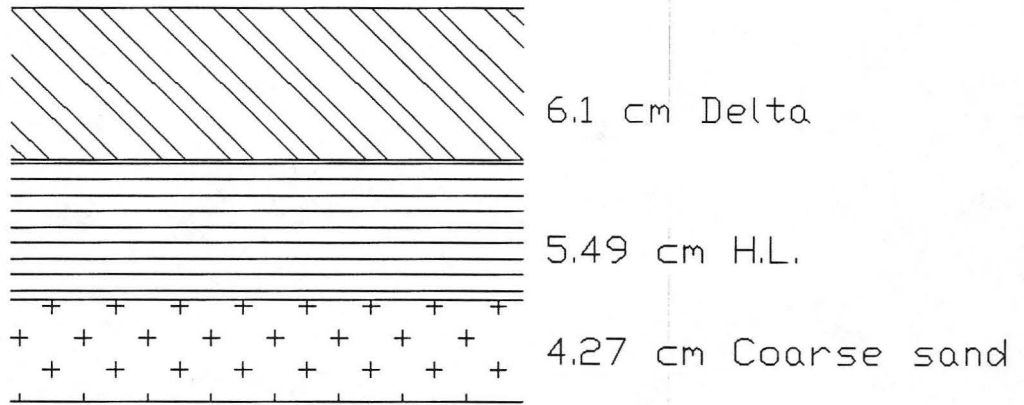
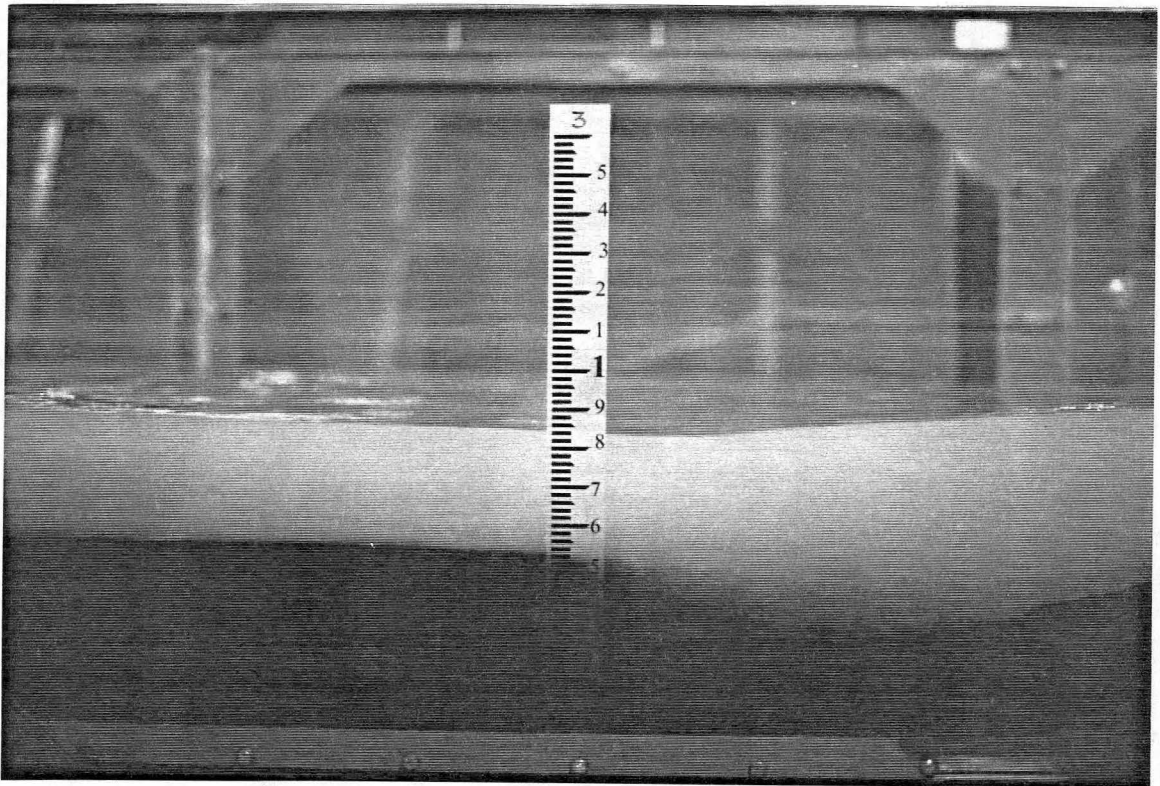


Figure 24. The deposition of step 3-D3



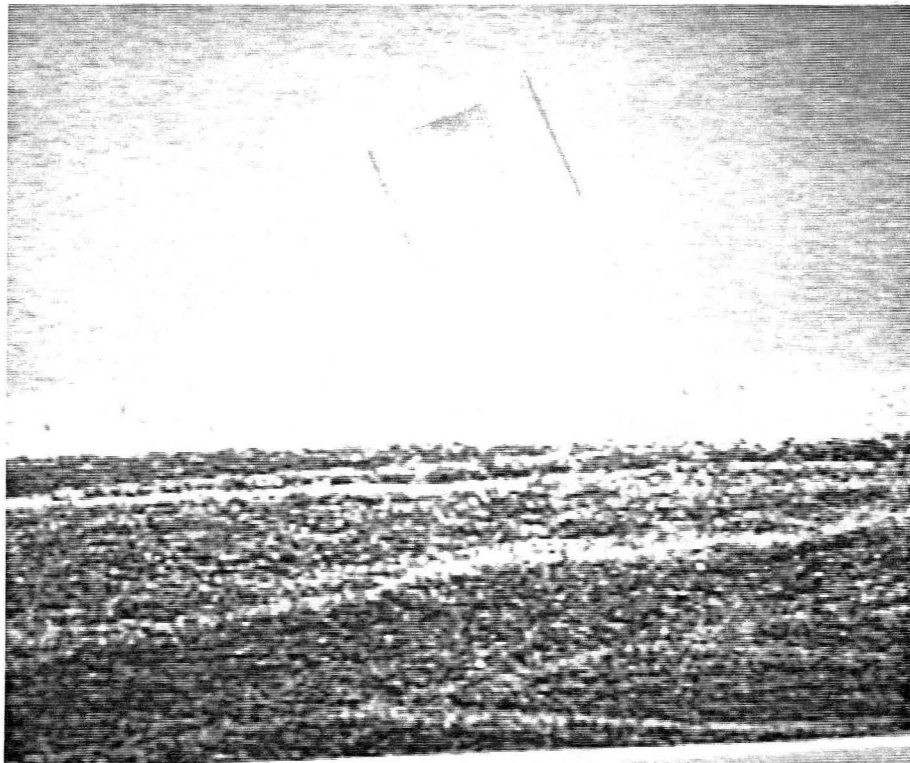
Picture 35. Longitudinal view of step 3-D3

Table 6. Summary results for run 3

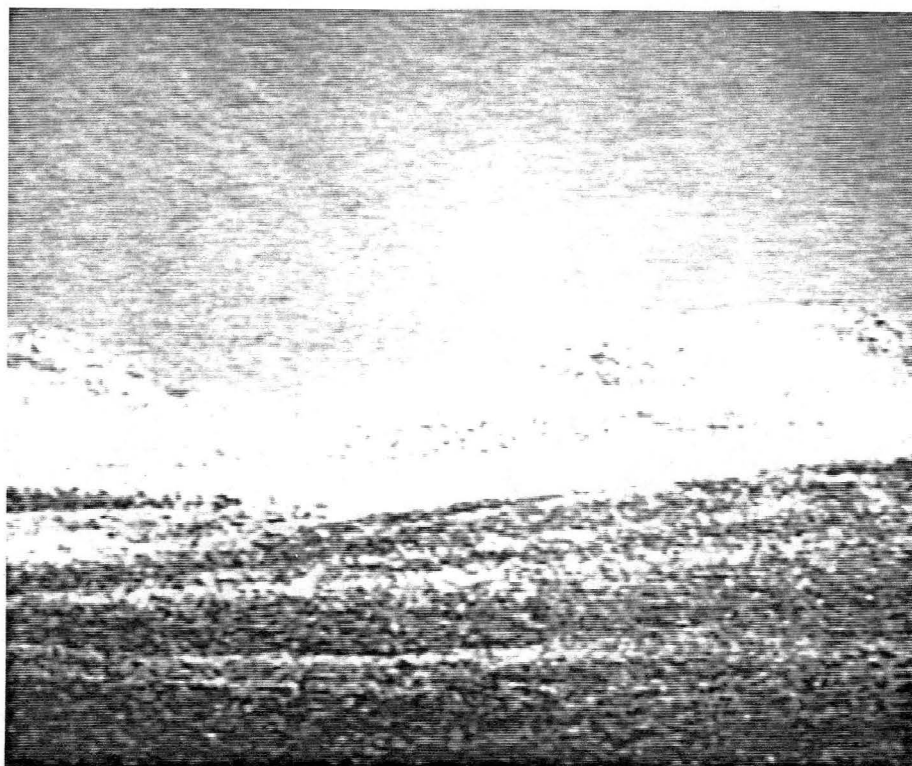
Step	Gate	Q m ³ /s	h cm	V _m cm/s	S _f	Shear N/m ²	Fr	U _* m/s	f	Bedform
3-U1	2	0.04	7.92	42.09	0.00787	5.39	0.48	0.0735	0.244	plane bed
3-U2	4	0.125	23.27	44.76	---	---	0.3	---	---	ripples
3-U3	4	0.125	17.78	58.59	0.00252	3.38	0.44	0.0582	0.079	long dunes
3-U4	5	0.125	23.57	44.19	0.00408	6.77	0.29	0.0823	0.277	dunes
3-D1	3	0.04	10.57	31.54	0.00392	3.45	0.31	0.0588	0.278	dunes
3-D2	3	0.04	14.58	22.86	0.00456	5.25	0.19	0.0725	0.804	dunes
3-D3	3	0.04	11.84	28.15	0.00854	8.28	0.26	0.091	0.836	dunes

Table 7. Data summary for all runs

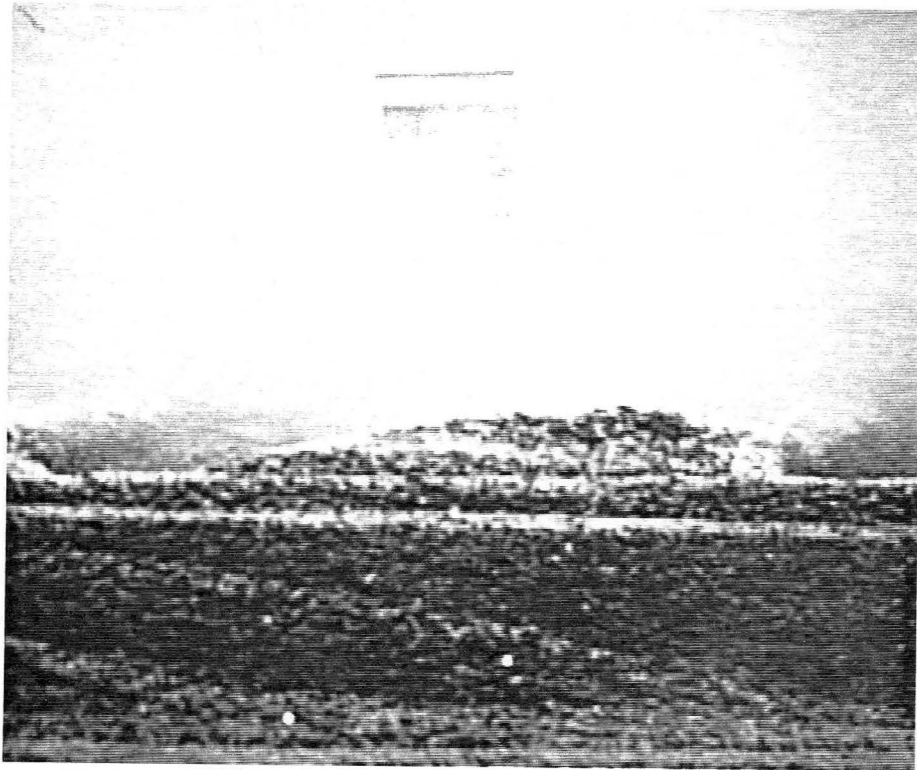
Step	Q m ³ /sec	h cm	V _m cm/sec	S _f	F _n	R cm	Shear N/m ²	U _* cm/sec	f	Bed condition
1-U1	0.125	10.31	101.03	0.005577	1	8.8	4.81	6.94	.038	plane bed
1-U2	0.125	13.77	75.65	0.005066	0.65	11.2	5.56	7.46	0.078	ripples downstream
1-U3	0.125	17.12	60.85	0.004491	0.47	13.32	5.86	7.66	0.127	ripples cover the bed
1-U4	0.125	18.54	56.18	0.00439	0.42	14.16	6.09	7.81	0.155	washed out ripples
2-U1	0.125	8.53	122.12	0.018966	1.33	7.47	13.88	11.79	0.075	---
2-U2	0.125	13.56	76.82	0.003735	0.67	11.06	4.05	6.36	0.055	ripples delta
2-U3	0.125	18.9	55.11	---	0.40	14.37	---	---	---	ripples cover the bed
2-D1	0.125	7.37	141.34	0.002641	1.66	6.56	1.7	4.12	0.007	plane bed
2-D2	0.04	6.6	50.51	0.007625	0.63	5.95	4.44	6.67	0.139	delta
2-D3	0.04	7.11	46.88	0.012107	0.56	6.36	7.54	8.69	0.275	delta
3-U1	0.04	7.92	42.09	0.007865	0.48	7	5.39	7.35	0.244	plane bed, ripples upstream
3-U2	0.125	23.27	44.76	---	0.3	16.77	---	---	---	ripples cover the bed
3-U3	0.125	17.78	58.59	0.002515	0.44	13.72	3.38	5.82	0.079	long dunes
3-U4	0.125	23.57	44.19	0.004082	0.29	16.92	6.77	8.23	0.277	dunes
3-D1	0.04	10.57	31.54	0.003919	0.31	8.99	3.45	5.88	0.278	dunes
3-D2	0.04	14.58	22.86	0.004564	0.19	11.73	5.25	7.25	0.804	dunes
3-D3	0.04	11.84	28.15	0.008543	0.26	9.89	8.28	9.10	0.836	dunes



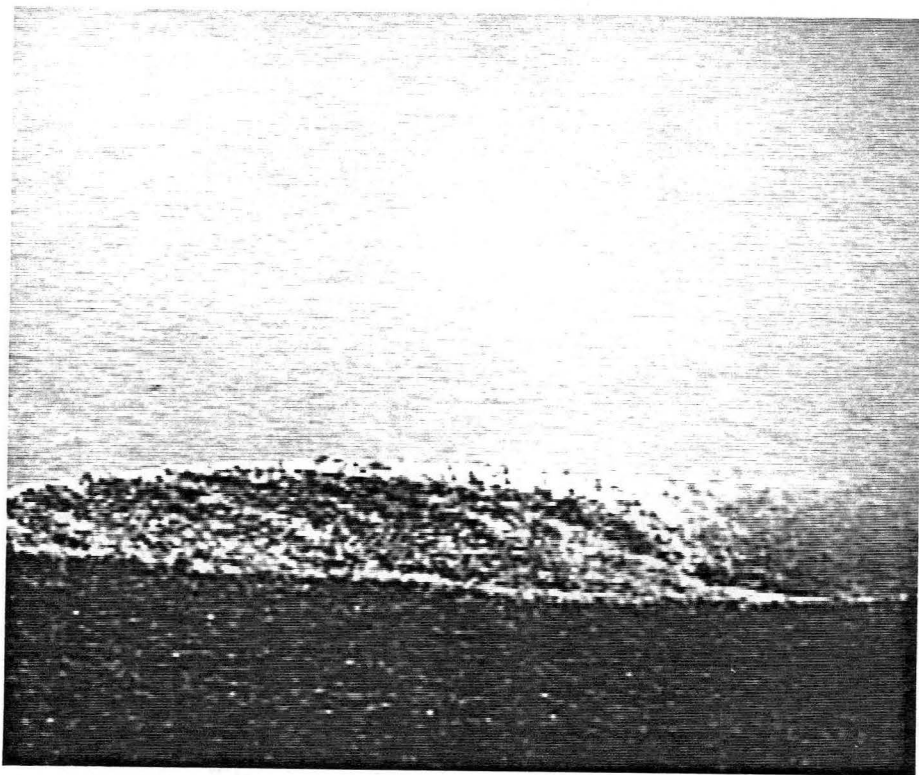
Picture 36a. Time sequence of ripple formation



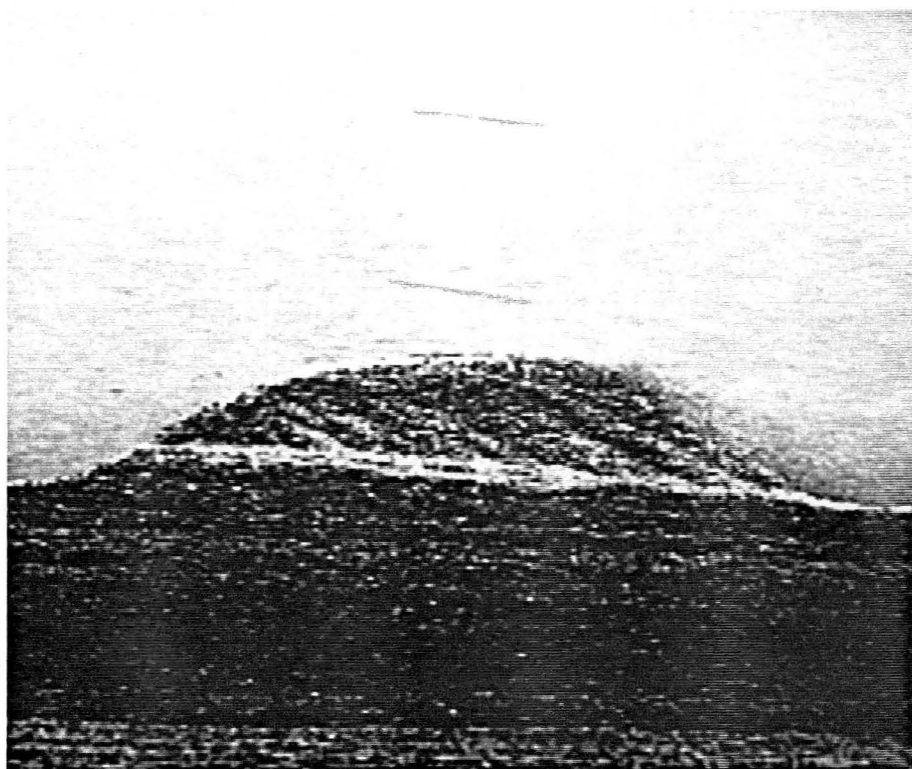
Picture 36b. Time sequence of ripple formation



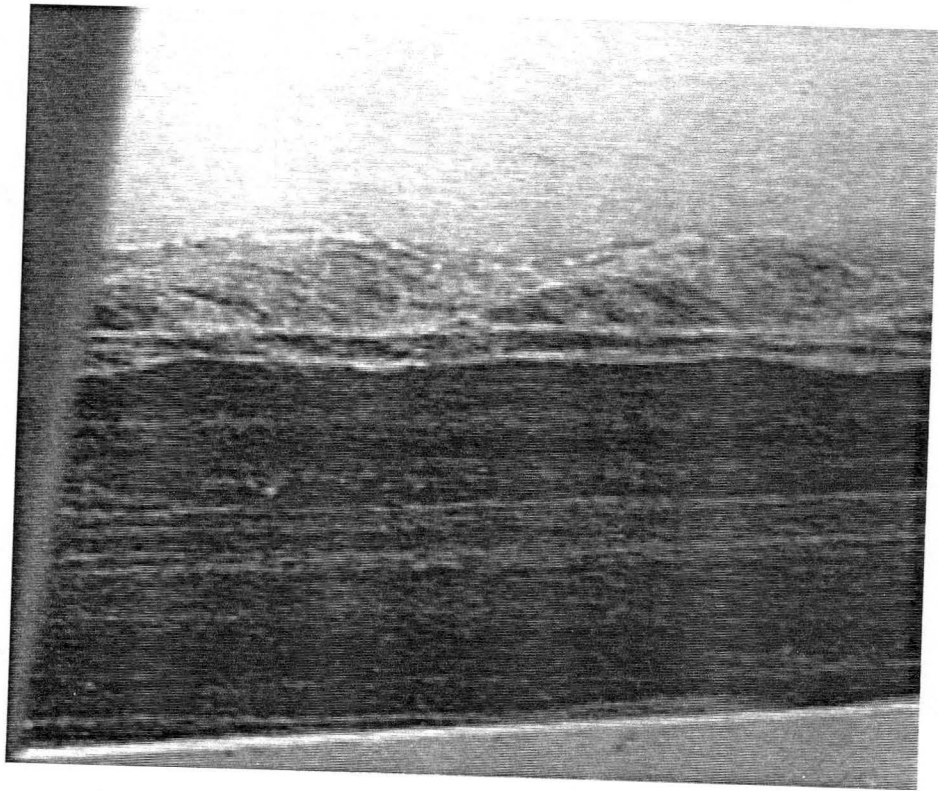
Picture 36c. Time sequence of ripple formation



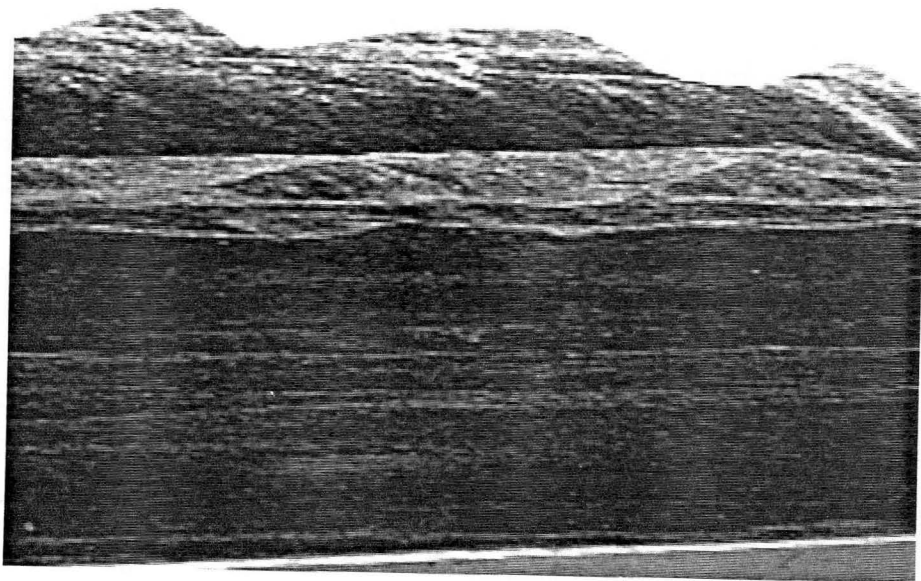
Picture 36d. Time sequence of ripple formation



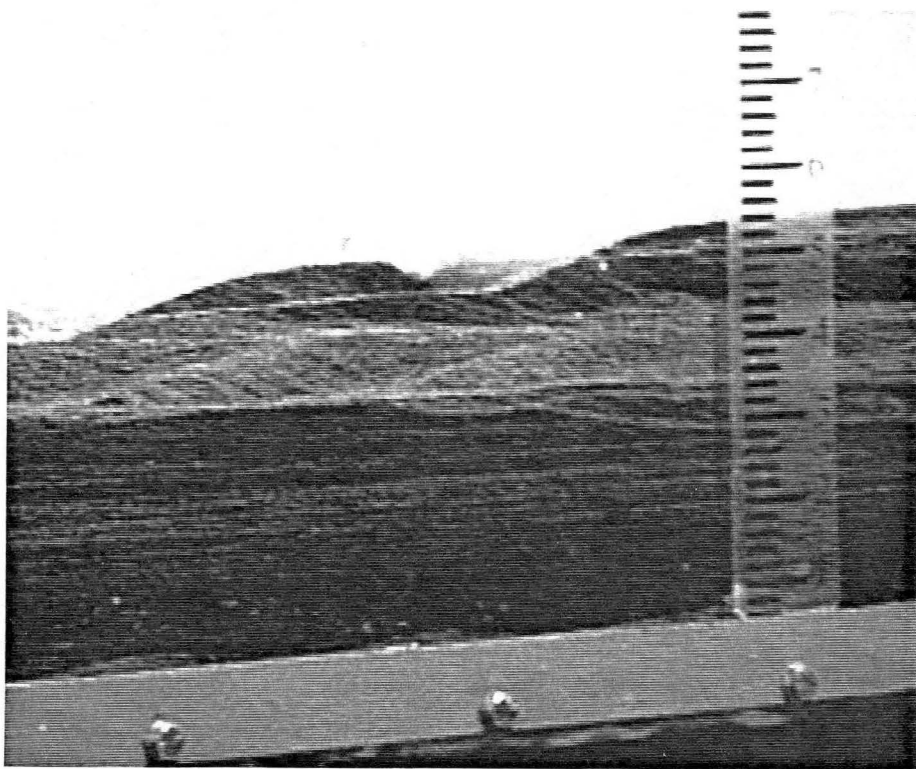
Picture 36e. Time sequence of ripple formation



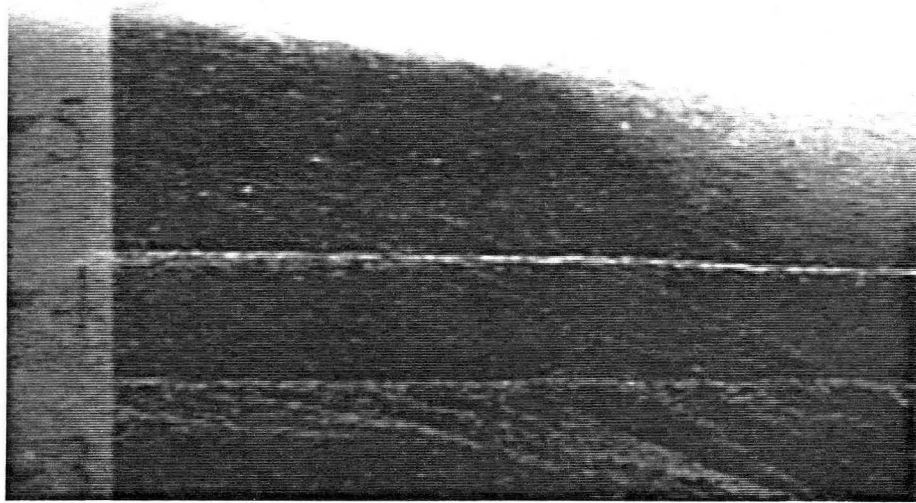
Picture 37a. Examples of climbing ripples



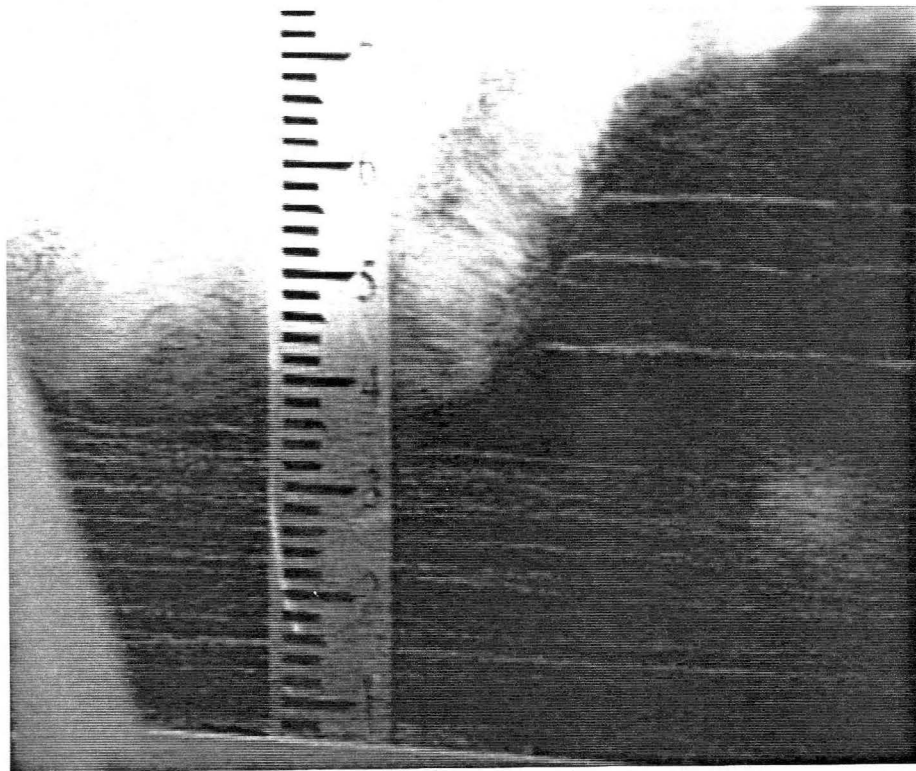
Picture 37b. Examples of climbing ripples



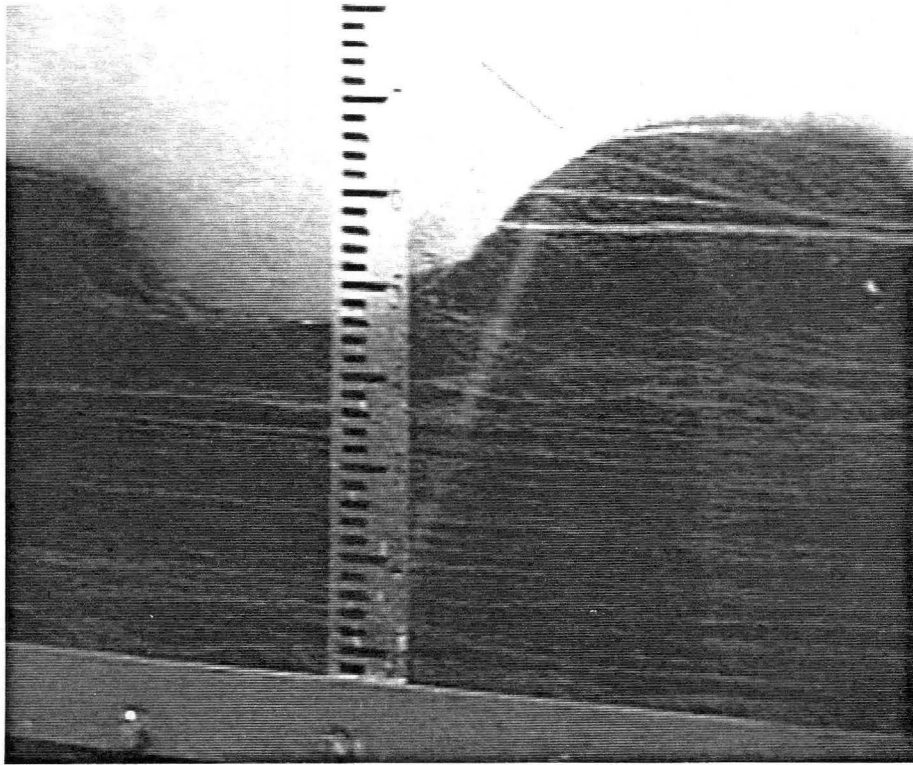
Picture 37c. Examples of climbing ripples



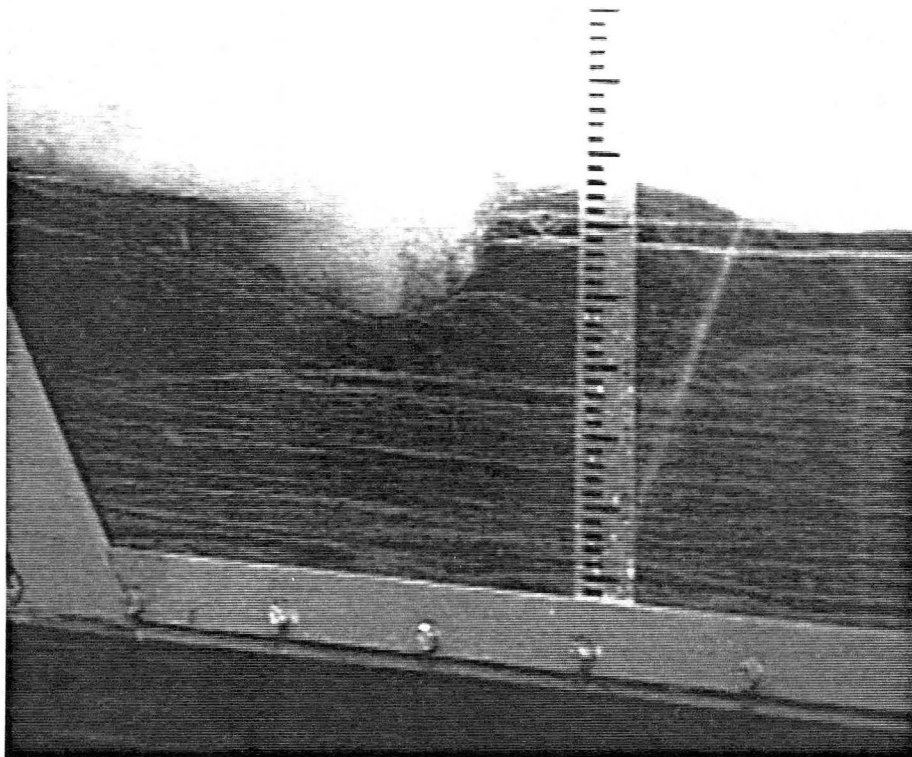
Picture 38. Topset and foreset slopes of a dune in formation



Picture 39. Upstream degradation of stratified deposits during dune formation



Picture 40. Example of combined aggradation and degradation during dune formation



Picture 41. Combined aggradation and degradation during dune formation

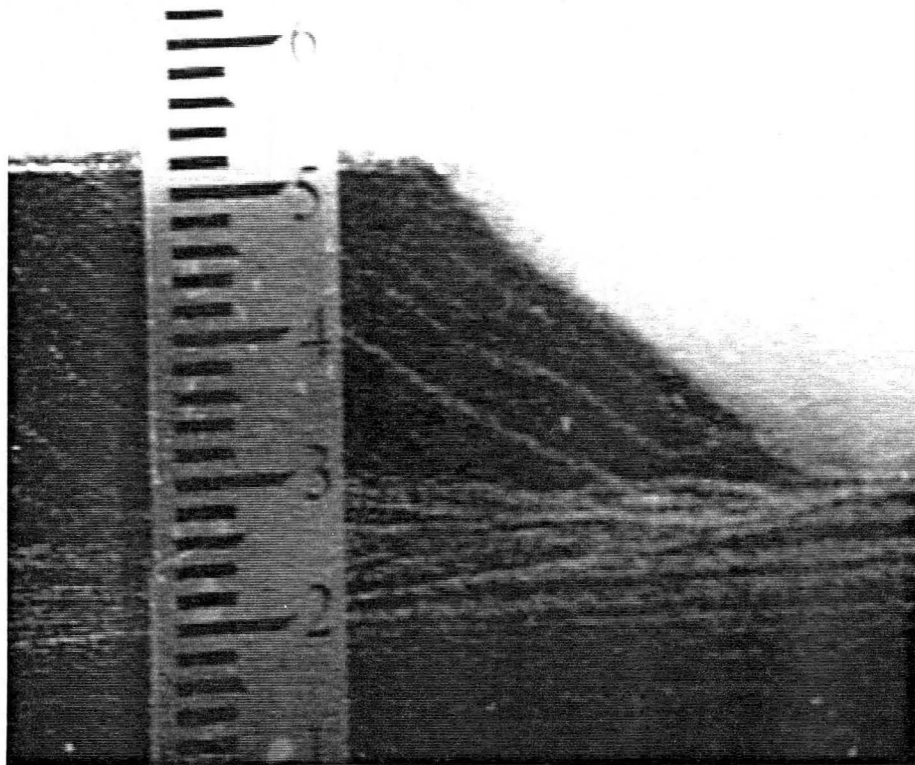


Picture 42. Typical stratified deposit of a long dune

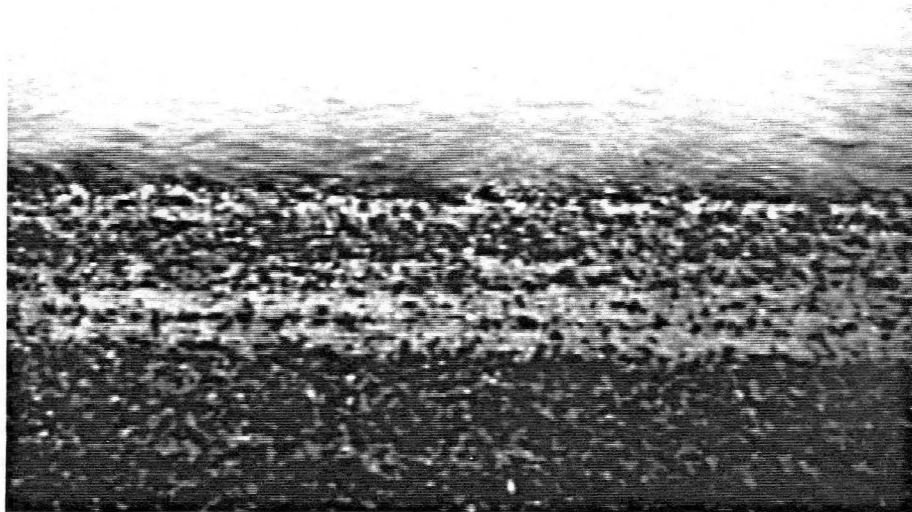
3.6 Stratified Delta

In order to examine the structure of a stratified delta, A simple run with carried out with a discharge of $0.125 \text{ m}^3/\text{sec}$. The total number of the tail gates used was 6 and the flume floor slope was 1.9%. The flow depth and the mean velocity were not recorded.

During this run, it was possible to observe the formation of a delta as shown in Picture 43. Coarse sand particles in black roll on top of the topset slope of the delta which is aggrading with time and primarily composed of fine sand in white, as shown on Picture 44. The resulting stratified deposit in formation is shown on Picture 45. The top surface of the delta was characterized by a plane bed and the topset of the delta was formed from thin layer of fine white sand. The black coarse particles were observed moving on top of the delta as a bed load.



Picture 43. Typical delta in formation

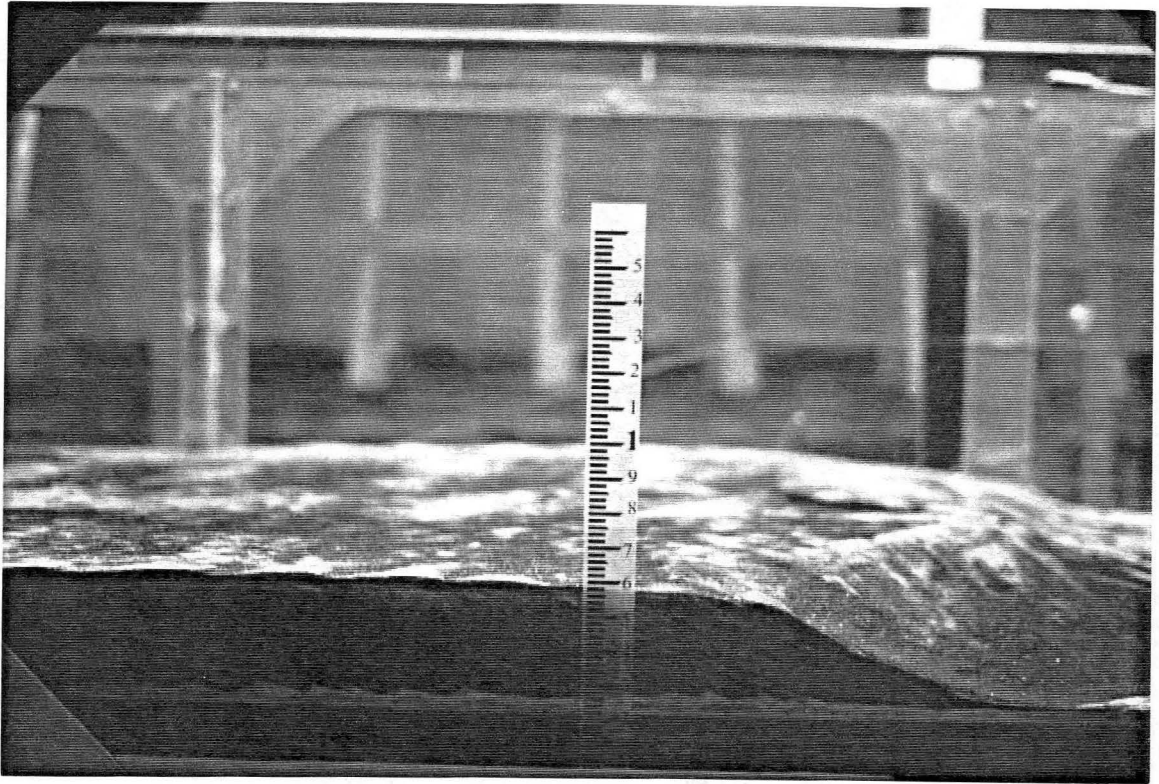


Picture 44. Coarse particles rolling on top of fine particles on topset slope



Picture 45. Stratified deposit in formation

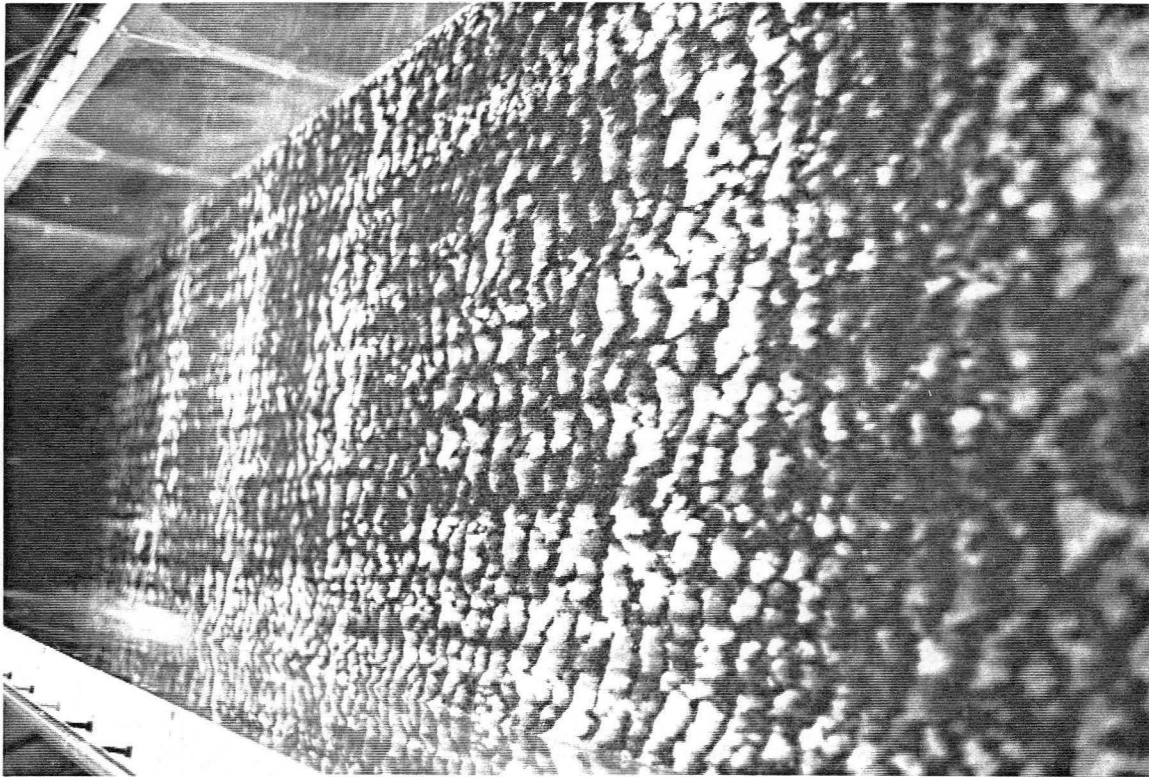
After the flume experiment, the deposit is dried in the flume over a period of 5-7 days. Picture 46a shows the deltaic structure and Picture 46b shows an enlarged view of the dried delta deposit. The bottomset of the delta is shown as white fine sand. The topset of the delta consists of a plane bed of fine sands partially covered with coarse sands, as shown on Pictures 47 and 48. A cross-section is cut through the delta on Picture 49 and the enlarged view (Picture 50) clearly illustrates the stratified sediment deposit that developed from a continuous supply of coarse sands in black and fine sands in white under steady non-uniform flow.



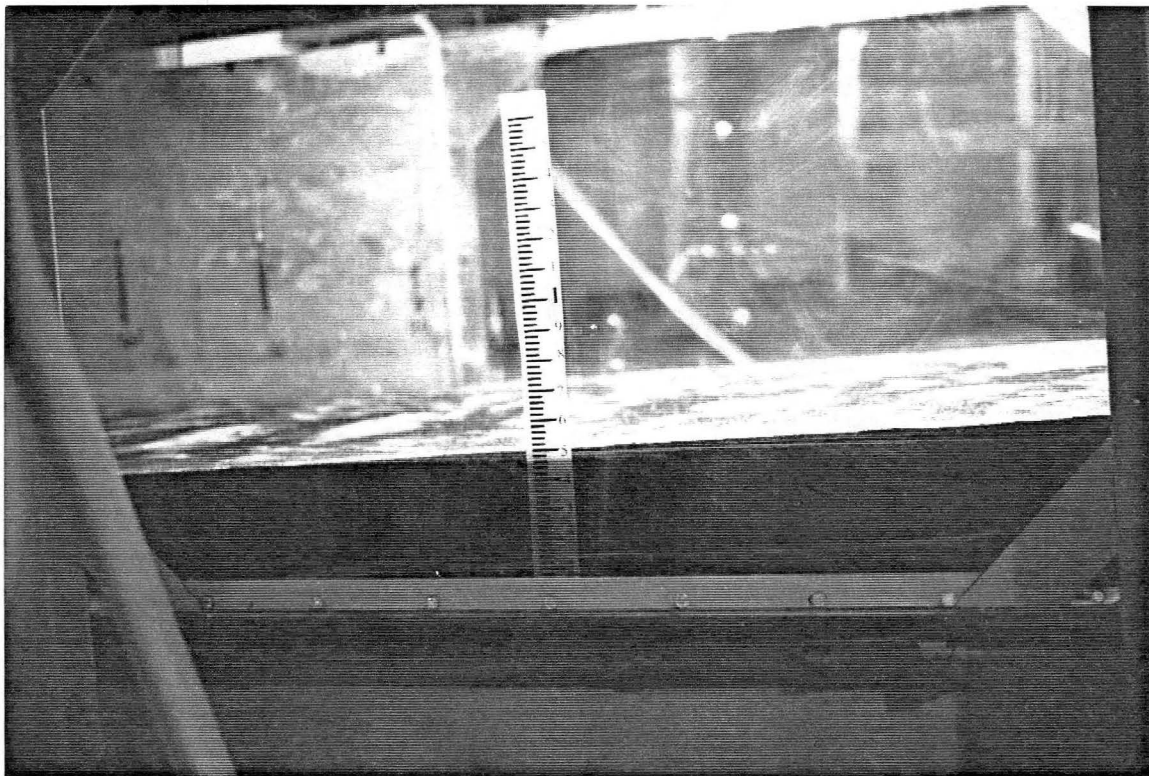
Picture 46a. Typical dried delta



Picture 46b. Typical dried delta, enlarged view



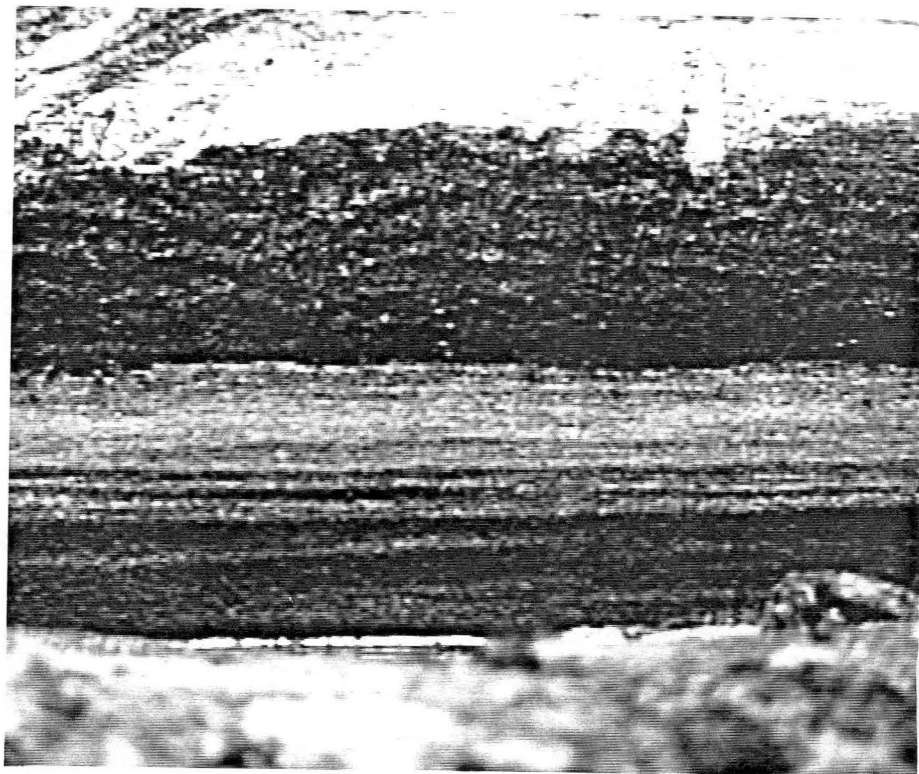
Picture 47. Top view of a dry delta



Picture 48. Side view of a dry delta



Picture 49. Cross-section of a dry delta



Picture 50. Enlarged cross-section of a dry delta

4. CONCLUSIONS

This study focused on 5 main aspects; 1) segregation of particles, 2) settling in air, 3) settling in fresh and salt water, 4) settling in vacuum, and 5) stratification in laboratory flume. Those experiments were carried out with one mixture of two different sands. They were different in size, color, shape and density.

4.1 Particle Segregation

Segregation of particles is observed from a sand mixture under lateral movement. For a mixture of black coarse particles and fine white particles, the fine particles fall in the interstices between coarse particles. Coarse particles roll on top of the fine particles. Because the fine particles have a lower kinetic energy than the coarse particles, they form a thin layer on the bottom of the moving sediment layer.

4.2 Lamination in Air

Settling in air is examined using U-shaped settling tubes. This equipment is designed to visualize the internal structure of two-dimensional settling. Clear lamination is observed when the sand mixture is poured freely at a constant rate.

After the initial splash from the impact of particles, the mixture slides down the incline near the angle of repose of the coarse sand. Fine and coarse particles segregate in the moving layer until a lamina has formed up the incline. Successive layers form and result in a laminated deposit.

Tilted settling in air results in a thin film of fine particles on the lower side of the settling tube. While the coarse particles were rolling on top. Lamination therefore results from repetitive segregation.

4.3 Lamination in Fresh Water and Salt Water

Settling in fresh and salt water at two different salt concentrations showed the laminae could be formed in salt water as well as in fresh water.

Unlike settling in air, fine particles in salt water tend to remain in suspension and settle at the edge of the tube. The concentration of coarse particles is higher toward the center of the settling tube. Lamination is less distinct in salt water than fresh water. Distinct lamination was observed in the air. This is due to the effect of differential settling velocity of submerged particles, and the increased suspension of fines which interferes with the segregation mechanism in the moving layer.

4.4 Lamination in Vacuum

Above all, the most significant experiment confirms the clear formation of laminae near complete vacuum conditions at -560 mm of Hg (or -22 in of Hg). The hypothesis formulated by numerous researchers that lamination is caused by turbulence must therefore be rejected.

4.5 Stratification in a Large Laboratory Flume

Laboratory experiments on stratification were conducted in a 60 ft long, 4 ft wide flume under a constant discharge and continuous supply of sediment. Three sets of experiments with horizontal, mild and adverse slopes included phases where the water level was increased, then decreased.

Starting from initially plane bed conditions, the increase in flow depth resulted in the complex formation of sequences of ripples, dunes and deltas. Ripples tended to be small and fine-grained early on but the grain size distribution changed and the median grain size increased overtime.

In the case of formation of dunes, long dunes showed a stratified deposit characterized by superposed sequences of deltas with thin topset deposits of fine particles on top of thick foreset deposits of coarse particles. As the amplitude of dunes increased over time, the stratified deposit was gradually scoured in the downstream direction.

A simple delta was modeled in the laboratory to illustrate simple stratification features resulting from a continuous supply of a heterogeneous sand mixture under a constant discharge. A clear stratified deposit was observed in which the interface slope between each strata was neither horizontal nor parallel to the flume slope. The interface slope between the bottom set and the foreset slope slightly less than the flume slope. The interface slope between foreset and topset deposits was about one-third of the flume slope. The topset slope was close to the initial flume slope.

The video cassette "Fundamental Experiments on Stratification" illustrates the dynamic formation of deltas under a constant discharge and a continuous sediment supply. The experiments replicate the results reported at a smaller scale in the earlier experimental program in 1990. The results confirm earlier observations on the segregation mechanism. The experimental fact that lamination occurs under vacuum settling forcibly rejects the hypothesis that lamination results from periodic cycles of turbulence. The stratification of sand mixtures under a steady discharge and continuous supply of heterogeneous sands provides clear experimental evidence that layers and strata are not necessarily identical, as explained by Julien et al. (1993). This year's experiments on changes in flow depth demonstrate that complex stratified deposits result with simultaneous formation of ripples, dunes and deltas at various stages of development. The formation of long dunes, for instance, involves simultaneous erosion and deposition of sediment at various locations in the flume. Although near horizontal strata can be observed through the flume sidewalls, it is difficult, if not

impossible, to associate chronological time sequences of their formation as viewed from sidewall views, or cross-sections, of the deposits.

In summary, the specific contributions of this year's research program are the following:

- 1) physical explanation of the segregation process based on the kinetic energy of rolling particles;
- 2) experiment observation of clear lamination under substantial vacuum (-560 mm of Hg);
- 3) new apparatus showing clear lamination in air, under water, salt water, and near complete vacuum;
- 4) clear stratification of sand mixtures in large flumes, which confirms previous observations in small flumes;
- 5) clear visualization of segregation, lamination and stratification, as presented on photographs and video-tape;
- 6) preparation of a top-quality video-cassette entitled "fundamental Experiments on Stratification" available in English or French on NTSC or PAL systems;
- 7) final preparation of the publication at the Société Géologique de France issued in Fall, 1993, including a new particle segregation diagram.

5. REFERENCES

- Berthault, G., 1986. "Sedimentology-experiments on lamination of sediments," C.R. Acad. Sci. Paris, t303, Serie II. No. 17, pp. 1569-1574.
- Berthault, G., 1988. "Sedimentation of heterogranular mixture--experimental lamination in still and running water," C.R. Acad. Sci. Paris, t306, Serie II, pp. 717-724.
- Julien, P.Y., 1987. "Erosion and Sedimentation," teaching guide for CE-716, Erosion and Sedimentation. Engineering Research Center, Colorado State University.
- Julien, P.Y. and Y.Q. Lan, 1989. "Experimental Formation of Alluvial Channel in Wide Rectangular Flume," Civil Engineering Report, CER89-90PYJ-YQL2, Department of Civil Engineering, Colorado State University, Fort Collins, CO, 29 p.
- Julien, P.Y. and Y.Q. Lan, 1990. "Sedimentation of Heterogranular Mixtures in a Vertical Cylinder," Civil Engineering Report, CER89-90PYJ-YQL13, Colorado State University, Fort Collins, CO, 48 p.
- Julien, P.Y. and Y.C. Chen, 1989a. "A short report about the experiment of lamination in a small flume," Unpublished Report, Colorado State University.
- Julien P.Y. and Y.C. Chen, 1989b. "Experimental Study of Horizontal Lamination in a Recirculating Flume," Civil Engineering Report CER88-89PYJ-YCC14, Colorado State University, Fort Collins, CO, 63 p.
- Julien, P.Y. and Y.C. Chen, 1989. "Experiment Study of the Deposition and Drying of Bijou Creek Sand in a Recirculating Flume," Civil Engineering Report, CER89-90-PYJ-YCC4, Colorado State University, Fort Collins, CO, 35 p.

Julien, P.Y. and Y.Q. Lan, 1990. "Laboratory Experiments on Lamination Stratification and Desiccation," Civil Engineering Report CER-89-90PYJ-YQL15, Colorado State University, Fort Collins, CO, 177 p.

Julien, P.Y., Y.Q. Lan and G. Berthault, 1993. "Experiments on Segregation, Lamination, Stratification as Desiccation of Heterogeneous Sand Mixtures," Bulletin de la Société Géologique de France, t164, No. 5, pp. 649-660.